Solution Manual

for the exercises in the textbook

Wireless Communications by A. F. Molisch,

created by

Peter Almers, Ove Edfors, Fredrik Floren, Anders Johanson, Johan Karedal, Buon Kiong Lau, Andreas F. Molisch, Andre Stranne, Fredrik Tufvesson, Shurjeel Wyne, and Hongyuan Zhang

In this solution manual, references to figures and equations in the textbook have a prefix B (e.g., Eq. (B-13.47)). Equations and figures without this prefix refer to the solution manual itself.

Chapter 1

Applications and requirements of wireless services

1. (i) 30 years, (ii) 10 years, (iii) 3 years.
2. (iii) pager and (v) TV broadcast cannot transmit in both directions.
3. A 10 s voice message requires $10 \cdot 10000 = 10^5$ bits. For a pager message, each letter requires 8 bit (extended alphabet encoding), so that a 128-letter message requires about 1000 bits. The voice message thus requires 100 times as many bits to be transmitted.
4. Private PABX and cellular systems are very similar, and are distinguished only by (i) the size of the coverage region, and (ii) the way the mobility is implemented. Paging systems and wireless LANs show large differences, especially the fact that wireless LANs allow duplex transmission while paging systems don't; also the data rates are completely different. (iii) cellular systems with closed user groups are quite similar to trunking radio. Depending on a cellular operator, a prioritization might be implemented (but almost always exists for trunking radio). The cellular system can also allow to reach participants outside the closed group.
5. The high data rate requires a considerable amount of spectrum. Since the transmission is done over a larger distance d, it means that this spectrum cannot be used for any other purpose at least in a circle of distance d around the MS (this is a rough approximation). Furthermore, remember that for a successful transmission, a certain minimum bit energy is required. Transmission over a large distance means that the transmit bit energy has to be high, in order to compensate for the large path loss. Thus, the transmission of a large number of bits implies a high energy consumption, which leads to short battery lifetime for the MS.
6. As explained in Sec. 1.4.2, the key factors are
   - *price of the offered services:* the price of the services is in turn influenced by the amount of competition, the willingness of the operators to accept losses in order to gain greater market penetration, and the external costs of the operators (especially the cost of spectrum licenses).
   - *price of the MSs:* the MSs are usually subsidized by the operators, and are either free, or sold at a nominal price, if the consumer agrees to a long-term contract.
   - *attractiveness of the offered services:* in many markets, the price of the services offered by different network operators is almost identical. Operators try to distinguish themselves by different features, like better coverage, text- and picture message service, etc. The offering of those improved features also helps to increase the market size in general, as it allows customers to find services tailored to their needs.
   - *general economic situation:* obviously, a good general economic situation allows the general population to spend more money on such "non-essential" things as mobile communications services.
   - *existing telecom infrastructure:* in countries or areas with a bad existing landline-based telecom infrastructure, cellular telephony and other wireless services can be the only way of communicating. This would enable high market penetration.

- *predisposition of the population*: there are several social factors that can increase the cellular market: (i) people have a positive attitude to new technology (gadgets) - e.g., Japan and Scandinavia; (ii) people consider communication an essential part of their lives - e.g., China, and (iii) high mobility of the population, with people being absent from their offices or homes for a significant part of the day, e.g., USA.

Chapter 2

Technical challenges of wireless communications

1. The carrier frequency has a strong impact on fading. The small-scale fading shows strong variations on the order of half a wavelength or less. Thus, variations of the channel are stronger (over a fixed distance x) at higher carrier frequencies. The dependence of the shadowing on the carrier frequency also shows a similar trend. At higher frequencies, objects tend to throw sharper "shadows", so that the transition from the "fully illuminated" to the "completely shadowed" state occurs over a shorter distance. Note, however, that the distance from the object that is throwing shadows plays a crucial role as well.

2. The pathlength via the mountain range is $2 \cdot 14 = 28$ km, which is 18 km longer than the direct path. Each km additional runlength corresponds to $\frac{10^3}{3 \cdot 10^8} s = \frac{10}{3}$ μs excess delay. Thus, the 18 km distance corresponds to 60 μs excess delay. As the goal is to keep this excess delay to less than 0.1 symbol durations, the symbol duration must be 600 μs, implying a symbol rate of 1.33 ksymbols/s. This is clearly too low for many applications. For this reason, equalizers or similar devices (see Chapter 16) are often used.

3. Low carrier frequencies make it difficult to build high-gain antennas. Note that for satellite TV, high-gain antennas are used at both link ends, leading to a better link budget. This will be explored further in Chapter 3. Furthermore, a large absolute bandwidth (required for the transmission of many channels) is more easily available at higher frequencies. For this reason, the Ku-band (above 10 GHz) is most frequently used. At very high frequencies the atmospheric attenuation, especially in bad weather, can become prohibitive.

4. Cellphones mainly operate in the $800 - 1000$ MHz band, and in the $1800 - 2000$ MHz band, though some systems also occupy the $400 - 500$ MHz band. In general, the higher frequency bands provide high capacity (can accommodate many users), both because a larger absolute bandwidth is available, and because the higher pathloss at those frequencies leads to smaller cell sizes (see also Chapter 17). Lower frequencies are better suited for outdoor-to-indoor penetration, as well as the coverage of large rural and mountainous regions. This is also the reason why, e.g., NMT 450 (an analogue system operating at 450 MHz carrier frequencies remained operative in the sparsely inhabited areas of Scandinavia even after GSM (a digital system operating at 900 and 1800 MHz carrier frequency) was introduced.

5. The first advantage is a reduction of interference to other users that utilize the same carrier frequency. this is true for both CDMA and TDMA based systems, as will be explained in more detail in Chapters 17 and 18. Furthermore, the power control improves the battery lifetime, as energy is not wasted (such a waste would occur if the transmitter always sends at full power, even if the receiver could receive with sufficient quality when less power is used.

Chapter 3

Noise- and interference-limited systems

1. First we convert the gains and noise figures to a linear scale.

   1.5 dB = 3/2 dB= $\sqrt{2} = 1.4$

   10 dB = 10

   4 dB = 10 − 3 − 3 dB= $10/(2 \cdot 2) = 2.5$;

   1 dB = 10 − 3 − 3 − 3 dB=$10/(2 \cdot 2 \cdot 2) = 1.25$;

   The noise figure can be computed from (compare also Eq. (B-3.6)).

$$\begin{aligned} F_{\text{eq}} &= F_1 + \frac{F_2 - 1}{G_1} + \frac{F_3 - 1}{G_1 G_2} && (3.1)\\ &= 1.4 + \frac{2.5 - 1}{1} + \frac{0.25}{10} && (3.2)\\ &= 2.925 && (3.3) \end{aligned}$$

   which is approximately 4.7 dB. As we can see, the noise figure is dominated by the stages before the low-noise amplifier and the noise figure of the amplifier itself.

2. The thermal noise for a system with 100 kHz bandwidth is

$$(-173 \text{ dBm/Hz}) + (50 \text{ dBHz}) = -123 \text{ dBm} \quad (3.4)$$

   As can be seen from Fig. 3.1, the noise enhancement due to man-made noise is approximately 31 dB at 50 MHz carrier frequency. Thus, the noise power is −92 dBm.

   Next, we compute the signal power arriving at the receiver. At 50 MHz, the wavelength is 6 m. According to Eq. (B-3.1),

$$\begin{aligned} P_{\text{RX}} &= P_{\text{TX}} G_{\text{RX}} G_{\text{TX}} \left(\frac{\lambda}{4\pi d}\right)^2 && (3.5)\\ &= 10^{-4} \cdot 1 \cdot 1 \cdot (\frac{6}{4\pi \cdot 100})^2 && (3.6)\\ &= 2.28 \cdot 10^{-9} && (3.7)\\ &= -86 \text{ dBW} && (3.8)\\ &= -56 \text{ dBm} && (3.9) \end{aligned}$$

   Consequently, the SNR at the receiver is 36 dB. Due to the receiver noise (noise figure 5 dB), it decreases to 31 dB.

   Consider next the result at 500 MHz. The noise power decreases by 23 dB, due to the strong reduction in the man-made noise (see again Fig. 3.1). However, the wavelength decreases by a factor of 10, so that the free-space attenuation increases by $10^2 = 20$ dB. The SNR is thus $31 + 23 - 20 = 34$ dB.

Increasing the center frequency further to 5 GHz, leads to a reduction of the total noise by another 8 dB. However, the signal power decreases by another 20 dB. Thus, the SNR gets worse by 12 dB, reducing to 22 dB.

3. The following link budget results:

Transmit power	20	dBm
Attenuation up to 50 m	−66	dB
Attenuation from 50 to 500 m	−42	dB
Transmit antenna gain	−7	dB
Receive antenna gain	9	dB
Total arriving power	−86	dBm
Receiver sensitivity	−105	dBm
Fading margin	19	dB

4. The following link budget can be created:

Receive noise power spectral density	−173	dBm/Hz
Receive bandwidth	73	dBHz
Receive noise power	−100	dBm
Transmit power	20	dBm
TX and RX antenna gains	4	dB
TX losses	−3	dB
Fading margin	-16	dB
Path loss	−90	dB
Arriving RX power	−85	dBm
SNR at RX input	15	dB
Required SNR	5	dB

From this it follows that the admissible noise figure of the RX is 10 dB.

5. We use the conservative estimate that the link margin for 90% of sufficient SIR is the sum of the link margins for the desired and the interfering signals, i.e., 20 dB. The *average* SIR at the MS thus needs to be 28 dB. The signal from the serving BS decreases as d^{-4}, so that at the cell boundary it is proportional to R^{-4}, while for the interfering signal, it is $(D-R)^4$. We thus require

$$\left(\frac{D-R}{R}\right)^4 = 10^{2.8} \tag{3.10}$$

from which $D/R = 6$ follows.

Chapter 4

Propagation mechanisms

1. The gain of an antenna relative to an isotropic antenna is defined as

$$G = \frac{A_{\text{eff}}}{A_{\text{iso}}}, \tag{4.1}$$

where A_{eff} is the effective area of the antenna and $A_{\text{iso}} = \lambda^2/4\pi$ is the effective area of the isotropic antenna. For the parabolic antenna we have an effective area of $A_{\text{eff}} = 0.55A$, where A is the physical aperture area. Thus,

$$\begin{aligned} G_{\text{par}} &= \frac{0.55A}{\frac{\lambda^2}{4\pi}} \\ &= \frac{4\pi}{\lambda^2} \cdot 0.55 \cdot \pi r^2 \\ &= 2.2 \left(\frac{\pi r}{\lambda}\right)^2. \end{aligned} \tag{4.2}$$

2. We have a distance between the TX and the RX of $d = 35 \cdot 10^6$ m. The antenna gains are $G_{\text{TX}} = 60$ dB (Earth) and $G_{\text{RX}} = 20$ dB (sat.), and the carrier frequency is $f_c = 11$ GHz.

   (a) The link budget is shown in Figure 4.1.

   (b) The total attenuation (including the antenna gain) from TX to RX is

$$\begin{aligned} P_{\text{TX|dB}} - P_{\text{RX|dB}} &= -G_{\text{TX|dB}} - G_{\text{RX|dB}} + L_{free} \\ &= -G_{\text{TX|dB}} - G_{\text{RX|dB}} + 20\log_{10}\left(\frac{4\pi d}{\lambda}\right) \\ &= -60 - 20 + 20\log_{10}\left(\frac{11 \cdot 10^9 \cdot 4\pi \cdot 35 \cdot 10^6}{3 \cdot 10^8}\right) \\ &= 124.2 \text{ dB}, \end{aligned} \tag{4.3}$$

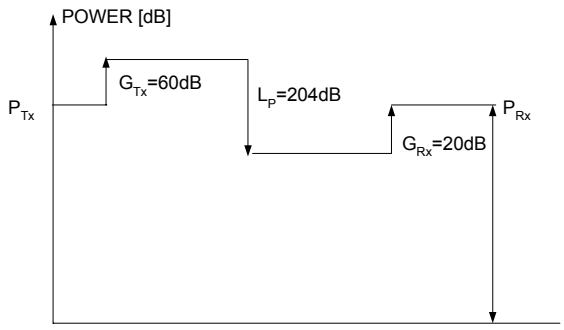

Figure 4.1: The link budget.

where we have used $\lambda = c/f_c$.

(c) Since the received power is

$$P_{\mathrm{RX|dB}} = P_{\mathrm{TX|dB}} - 124.2, \tag{4.4}$$

the transmit power required to keep the receiver at a received power level of -120 dBm is

$$P_{\mathrm{TX|dB}} = P_{\mathrm{RX|dB}} + 124.2 = -120 + 124.2 = 4.2 \text{ dBm}. \tag{4.5}$$

3. We are given the following parameters:

$$\begin{aligned} f_c &= 10^9 \text{ Hz} \\ \lambda &= \frac{3 \cdot 10^8}{10^9} = 0.3 \text{ m} \\ d &= 90 \text{ m} \\ L_a &= 15 \text{ m}, \end{aligned} \tag{4.6}$$

where d is the separation distance between the antennas, and L_a the maximum dimension of the antennas (in this case the diameter of the parabolic dishes).

(a) The Rayleigh distance is

$$\begin{aligned} d_R &= \frac{2L_a^2}{\lambda} \\ &= \frac{2 \cdot 15^2}{0.3} = 1500 \text{ m}, \end{aligned} \tag{4.7}$$

which means that $d < d_R$, and hence, Friis' law is not valid.

(b) Assuming that Friis' law is valid (despite the results in (a)), we find that the received power is

$$\begin{aligned} P_{\mathrm{RX|dB}} &= P_{\mathrm{TX|dB}} + G_{\mathrm{TX|dB}} - 20\log_{10}\left(\frac{4\pi d}{\lambda}\right) + G_{\mathrm{RX|dB}} \\ &= P_{\mathrm{TX|dB}} + 2 \cdot 10\log_{10}\left(\frac{0.55A}{\frac{\lambda^2}{4\pi}}\right) - 20\log_{10}\left(\frac{4\pi d}{\lambda}\right) \\ &= P_{\mathrm{TX|dB}} + 20\log_{10}\left(\frac{0.55A}{\frac{\lambda^2}{4\pi}} \cdot \frac{\lambda}{4\pi d}\right) \\ &= P_{\mathrm{TX|dB}} + 20\log_{10}\left(\frac{0.55A}{\lambda d}\right). \end{aligned} \tag{4.8}$$

With the values given, we have

$$\begin{aligned} P_{\mathrm{RX|dB}} &= P_{\mathrm{TX|dB}} + 20\log_{10}\left(\frac{0.55 \cdot \pi \cdot 7.5^2}{0.3 \cdot 90}\right) \\ &= P_{\mathrm{TX|dB}} + 11 \text{ dB}. \end{aligned} \tag{4.9}$$

Apparently, more power is received than is transmitted! This shows that using propagation models outside their range of validity may give very inaccurate results.

(c) The Rayleigh distance is

$$d_R = \frac{2L_a^2}{\lambda}, \tag{4.10}$$

and for a circular parabolic antenna, $L_a = 2r$. Thus,

$$d_R = \frac{2 \cdot 4r^2}{\lambda}. \tag{4.11}$$

But for the circular parabolic we also have the antenna gain

$$G_{\text{par}} = 2.2\left(\frac{\pi r}{\lambda}\right)^2, \tag{4.12}$$

which can be rewritten as

$$r^2 = \frac{G_{\text{par}}}{2.2}\left(\frac{\lambda}{\pi}\right)^2. \tag{4.13}$$

Thus,

$$\begin{aligned} d_R &= \frac{8}{\lambda}\cdot\frac{G_{\text{par}}}{2.2}\left(\frac{\lambda}{\pi}\right)^2 \\ &= 0.37\cdot\lambda\cdot G_{\text{par}}. \end{aligned} \tag{4.14}$$

4. We have the following parameters:

$$\begin{aligned} f_c &= 900\text{ MHz} \Rightarrow \lambda = 1/3\text{ m} \\ \varepsilon_r &= 4 \\ \Delta d &= 10\text{ cm} \\ d_{TX} &= 20\text{ m} \\ d_{RX} &= 60\text{ m} \\ h_{TX} &= 1.4\text{ m} \\ h_{RX} &= 1.4\text{ m} \\ h_{wall} &= 58\text{ m} \end{aligned} \tag{4.15}$$

(a) Since the brick wall can be treated as lossless, we have $\delta_{brick} = \delta_2 = \varepsilon_0\varepsilon_r$ and $\delta_{air} = \delta_1 = \varepsilon_0$. The reflection coefficient for TE-waves incident from air to brick is then given by

$$\begin{aligned} \rho_1 &= \frac{\sqrt{\delta_1}\cos\Theta_e - \sqrt{\delta_2}\cos\Theta_t}{\sqrt{\delta_1}\cos\Theta_e + \sqrt{\delta_2}\cos\Theta_t} = \frac{\sqrt{\varepsilon_0}\cos 0 - \sqrt{\varepsilon_0\varepsilon_r}\cos 0}{\sqrt{\varepsilon_0}\cos 0 + \sqrt{\varepsilon_0\varepsilon_r}\cos 0} = \\ &= \frac{1-\sqrt{\varepsilon_r}}{1+\sqrt{\varepsilon_r}} = \frac{1-2}{1+2} = -\frac{1}{3} \end{aligned} \tag{4.16}$$

while the reflection coefficient from brick to air is

$$\rho_2 = \frac{\sqrt{\delta_2}\cos\Theta_e - \sqrt{\delta_1}\cos\Theta_t}{\sqrt{\delta_2}\cos\Theta_e + \sqrt{\delta_1}\cos\Theta_t} = -\rho_1 = \frac{1}{3} \tag{4.17}$$

The corresponding transmission coefficents are

$$\begin{aligned} T_1 &= \frac{2\sqrt{\delta_1}\cos\Theta_e}{\sqrt{\delta_1}\cos\Theta_e + \sqrt{\delta_2}\cos\Theta_t} = \frac{2}{1+\sqrt{\varepsilon_r}} = \frac{2}{3} \\ T_2 &= \frac{2\sqrt{\delta_2}\cos\Theta_e}{\sqrt{\delta_1}\cos\Theta_e + \sqrt{\delta_2}\cos\Theta_t} = \frac{2\sqrt{\varepsilon_r}}{1+\sqrt{\varepsilon_r}} = \frac{4}{3} \end{aligned} \tag{4.18}$$

Then, the total transmission coefficient can be written as

$$T = \frac{T_1 T_2 e^{-j\alpha}}{1+\rho_1\rho_2 e^{-2j\alpha}} \tag{4.19}$$

With $\alpha = \frac{2\pi}{\lambda}\sqrt{\varepsilon_r}\Delta d\cos\Theta_t = \frac{2\pi}{1/3}\sqrt{4}\cdot 0.1\cdot 1 = 1.2\pi$, this becomes

$$T = \frac{\frac{4}{3}\frac{2}{3}e^{-j1.2\pi}}{1-\left(\frac{1}{3}\right)^2 e^{-j2.4\pi}} = -0.677 + j0.615 \tag{4.20}$$

Hence, the total received field, as transmitted through the wall, is given by

$$E_{\text{through}} = E_0\left(-0.677 + j0.615\right) \tag{4.21}$$

where E_0 is the electric field strength at the receiver if there hadn't been a screen.

(b) The diffracted field is given by

$$E_{\text{diff}} = E_0 \left(\frac{1}{2} - \frac{\exp(j\pi/4)}{\sqrt{2}} F(\nu_F) \right) \tag{4.22}$$

The Fresnel parameter ν_F is given by

$$\nu_F = \theta_d \sqrt{\frac{2 d_{TX} d_{RX}}{\lambda (d_{TX} + d_{RX})}} = 1.99 \sqrt{\frac{2400}{1/3 \cdot 80}} = 18.854 \tag{4.23}$$

where the diffraction angle θ_d has been determined as

$$\begin{aligned} \theta_d &= \arctan\left(\frac{h_{\text{wall}} - h_{\text{TX}}}{d_{\text{TX}}}\right) + \arctan\left(\frac{h_{\text{wall}} - h_{\text{RX}}}{d_{\text{RX}}}\right) = \\ &= \arctan\left(\frac{56.6}{20}\right) + \arctan\left(\frac{56.6}{60}\right) = 1.99 \end{aligned} \tag{4.24}$$

A numerical evaluation of the Fresnel integral yields $F(18.85) \approx 0.4875 - 0.4886i$. Thus, the diffracted field becomes

$$\begin{aligned} E_{\text{diff}} &= E_0 \left(\frac{1}{2} - \frac{\exp(j\pi/4)}{\sqrt{2}} (0.4875 - 0.4886i) \right) = \\ &= E_0 (0.0119 + 0.0005i) \end{aligned} \tag{4.25}$$

(c) The ratio becomes

$$\begin{aligned} \frac{|E_{\text{through}}|}{|E_{\text{diff}}|} &= \frac{|E_0 (-0.677 + j0.615)|}{|E_0 (-0.012 - j0.001)|} = \\ &= \frac{|-0.677 + j0.615|}{|-0.012 - j0.001|} = \frac{0.915}{0.012} = 76 \ . \end{aligned} \tag{4.26}$$

Hence, much more power is transmitted through the wall than is diffracted over it.

5. Since medium 1 is air, we have $\delta_1 = \varepsilon_0$. Medium 2 is assumed to be lossless, hence $\sigma_2 = 0$ and thus the dielectric constant δ_2 is real and equal to $\varepsilon_r \varepsilon_0$. Eq. (B-4.13) yields

$$\begin{aligned} \rho_{\text{TM}} &= \frac{\sqrt{\delta_2}\cos\Theta_e - \sqrt{\delta_1}\cos\Theta_t}{\sqrt{\delta_2}\cos\Theta_e + \sqrt{\delta_1}\cos\Theta_t} = \frac{\sqrt{\varepsilon_r\varepsilon_0}\cos\Theta_e - \sqrt{\varepsilon_0}\cos\Theta_t}{\sqrt{\varepsilon_r\varepsilon_0}\cos\Theta_e + \sqrt{\varepsilon_0}\cos\Theta_t} = \\ &= -\frac{\cos\Theta_t - \sqrt{\varepsilon_r}\cos\Theta_e}{\cos\Theta_t + \sqrt{\varepsilon_r}\cos\Theta_e} \end{aligned} \tag{4.27}$$

But using Eq. (B-4.12), we can rewrite $\cos\Theta_t$ as

$$\cos\Theta_t = \sqrt{1 - \sin^2\Theta_t} = \sqrt{1 - \frac{1}{\varepsilon_r}\sin^2\Theta_e} \tag{4.28}$$

Hence,

$$\rho_{\text{TM}} = -\frac{\sqrt{1 - \frac{1}{\varepsilon_r}\sin^2\Theta_e} - \sqrt{\varepsilon_r}\cos\Theta_e}{\sqrt{1 - \frac{1}{\varepsilon_r}\sin^2\Theta_e} + \sqrt{\varepsilon_r}\cos\Theta_e} = \frac{\varepsilon_r\cos\Theta_e - \sqrt{\varepsilon_r - \sin^2\Theta_e}}{\varepsilon_r\cos\Theta_e + \sqrt{\varepsilon_r - \sin^2\Theta_e}} \tag{4.29}$$

Similarily, for TE waves we have

$$\begin{aligned} \rho_{\text{TE}} &= \frac{\sqrt{\delta_1}\cos\Theta_e - \sqrt{\delta_2}\cos\Theta_t}{\sqrt{\delta_1}\cos\Theta_e + \sqrt{\delta_2}\cos\Theta_t} = \frac{\sqrt{\varepsilon_0}\cos\Theta_e - \sqrt{\varepsilon_r\varepsilon_0}\cos\Theta_t}{\sqrt{\varepsilon_0}\cos\Theta_e + \sqrt{\varepsilon_r\varepsilon_0}\cos\Theta_t} = \\ &= \frac{\cos\Theta_e - \sqrt{\varepsilon_r}\cos\Theta_t}{\cos\Theta_e + \sqrt{\varepsilon_r}\cos\Theta_t} = \frac{\cos\Theta_e - \sqrt{\varepsilon_r}\sqrt{1 - \frac{1}{\varepsilon_r}\sin^2\Theta_e}}{\cos\Theta_e + \sqrt{\varepsilon_r}\sqrt{1 - \frac{1}{\varepsilon_r}\sin^2\Theta_e}} = \\ &= \frac{\cos\Theta_e - \sqrt{\varepsilon_r - \sin^2\Theta_e}}{\cos\Theta_e + \sqrt{\varepsilon_r - \sin^2\Theta_e}} \end{aligned} \tag{4.30}$$

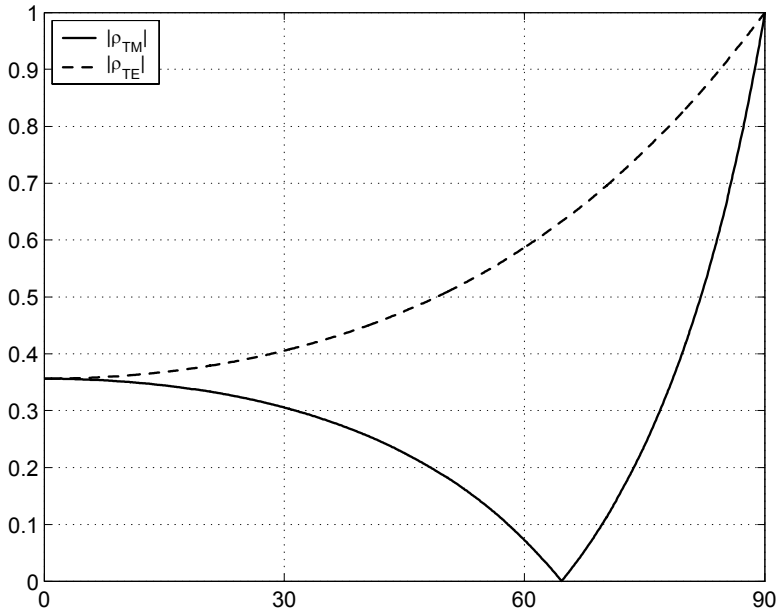

Figure 4.2: Reflection coefficients for TM and TE polarization.

6. (a) Following Problem 5, we have

$$\rho_{TM} = \frac{\varepsilon_r \cos\Theta_e - \sqrt{\varepsilon_r - \sin^2\Theta_e}}{\varepsilon_r \cos\Theta_e + \sqrt{\varepsilon_r - \sin^2\Theta_e}} \tag{4.31}$$

which is equal to zero when $\sqrt{\varepsilon_r - \sin^2\Theta_e} = \varepsilon_r \cos\Theta_e$. Hence,

$$\begin{aligned} \varepsilon_r - \sin^2\Theta_e &= \varepsilon_r^2 \cos^2\Theta_e \Leftrightarrow \\ \varepsilon_r - 1 + \cos^2\Theta_e &= \varepsilon_r^2 \cos^2\Theta_e \Leftrightarrow \\ \cos^2\Theta_e &= \frac{\varepsilon_r - 1}{\varepsilon_r^2 - 1} \Leftrightarrow \\ \Theta_e &= \arccos\sqrt{\frac{\varepsilon_r - 1}{\varepsilon_r^2 - 1}} = \arctan\sqrt{\varepsilon_r} \end{aligned} \tag{4.32}$$

This angle for which there is no TM reflection is called the Brewster angle. For TE waves, the reflection is given by

$$\rho_{TE} = \frac{\cos\Theta_e - \sqrt{\varepsilon_r - \sin^2\Theta_e}}{\cos\Theta_e + \sqrt{\varepsilon_r - \sin^2\Theta_e}} \tag{4.33}$$

which is < 0 for all Θ_e since

$$\cos\Theta_e - \sqrt{\varepsilon_r - \sin^2\Theta_e} = \sqrt{1 - \sin^2\Theta_e} - \sqrt{\varepsilon_r - \sin^2\Theta_e} < 0 \tag{4.34}$$

for all $\varepsilon_r > 1$.

(b) For $\varepsilon_r = 4.44$, the magnitude of the reflection coefficients is plotted in Figure 4.2. The Brewster angle becomes

$$\Theta_e = \arccos\sqrt{\frac{4.44 - 1}{4.44^2 - 1}} = 64.6 \text{ deg} \tag{4.35}$$

7. The received power is given by the power flux density $|E|^2/120\pi$ (in W/m^2) multiplied by the effective receive antenna area A_{RX}, i.e.,

$$P_{RX}(d) = \frac{|E|^2}{120\pi} A_{RX} = E(1m)^2 \frac{1}{d^2} 4 \left(\frac{h_{TX} h_{RX}}{d}\right)^2 \frac{4\pi^2}{\lambda^2} \frac{1}{120\pi} A_{RX} \tag{4.36}$$

From Eq. (B-4.2), we have

$$G_{RX} = \frac{4\pi}{\lambda^2} A_{RX} \Leftrightarrow A_{RX} = \frac{G_{RX}\lambda^2}{4\pi} \tag{4.37}$$

This, substituted into the expression for P_{RX}, yields

$$\begin{aligned} P_{RX}(d) &= E(1m)^2 \frac{1}{d^2} 4 \left(\frac{h_{TX}h_{RX}}{d}\right)^2 \frac{4\pi^2}{\lambda^2} \frac{1}{120\pi} \frac{G_{RX}\lambda^2}{4\pi} = \\ &= \frac{4E(1m)^2}{120} G_{RX} \left(\frac{h_{TX}h_{RX}}{d^2}\right)^2 \end{aligned} \tag{4.38}$$

But

$$\frac{4E(1m)^2}{120} = 4\pi \frac{E(1m)^2}{120\pi} = EIRP(1m) = P_{TX}G_{RX} \tag{4.39}$$

Hence,

$$P_{RX}(d) = P_{TX}G_{TX}G_{RX} \left(\frac{h_{TX}h_{RX}}{d^2}\right)^2 . \tag{4.40}$$

8. The given parameters are:

BS	MS
$P_{\mathrm{TX,BS}} = 40$ W	$P_{\mathrm{TX,MS}} = 0.1$ W
$L_{a,\mathrm{BS}} = 0.5$ m	$L_{a,\mathrm{MS}} = 0.15$ m
$h_{\mathrm{BS}} = 10$ m	$h_{\mathrm{MS}} = 1.5$ m
$G_{\mathrm{BS}} = 6$ dB	$G_{\mathrm{MS}} = 2$ dB
$f_c = 900$ MHz $\Longrightarrow \lambda = \frac{1}{3}$ m.	

The received power at the RX a distance d from the TX is given by

$$P_{\mathrm{RX}}(d) = \frac{P_{\mathrm{TX}}G_{\mathrm{TX}}G_{\mathrm{RX}}}{\left(\frac{d^2}{h_{\mathrm{TX}}h_{\mathrm{RX}}}\right)^2}, \tag{4.41}$$

provided that $d \geq 4h_{\mathrm{TX}}h_{\mathrm{RX}}/\lambda$.

(a) The power available at the mobile station is

$$\begin{aligned} P_{\mathrm{RX,MS}} &= 10\log_{10}(40) + 6 + 2 - 20\log_{10}\left(\frac{d^2}{15}\right) \\ &= 47.5 - 40\log_{10}(d) \text{ dBW}, \end{aligned} \tag{4.42}$$

and the power at the base station is

$$\begin{aligned} P_{\mathrm{RX,BS}} &= 10\log_{10}(0.1) + 6 + 2 - 20\log_{10}\left(\frac{d^2}{15}\right) \\ &= 21.5 - 40\log_{10}(d) \text{ dBW}. \end{aligned} \tag{4.43}$$

The received power varies inversely as the fourth power of the separation distance between TX and RX.

(b) To determine the valid range of separation distance between 200 m and 3 km, we start with the condition for the ground plane propagation model to be valid. The condition is

$$\frac{4h_{\mathrm{TX}}h_{\mathrm{RX}}}{\lambda} = \frac{4 \cdot 10 \cdot 1.5}{1/3} = 180 < d = 200 \text{ m}, \tag{4.44}$$

and hence the propagation formula holds (note, though, that the stricter condition Eq. (B-4.65) does not hold). Next, the condition for Friis' law to hold is

$$d \geq d_R = \frac{2L_a^2}{\lambda}. \tag{4.45}$$

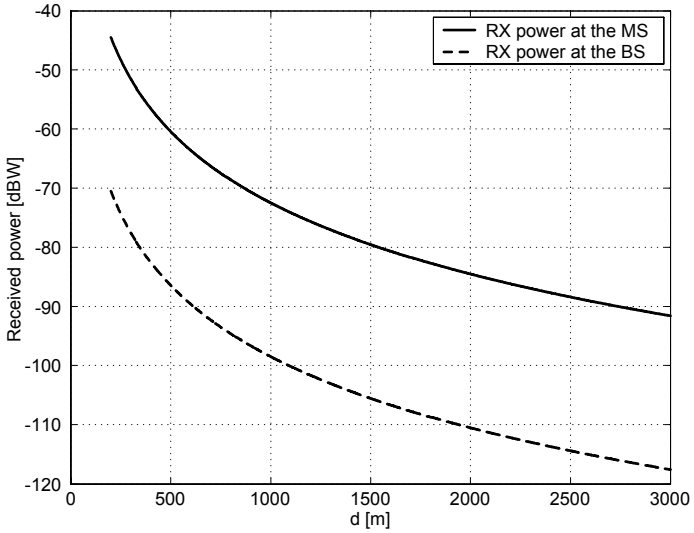

Figure 4.3: Received power at the BS and MS as a function of separation distance.

For the mobile station we have

$$d_{R,\mathrm{MS}} = \frac{2 \cdot 0.15^2}{1/3} = 0.135 \text{ m}, \tag{4.46}$$

and for the base station we have

$$d_{R,\mathrm{BS}} = \frac{2 \cdot 0.5^2}{1/3} = 1.5 \text{ m}, \tag{4.47}$$

which means that Friis' law also holds for all distances in this exercise.

(c) The plots of received power over distances of 200 m to 3 km between MS and BS is shown in Figure 4.3.

9. The parameters given are:

BS	MS
$P^{\min}_{\mathrm{RX,BS}} = P^{\min}_{\mathrm{RX,MS}} - 10$ dB	$P^{\min}_{\mathrm{RX,MS}}$
$h_{\mathrm{BS}} = 10$ m	$h_{\mathrm{MS}} = 1.5$ m
$G_{\mathrm{BS}} = 6$ dB	$G_{\mathrm{MS}} = 2$ dB

$f_c = 900$ MHz $\Longrightarrow \lambda = \frac{1}{3}$ m.

The scenario is illustrated in Figure 4.4. The received power at the MS and the reference antenna with the BS as a transmitter is

$$P_{\mathrm{RX|dB}}(d) = P_{\mathrm{TX|dB}} + G_{\mathrm{TX|dB}} - 20\log_{10}\left(\frac{d^2}{h_{\mathrm{TX}} h_{\mathrm{RX}}}\right) + G_{\mathrm{RX|dB}}. \tag{4.48}$$

The received power at the reference antenna with the MS as a transmitter is

$$P_{\mathrm{RX|dB}}(d) = P_{\mathrm{TX|dB}} + G_{\mathrm{TX|dB}} - 20\log_{10}\left(\frac{4\pi d}{\lambda}\right) + G_{\mathrm{RX|dB}}. \tag{4.49}$$

(a) The minimum received power required by the MS is $P^{\min}_{\mathrm{RX,MS}}$ and the distance between MS and BS is d.

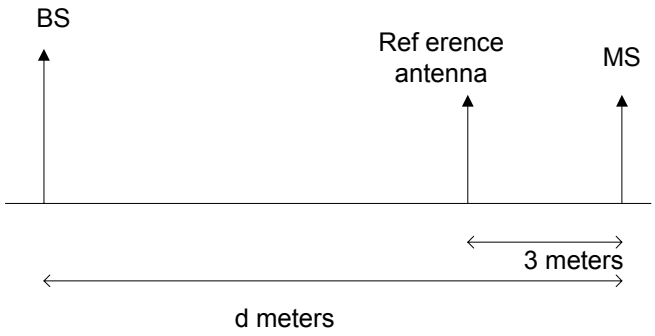

Figure 4.4: Reference antenna with gain G_{ref} to measure the radiation from the BS and MS.

i. The expression for the minimum required BS transmit power is calculated using

$$P^{\text{min}}_{\text{RX,MS}} = P_{\text{TX,BS}} + 6 - 20\log_{10}\left(\frac{d^2}{15}\right) + 2, \tag{4.50}$$

which results in

$$\begin{aligned} P_{\text{TX,BS}} &= P^{\text{min}}_{\text{RX,MS}} - 8 - 20\log_{10}(15) + 40\log_{10}(d) \\ &= P^{\text{min}}_{\text{RX,MS}} - 31.5 \text{ dB} + 40\log_{10}(d) \end{aligned} \tag{4.51}$$

ii. The expression for the minimum required MS transmit power is calculated using

$$P^{\text{min}}_{\text{RX,BS}} = P_{\text{TX,MS}} + 6 - 20\log_{10}\left(\frac{d^2}{15}\right) + 2, \tag{4.52}$$

which results in

$$\begin{aligned} P_{\text{TX,MS}} &= P^{\text{min}}_{\text{RX,BS}} - 31.5 \text{ dB} + 40\log_{10}(d) \\ &= P^{\text{min}}_{\text{RX,MS}} - 41.5 \text{ dB} + 40\log_{10}(d), \end{aligned} \tag{4.53}$$

since $P^{\text{min}}_{\text{RX,BS}} = P^{\text{min}}_{\text{RX,MS}} - 10$ dB.

iii. The received power at the reference antenna from the BS is

$$\begin{aligned} P^{\text{BS}}_{\text{RX,ref}} &= P_{\text{TX,BS}} + 6 + G_{\text{ref}} + 20\log_{10}(15) - 40\log_{10}(d) \\ &= P_{\text{TX,BS}} + G_{\text{ref}} + 29.5 \text{ dB} - 40\log_{10}(d), \end{aligned} \tag{4.54}$$

and using the result in 9(a)i we have

$$\begin{aligned} P^{\text{BS}}_{\text{RX,ref}} &= P^{\text{min}}_{\text{RX,MS}} - 31.5 \text{ dB} + 40\log_{10}(d) \\ &\quad + G_{\text{ref}} + 29.5 \text{ dB} - 40\log_{10}(d) \\ &= P^{\text{min}}_{\text{RX,MS}} + G_{\text{ref}} - 2 \text{ dB}. \end{aligned} \tag{4.55}$$

iv. With the distance $d_{\text{ref,MS}} = 3$ m between reference antenna and MS, the received power at the reference antenna from the MS is

$$\begin{aligned} P^{\text{MS}}_{\text{RX,ref}} &= P_{\text{TX,MS}} + 2 - 20\log_{10}\left(\frac{4\pi d_{\text{ref,MS}}}{\lambda}\right) + G_{\text{ref}} \\ &= P_{\text{TX,MS}} + G_{\text{ref}} + 2 \text{ dB} - 41 \text{ dB} \\ &= P_{\text{TX,BS}} - 10 \text{ dB} + G_{\text{ref}} + 2 \text{ dB} - 41 \text{ dB} \\ &= P_{\text{TX,BS}} + G_{\text{ref}} - 49 \text{ dB}, \end{aligned} \tag{4.56}$$

and using the result in 9(a)i we have

$$\begin{aligned} P^{\text{MS}}_{\text{RX,ref}} &= P^{\text{min}}_{\text{RX,MS}} - 31.5 \text{ dB} + 40\log_{10}(d) + G_{\text{ref}} - 49 \text{ dB} \\ &= P^{\text{min}}_{\text{RX,MS}} + G_{\text{ref}} - 80.5 \text{ dB} + 40\log_{10}(d). \end{aligned} \tag{4.57}$$

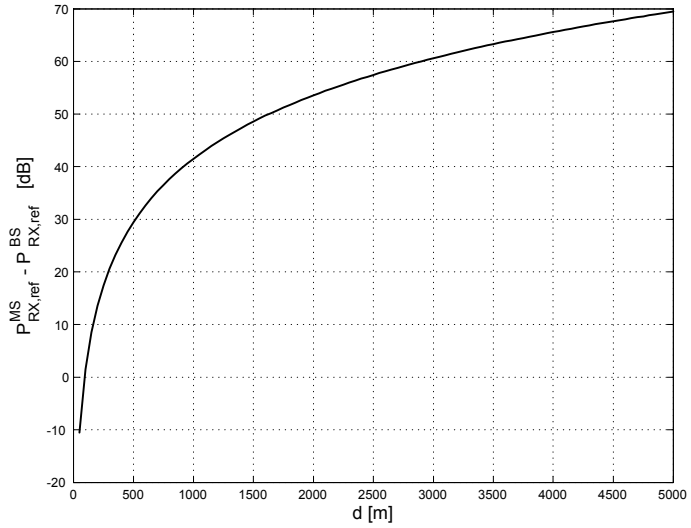

Figure 4.5: The difference $P^{\mathrm{MS}}_{\mathrm{RX,ref}} - P^{\mathrm{BS}}_{\mathrm{RX,ref}}$, as a function of the separation distance d.

(b) The difference in dB between $P^{\mathrm{MS}}_{\mathrm{RX,ref}}$ and $P^{\mathrm{BS}}_{\mathrm{RX,ref}}$ as a function of d is

$$\begin{aligned} P^{\mathrm{MS}}_{\mathrm{RX,ref}} - P^{\mathrm{BS}}_{\mathrm{RX,ref}} &= P_{\mathrm{TX,BS}} + G_{\mathrm{ref}} - 49 \text{ dB} - P_{\mathrm{TX,BS}} \\ &\quad -G_{\mathrm{ref}} - 29.5 \text{ dB} + 40\log_{10}(d) \\ &= -78.5 \text{ dB} + 40\log_{10}(d). \end{aligned} \tag{4.58}$$

The plot of $P^{\mathrm{MS}}_{\mathrm{RX,ref}} - P^{\mathrm{BS}}_{\mathrm{RX,ref}}$ for d in the range of 50 m to 5 km is shown in Figure 4.5. Note, however, that the breakpoint d_{break} lies at $d = 180$ m, so that the assumed d^4 law for the radiation from the BS is valid only at that distance

We determine the distance at which the MS and the BS produce the same radiation at the reference antenna. From

$$P^{\mathrm{MS}}_{\mathrm{RX,ref}} - P^{\mathrm{BS}}_{\mathrm{RX,ref}} = -78.5 \text{ dB} + 40\log_{10}(d) = 0 \text{ dB} \tag{4.59}$$

we find the distance to be

$$d = 10^{78.5/40} \approx 92 \text{ m}. \tag{4.60}$$

Hence, for a separation distance between the BS and the MS of $d \geq 92$ m, the radiation from a mobile unit at a distance of 3 m will be greater than the radiation from the BS (note, however, again the breakpoint). In many real-life situations the distance from a mobile to the base station is much greater than that, and the distance to people using mobile phones less than 3 meters. This means that exposure to radiation from surrounding base stations is less than the exposure to radiation from mobiles used by surrounding people. (Remember, though, that the studied case is based on very simple models.)

10. First we redraw the geometry according to Figure 4.6 in order to determine the size and position of the equivalent screen. The height h and the distance from the transmitter d_{TX} are given by simple trigonometry as

$$\left\{ \begin{array}{c} \frac{6}{8} = \frac{d_{TX}}{h-2} \\ \frac{10}{14} = \frac{40-d_{TX}}{h-2} \end{array} \right. \Rightarrow \left\{ \begin{array}{c} d_{TX} = \frac{840}{41} \approx 20.49 \text{ m} \\ h = \frac{1202}{41} \approx 29.32 \text{ m} \end{array} \right. \tag{4.61}$$

Note that the middle screen does not affect the result.

(a) $f = 900$ MHz implies $\lambda = 1/3$ m. Eq. (B-4.29) and (B-4.30) give the diffraction angle and Fresnel

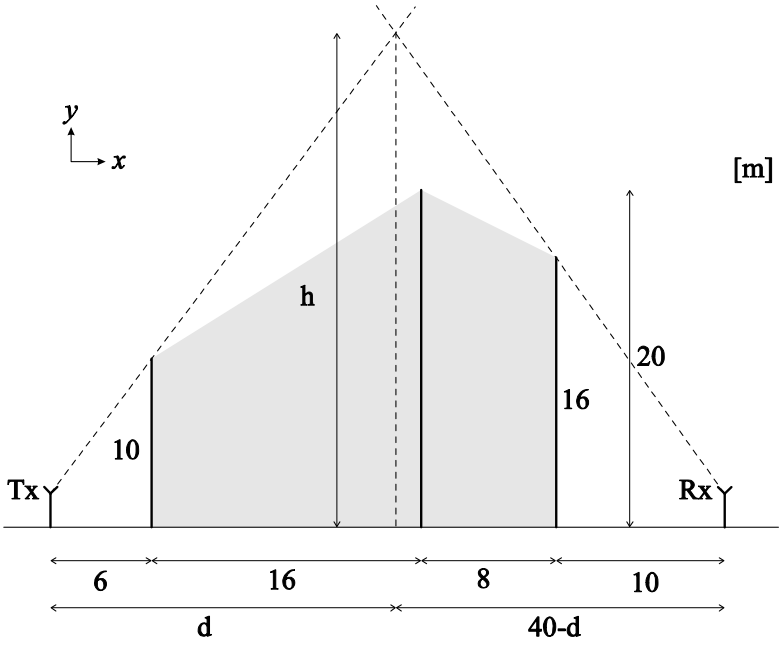

Figure 4.6: Redrawn geometry for Problem 10.

parameter for this equivalent screen as

$$\begin{aligned} \theta_d &= \arctan\left(\frac{h-h_{TX}}{d_{TX}}\right)+\arctan\left(\frac{h-h_{RX}}{d_{RX}}\right)= \\ &= \arctan\left(\frac{29.32-2}{20.49}\right)+\arctan\left(\frac{29.32-2}{40-20.49}\right)= 1.88 \text{ rad} \end{aligned} \tag{4.62}$$

$$\nu_F = \theta_d\sqrt{\frac{2d_{TX}d_{RX}}{\lambda\left(d_{TX}+d_{RX}\right)}} = 1.88\sqrt{\frac{2\cdot 20.49\cdot(40-20.49)}{1/3\cdot 40}} = 14.54 \tag{4.63}$$

The total field is given by

$$E_{total} = E_0\left(\frac{1}{2}-\frac{\exp\left(j\pi/4\right)}{\sqrt{2}}F\left(14.54\right)\right) \tag{4.64}$$

where a numerical evaluation of the Fresnel integral yields

$$F\left(14.54\right) = \int_0^{14.54}\exp\left(-j\pi\frac{t^2}{2}\right)dt \approx 0.483-j0.486 \tag{4.65}$$

Hence the magnitude of the total received field is given by

$$\begin{aligned} \frac{|E_{total}|}{|E_0|} &= \left|\frac{1}{2}-\frac{\exp\left(j\pi/4\right)}{\sqrt{2}}\left(0.483-j0.486\right)\right| = \\ &= |0.0154+j0.0012| = 0.0155 \end{aligned} \tag{4.66}$$

(b) For $f = 1800$ MHz, $\lambda = 1/6$ m. While the diffraction angle becomes the same as in (a), the Fresnel parameter and Fresnel integral now become

$$\nu_F = \theta_d\sqrt{\frac{2d_{TX}d_{RX}}{\lambda\left(d_{TX}+d_{RX}\right)}} = 1.88\sqrt{\frac{2\cdot 20.49\cdot(40-20.49)}{1/6\cdot 40}} = 20.56 \tag{4.67}$$

$$F(20.56) = \int_0^{20.56} \exp\left(-j\pi\frac{t^2}{2}\right) dt \approx 0.485 - j0.502 \tag{4.68}$$

Thus, the magnitude of the total received field is given by

$$\begin{aligned} \frac{|E_{total}|}{|E_0|} &= \left|\frac{1}{2} - \frac{\exp(j\pi/4)}{\sqrt{2}}(0.485 - j0.502)\right| = \\ &= |0.0065 + j0.0088| = 0.0109 \end{aligned} \tag{4.69}$$

(c) For $f = 2.4$ GHz, $\lambda = 0.125$ m. We have still the same diffraction angle as in (a), while the new Fresnel parameter and Fresnel integral become

$$\nu_F = \theta_d\sqrt{\frac{2d_{TX}d_{RX}}{\lambda(d_{TX}+d_{RX})}} = 1.88\sqrt{\frac{2\cdot 20.49\cdot(40-20.49)}{0.125\cdot 40}} = 23.75 \tag{4.70}$$

$$F(23.75) = \int_0^{23.75} \exp\left(-j\pi\frac{t^2}{2}\right) dt \approx 0.4973 - 0.4869i \tag{4.71}$$

Thus, the magnitude of the total received field is given by

$$\begin{aligned} \frac{|E_{total}|}{|E_0|} &= \left|\frac{1}{2} - \frac{\exp(j\pi/4)}{\sqrt{2}}(0.497 - j0.487)\right| = \\ &= |0.0079 - j0.0052| = 0.0095 \end{aligned} \tag{4.72}$$

Chapter 5

Statistical description of the wireless channel

1. Using the complex baseband notation:

$$\begin{aligned} E_1(t) &= 0.1\exp[-j2\pi\upsilon_{\max}\cos(\gamma_1)\,t] \\ E_2(t) &= 0.2\exp[-j2\pi\upsilon_{\max}\cos(\gamma_2)\,t] \end{aligned} \tag{5.1}$$

The squared amplitude of the total field at time t is given by

$$P(t) = \left|\sum_{i=1}^{2} E_i(t)\right|^2 \tag{5.2}$$

The power per unit area is given by

$$S(t) = \frac{P(t)}{Z}\ W\cdot m^{-2} \tag{5.3}$$

$t = 0$

$$\begin{aligned} E_1(0) &= 0.1\exp(0) = 0.1 \\ E_2(0) &= 0.2\exp(0) = 0.2 \end{aligned} \tag{5.4}$$

$$P(0) = |E_1(0) + E_2(0)|^2 = 0.1^2 + 0.2^2 = .05 \tag{5.5}$$

The power per unit area is

$$S(0) = \frac{P(0)}{377}\ W\cdot m^{-2} \tag{5.6}$$

$t = 0.1$
The two multipath components experience a phase-change of equal magnitude but reverse direction due to their respective propagation directions relative to the receiver.

$$\begin{aligned} E_1(0.1) &= 0.1\exp\left[-j2\pi\frac{\mathrm{v}}{\lambda}\cos(\pi)\cdot 0.1\right] \\ &= 0.1\exp[104.7j] = 0.1\exp[4.17j] \\ &= -0.052 - j0.086 \\ E_2(0.1) &= 0.2\cos\left[-j2\pi\frac{\mathrm{v}}{\lambda}\cos(0)\cdot 0.1\right] \\ &= 0.2\cos[-104.7j] = 0.2\exp[-4.17j] \\ &= -0.103 + j0.171 \end{aligned} \tag{5.7}$$

$$P(0.1) = |-0.052 - j0.086 - 0.103 + j0.171|^2 = 0.03 \tag{5.8}$$

The power per unit area is

$$S(0.1) = \frac{P(0.1)}{377} W\cdot m^{-2} \tag{5.9}$$

$t = 0.2$

$$\begin{aligned} E_1(0.2) &= 0.1\cos\left[-j2\pi\frac{\mathrm{v}}{\lambda}\cos(\pi)\cdot 0.2\right] \\ &= 0.1\exp[209.4j] = 0.1\exp[2.0549j] \\ &= -0.047 + j0.086 \\ E_2(0.2) &= 0.2\cos\left[-2\pi\frac{\mathrm{v}}{\lambda}\cos(0)\cdot 0.2\right] \\ &= 0.2\exp[-j209.4] = 0.2\exp[-j2.0549] \\ &= -0.093 - j0.177 \end{aligned} \tag{5.10}$$

$$P(0.2) = |-0.047 + j0.086 - 0.093 - j0.177|^2 = 0.028 \tag{5.11}$$

The power per unit area is

$$S(0.2) = \frac{P(0.2)}{377}\ W\cdot m^{-2}$$

The small-scale averaged power per unit area is determined as

$$S_{\text{small scale avg}} = \frac{P(0) + P(0.1) + P(0.2)}{377\cdot 3} = \frac{.05 + .03 + .028}{377\cdot 3} = 95.5\text{x}10^{-6}\ W\cdot m^{-2}$$

2. The pdf of the Rice distributed amplitude r is given as

$$pdf_r(r) = \frac{r}{\sigma^2}\cdot\exp\left[-\frac{r^2+A^2}{2\sigma^2}\right]\cdot I_0\left(\frac{rA}{\sigma^2}\right) \qquad 0 \le r < \infty \tag{5.12}$$

$I_0(x)$ is the modified Bessel function of the first kind, zero order. For $K_\mathrm{r} >> 1$, we can use the approximation for a large argument of the modified Bessel function, *i.e.*,

$$I_0(x) \approx \frac{1}{\sqrt{2\pi x}}\exp[x] \qquad x >> 1. \tag{5.13}$$

For $K_\mathrm{r} = \frac{A^2}{2\sigma^2} >> 1$, the pdf can be written as

$$\begin{aligned} pdf_r(r) &= \frac{r}{\sigma^2}\cdot\exp\left[-\frac{r^2+A^2}{2\sigma^2}\right]\cdot\frac{1}{\sqrt{2\pi\left(\frac{rA}{\sigma^2}\right)}}\exp\left[\frac{rA}{\sigma^2}\right] \\ &= \frac{1}{\sqrt{2\pi\left(\frac{rA}{\sigma^2}\right)}}\cdot\frac{r}{\sigma^2}\cdot\exp\left[-\frac{r^2+A^2}{2\sigma^2}+\frac{rA}{\sigma^2}\right] \\ &= \frac{1}{\sqrt{2\pi\sigma^2}}\cdot\frac{r}{\sqrt{rA}}\cdot\exp\left[-\frac{r^2+A^2-2rA}{2\sigma^2}\right]. \end{aligned} \tag{5.14}$$

For large K_r, we can approximate $\frac{r}{\sqrt{rA}} \approx 1$, giving

$$pdf_r(r) = \frac{1}{\sqrt{2\pi\sigma^2}}\exp\left[-\frac{(r-A)^2}{2\sigma^2}\right] \tag{5.15}$$

which is the pdf of $r \sim N\left(A, \sigma^2\right)$.

3. Since the receiver experiences both small- and large-scale fading, a conservative estimate of the fading margin (M) is obtained as

$$M_{dB} = M_{\text{Rayleigh}_{dB}} + M_{\text{large-scale}_{dB}}. \tag{5.16}$$

For small scale Rayleigh fading,

$$P_{\text{out}} = \Pr\{r < r_{\min}\} = 1 - \exp\left[-\frac{r_{\min}^2}{2\sigma^2}\right], \tag{5.17}$$

where $2\sigma^2$ is the small scale mean received power. Since the fading margin for an arbitrary threshold $r_{\min}$ is specified as $M_{\text{Rayleigh}} = \frac{2\sigma^2}{r_{\min}^2}$, and the system must not drop below 10% of the specified level,

$$\begin{aligned} P_{\text{out}} &= 1 - \exp\left[-\frac{1}{M_{\text{Rayleigh}}}\right] \\ M_{\text{Rayleigh}} &= -\frac{1}{\ln(1-P_{\text{out}})} = -\frac{1}{\ln(1-0.1)} = 9.49 \\ M_{\text{Rayleigh}_{dB}} &= 10 \cdot \log_{10}(M_{\text{Rayleigh}}) = 9.77 \text{ dB} \end{aligned} \tag{5.18}$$

For large-scale (log-normal) fading,

$$\begin{aligned} P_{\text{out}} &= \Pr\{r < r_{\min}\} = \Pr\{L_{\text{mean}_{dB}} + L_{dB} > L_{\max_{dB}}\} \\ &= \Pr\left\{\frac{L_{dB}}{\sigma_F} > \frac{L_{\max_{dB}} - L_{\text{mean}_{dB}}}{\sigma_F}\right\} \end{aligned} \tag{5.19}$$

where $L_{\text{mean}_{dB}}$ is the large-scale-averaged mean path loss at the cell boundary, L_{dB} is the normally distributed random path loss component, and $L_{\max_{dB}}$ is the maximum allowed path loss corresponding to $r_{\min}$. Substitute $M_{\text{large-scale}_{dB}} = L_{\max_{dB}} - L_{\text{mean}_{dB}}$, and note that the random variable $X = \frac{L_{dB}}{\sigma_F}$ has a normal distribution with zero mean and unit variance. Thus, the outage probability can be obtained as the tail probability of the normal distribution,

$$\begin{aligned} P_{\text{out}} &= \Pr\left\{\frac{L_{dB}}{\sigma_F} > \frac{M_{\text{large-scale}_{dB}}}{\sigma_F}\right\} \\ &= \int_{\frac{M_{\text{large-scale}_{dB}}}{\sigma_F}}^{\infty} pdf(x)dx \\ &= Q\left(\frac{M_{\text{large-scale}_{dB}}}{\sigma_F}\right) \\ 0.1 &= Q\left(\frac{M_{\text{large-scale}_{dB}}}{6}\right) \\ M_{\text{large-scale}_{dB}} &= 6 \cdot Q^{-1}(0.1) = 7.69 \text{ dB} \end{aligned} \tag{5.20}$$

as we required that an outage should not occur more than 10% of the time. The required fading margin, taking into account both the small and large scale fading is

$$M_{dB} = 9.77 + 7.69 = 17.5 \text{ dB} \tag{5.21}$$

4. We assume that only the mobile moves (in a stationary environment), and that the maximal Doppler spread is twice the maximal Doppler shift, i.e., $S_{\max} = 2\upsilon_{\max}$. We are to design a system communicating at both 900 MHz and 1800 MHz. For the Doppler shift we have the relation,

$$\upsilon = -\frac{\nu}{\lambda}\cos\gamma, \tag{5.22}$$

where

$$\begin{aligned} \upsilon &= \text{Doppler shift of the received carrier signal in Hz,} \\ \nu &= \text{velocity of mobile receiver in m/s,} \\ \lambda &= \text{wavelength of carrier signal in m,} \\ \gamma &= \text{angle between direction of arrival of signal and direction of motion.} \end{aligned}$$

As can be seen in Eq. (5.22), the Doppler shift can be both positive and negative depending on the angle of incidence of the received signal at the mobile receiver. The maximal amount of Doppler shift (positive or negative) occurs for $\gamma = k\pi$, where $k = 0, 1, 2, \ldots$. Thus,

$$\upsilon_{\max} = \max_{\gamma} |\upsilon| = \frac{\text{v}}{\lambda}. \tag{5.23}$$

(a) To calculate the maximal Doppler spread when communicating at a mobile speed of 200 km/h, we convert the speed to m/s as

$$\mathrm{v} = \frac{200 \cdot 10^3}{3600} = 55.6 \text{ m/s},$$

and use $c_0 = \lambda f_c$ to obtain the maximal Doppler shift as

$$\nu_{\max,900} = \frac{\mathrm{v}}{\lambda} = \frac{55.6 \cdot 900 \cdot 10^6}{3 \cdot 10^8} = 167 \text{ Hz} \tag{5.24}$$

for the 900 MHz case and

$$\nu_{\max,1800} = \frac{55.6 \cdot 1800 \cdot 10^6}{3 \cdot 10^8} = 334 \text{ Hz} \tag{5.25}$$

in the 1800 MHz case, which means that

$$S_{\max} = 2\nu_{\max} = 2\nu_{\max,1800} = 668 \text{ Hz}. \tag{5.26}$$

(b) If the system is designed for communication at 900 MHz and 200 km/h the maximal Doppler spread is

$$S_{\max} = 2\nu_{\max,900} = 334 \text{ Hz}, \tag{5.27}$$

and if the system is used at 1800 MHz instead of 900 MHz, the maximal mobile speed is

$$\nu_{\max} = \lambda\nu_{\max} = \frac{\lambda S_{\max}}{2} = \frac{3 \cdot 10^8 \cdot 334}{1800 \cdot 10^6 \cdot 2} = 27.8 \text{ m/s} = 100 \text{ km/h}.. \tag{5.28}$$

5. (a) We have a mean propagation loss of $L_0 = 127$ dB, and a log-normally distributed large-scale fading about that mean with a standard deviation of $\sigma_F = 7$ dB. The wireless system does not work properly when the propagation loss is larger than $L_{\max} = 135$ dB, and we want to determine how often this happens (outage probability), i.e., the probability of a log-normal component, L, larger than $M = L_{\max} - L_0 = 135 - 127 = 8$ dB. Expressed in statistical terms, the outage probability is given by

$$\begin{aligned} P_{\text{out}} &= \Pr\{L_0 + L > L_{\max}\} \\ &= \Pr\{\frac{L}{\sigma_F} > \frac{M}{\sigma_F}\} \\ &= \int_{\frac{M}{\sigma_F}}^{\infty} \frac{1}{\sqrt{2\pi}} e^{-\frac{1}{2}y^2} dy \\ &= \int_{\frac{8}{7}}^{\infty} \frac{1}{\sqrt{2\pi}} e^{-\frac{1}{2}y^2} dy, \end{aligned} \tag{5.29}$$

which is the tail probability from $\frac{8}{7}$ to infinity of a standard Gaussian distribution. Thus,

$$P_{\text{out}} = Q\left(\frac{8}{7}\right) = 0.127. \tag{5.30}$$

(b) i. Yes, increasing the transmit power will increase the average received power. The probability of receiving a power level below the sensitivity level decreases and therefore so does the outage probability. However, it might not be a possible solution due to spectrum regulations. Further, increased power may lead to unacceptable interference in the system.

ii. No, assuming that we want to communicate over a certain distance the only way to reduce the deterministic path loss is to change the environment (removing obstacles such as houses and hills), which is in most cases not an option.

iii. Yes, increasing the gain of the antennas will increase the average received power and decrease the outage probability. However, increasing the antenna gain will also increase the directivity so be sure to point the antennas in the right directions. Spectrum regulations often give the transmit power in EIRP, and increasing the antenna gain leads to increased EIRP.

iv. No, the σ_F is determined by the environment and cannot be changed.

v. Yes, a better receiver can tolerate a weaker received signal and therefore the outage probability can be decreased. However, a better receiver may be more complex and expensive, and may also use more power.

6. The Rayleigh CDF is

$$cdf(r_{\min}) = 1 - e^{-\frac{r_{\min}^2}{2\sigma^2}}, \tag{5.31}$$

where $2\sigma^2$ is the mean-square value of r, and $\sqrt{2}\sigma = r_{\text{rms}}$ is the root-mean-square (rms) value. The sensitivity level of the receiver is $r_{\min}$ and the outage probability is $P_{\text{out}} = \Pr\{r \leq r_{\min}\} = cdf(r_{\min})$.

(a) The amplitude, r, and the power, C, of the received signal are related as $C = K \cdot r^2$. With the instantaneous received power, C, the receiver sensitivity level (minimum received power for the system to work properly), $C_{\min}$, and the average received power, $\bar{C}$, we have

$$C_{\min} = K \cdot r_{\min}^2, \tag{5.32}$$

and

$$\bar{C} = K\overline{r^2} = \left[\overline{r^2} = r_{\text{rms}}^2 = 2\sigma^2\right] = K \cdot 2\sigma^2. \tag{5.33}$$

The outage probability is

$$P_{\text{out}} = 1 - e^{-\frac{r_{\min}^2}{2\sigma^2}}, \tag{5.34}$$

and by an expansion of K in the exponent, we have

$$P_{\text{out}} = 1 - e^{-\frac{r_{\min}^2}{2\sigma^2}} = 1 - e^{-\frac{Kr_{\min}^2}{K2\sigma^2}} = 1 - e^{-\frac{C_{\min}}{\bar{C}}}. \tag{5.35}$$

(b) The fading margin is defined as

$$M = \frac{\bar{C}}{C_{\min}}, \tag{5.36}$$

which means that

$$P_{\text{out}} = 1 - e^{-\frac{C_{\min}}{\bar{C}}} = 1 - e^{-\frac{1}{M}}. \tag{5.37}$$

Using this relation between outage probability and fading margin, we have

$$\begin{aligned} -\frac{1}{M} &= \ln(1 - P_{\text{out}}) \\ M &= -\frac{1}{\ln(1 - P_{\text{out}})}, \end{aligned} \tag{5.38}$$

and thus

$$M_{\text{dB}} = -10\log_{10}\left(-\ln(1 - P_{\text{out}})\right). \tag{5.39}$$

7. First, recall that

$$P_{\text{out}} = 1 - e^{-\frac{C_{\min}}{\bar{C}}} = 1 - e^{-\frac{1}{M}}, \tag{5.40}$$

where P_{out} is the outage probability and M is the fading margin. By using Taylor series expansion about $x = 1/M$, we have

$$P_{\text{out}} = 1 - e^{-x} \approx \left[e^{-x} = 1 - \frac{x}{1!} + \frac{x^2}{2!} + ... \Rightarrow 1 - e^{-x} \approx 1 - x\right] \approx x, \tag{5.41}$$

and thus, for small $x = 1/M$

$$P_{\text{out}} \approx \frac{1}{M} \tag{5.42}$$

and

$$M \approx \frac{1}{P_{\text{out}}}. \tag{5.43}$$

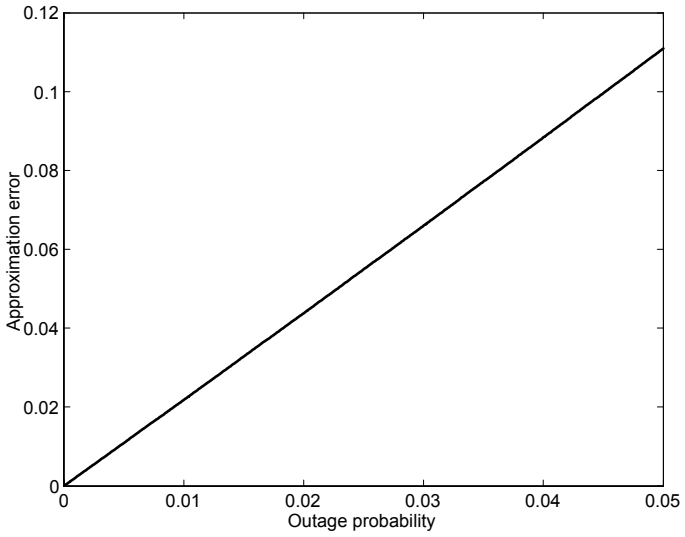

Figure 5.1: Approximation error ε as a function of P_{out}.

(a) If we use the approximation, we have

$$P_{\text{out}} = \Pr\{r \leq r_{\min}\} \approx \frac{r_{\min}^2}{2\sigma^2} = \frac{C_{\min}}{\overline{C}} = \frac{1}{M}, \tag{5.44}$$

and by denoting the approximate fading margin in dB by $\widetilde{M}_{\text{dB}}$, we get

$$\widetilde{M}_{\text{dB}} = -10\log_{10}(P_{\text{out}}). \tag{5.45}$$

(b) The error (in dB) when using the approximation is

$$\varepsilon = \widetilde{M}_{\text{dB}} - M_{\text{dB}}, \tag{5.46}$$

where M_{dB} is the exact expression from Exercise 6b and $\widetilde{M}_{\text{dB}}$ is the approximative expression from Exercise 7a. Using the derived expressions we have

$$\begin{aligned} \varepsilon &= -10\log_{10}(P_{\text{out}}) + 10\log_{10}(-\ln(1-P_{\text{out}})) \\ &= 10\log_{10}\left(-\frac{\ln(1-P_{\text{out}})}{P_{\text{out}}}\right), \end{aligned} \tag{5.47}$$

which is shown in Figure 5.1 for P_{out} between 0 and 0.05. It can be seen that the error increases with P_{out}. For $P_{\text{out}} = 0.05$ we have the maximum error in the specified range of P_{out}, $\varepsilon_{0.05} = \widetilde{M}_{\text{dB}} - M_{\text{dB}} = 0.11$ dB, which is not a large error in most situations of radio communication.

8. We have a small-scale fading described by the Rayleigh distribution, for which $\overline{r^2} = r_{\text{rms}}^2 = 2\sigma^2$ and $r_{50} = 1.18\sigma$.

(a) The Rayleigh *cdf* is given by

$$cdf(r) = 1 - e^{-\frac{r^2}{r_{\text{rms}}^2}}. \tag{5.48}$$

To express this *cdf* in terms of r_{50} instead of r_{rms} we use

$$r_{\text{rms}}^2 = 2\sigma^2 \tag{5.49}$$

and

$$\sigma = \frac{r_{50}}{1.18} \tag{5.50}$$

to obtain

$$r_{\text{rms}}^2 = 2\left(\frac{r_{50}}{1.18}\right)^2 = 1.44 r_{50}^2, \tag{5.51}$$

Inserting this into the Rayleigh *cdf* gives

$$cdf(r) = 1 - e^{-\frac{r^2}{1.44 r_{50}^2}}. \tag{5.52}$$

(b) The outage probability is given by the Rayleigh cdf

$$P_{\text{out}} = \Pr\left(r \le r_{\min}\right) = cdf(r_{\min}) = 1 - e^{-\frac{r_{\min}^2}{r_{\text{rms}}^2}} \tag{5.53}$$

using r_{rms}^2, and

$$P_{\text{out}} = 1 - e^{-\frac{r_{\min}^2}{1.44 r_{50}^2}} \tag{5.54}$$

using r_{50}^2. First, expressing the fading margin M_{mean} relative rms value, we have from a previous exercise

$$M_{\text{mean}} = \frac{r_{\text{rms}}^2}{r_{\min}^2}. \tag{5.55}$$

Then, using Eq. (5.53),

$$\begin{aligned} -\frac{r_{\min}^2}{r_{\text{rms}}^2} &= \ln(1 - P_{\text{out}}) \qquad (5.56)\\ \frac{1}{M_{\text{mean}}} &= -\ln(1 - P_{\text{out}}), \end{aligned}$$

which results in

$$M_{\text{mean}|\text{dB}} = -10\log_{10}\left(\ln\left(\frac{1}{1 - P_{\text{out}}}\right)\right). \tag{5.57}$$

Next, expressing the fading margin M_{median} relative median-value, we have

$$M_{\text{median}} = \frac{r_{50}^2}{r_{\min}^2}. \tag{5.58}$$

Using this in Eq. (5.54),

$$\begin{aligned} -\frac{r_{\min}^2}{1.44 r_{50}^2} &= \ln(1 - P_{\text{out}}) \qquad (5.59)\\ \frac{1}{M_{\text{median}}} &= -1.44\ln(1 - P_{\text{out}}), \end{aligned}$$

which results in

$$M_{\text{median}|\text{dB}} = -1.58\text{ dB} - 10\log_{10}\left(\ln\left(\frac{1}{1 - P_{\text{out}}}\right)\right). \tag{5.60}$$

(c) Comparing the two fading margins in Eqs. (5.57) and Eq. (5.60), it can be seen that they differ only by an additive constant (in dB) of 1.58 dB, as

$$M_{\text{mean}|\text{dB}} = M_{\text{median}|\text{dB}} + 1.58\text{ dB}. \tag{5.61}$$

It is also possible to arrive at that solution by simply observing that the ratio of the mean value to the median value is $\sqrt{2}/1.18$, which translates to 1.58 dB. Since the mean value is larger than the median value, the fading margin (referring to the mean value) has to be larger by those 1.58 dB than the fading margin (referring to the median value).

9. We have for $r_{\min}$ the level crossing rate (fading dips per second)

$$N_r\left(r_{\min}\right) = \sqrt{\frac{\Omega_2}{\pi\Omega_0}}\frac{r_{\min}}{\sqrt{2\Omega_0}}e^{-\frac{r_{\min}^2}{2\Omega_0}}, \tag{5.62}$$

and the average fading dip duration

$$ADF\left(r_{\min}\right) = \frac{cdf(r_{\min})}{N_r\left(r_{\min}\right)}, \tag{5.63}$$

where $\sqrt{2\Omega_0}$ is the rms-value of the signal amplitude over a local area. The parameter $\Omega_2 = \frac{1}{2}\Omega_0\left(2\pi\upsilon_{\max}\right)^2$, where $\upsilon_{\max}$ is the maximum Doppler frequency, is the second moment of the Doppler spectrum. We start by expressing $N_r\left(r_{\min}\right)$ in terms of $M = r_{\rm rms}^2/r_{\min}^2$ instead of Ω_0 and Ω_2. Since

$$\sqrt{2\Omega_0} = r_{\rm rms} \tag{5.64}$$

we obtain

$$\begin{aligned} \Omega_0 &= \frac{r_{\rm rms}^2}{2} = \frac{M}{2}r_{\min}^2 \\ M &= \frac{2\Omega_0}{r_{\min}^2} \end{aligned} \tag{5.65}$$

substituting Ω_2, Ω_0 into Eq. (5.62),

$$\begin{aligned} N_r\left(r_{\min}\right) &= \sqrt{\frac{\frac{1}{2}\Omega_0\left(2\pi\upsilon_{\max}\right)^2}{\pi\Omega_0}}\frac{r_{\min}}{\sqrt{2\Omega_0}}e^{-\frac{r_{\min}^2}{2\Omega_0}} \\ &= \sqrt{2\pi}\upsilon_{\max}\frac{1}{\sqrt{M}}e^{-\frac{1}{M}}. \end{aligned} \tag{5.66}$$

The expression for the average fade duration is rewritten as

$$\begin{aligned} ADF\left(r_{\min}\right) &= \frac{cdf(r_{\min})}{N_r\left(r_{\min}\right)} \\ &= \frac{1-e^{-\frac{r_{\min}^2}{r_{\rm rms}^2}}}{\sqrt{2\pi}\upsilon_{\max}\frac{1}{\sqrt{M}}e^{-\frac{1}{M}}} \\ &= \sqrt{\frac{M}{2\pi}}\frac{1}{\upsilon_{\max}}e^{\frac{1}{M}} - \sqrt{\frac{M}{2\pi}}\frac{1}{\upsilon_{\max}} \\ &= \sqrt{\frac{M}{2\pi}}\frac{1}{\upsilon_{\max}}\left(e^{\frac{1}{M}}-1\right). \end{aligned} \tag{5.67}$$

10. (a) We start by calculating the ground plane path loss

$$L_{\rm ground|dB} = 20\log_{10}\left(\frac{5000^2}{20\cdot 1.5}\right) = 118.4 \text{ dB} \tag{5.68}$$

and the additional loss from Egli's model

$$\Delta L_{|\rm dB} = 10\log_{10}\left(\frac{450^2}{1600}\right) = 21 \text{ dB}, \tag{5.69}$$

which results in a total median path loss of $L_{0|\rm dB} = 118.4 + 21 = 139.4$ dB. The link budget diagram is shown in Figure 5.2.

(b) The system is considered operational if the instantaneous received power is not below $C_{\min|\rm dB}$ more than 5% of the time. This corresponds to a maximum outage probability of $P_{\rm out} = 0.05$.

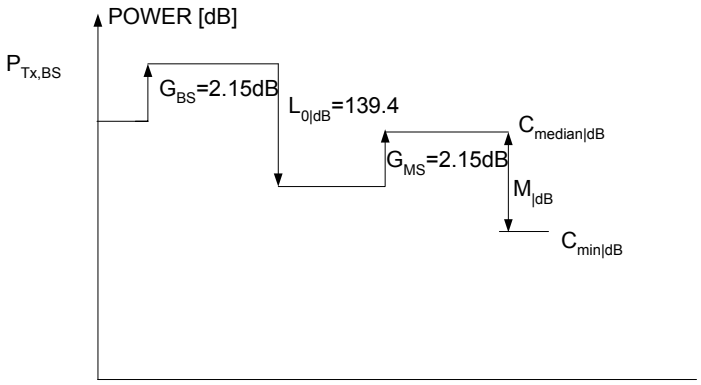

Figure 5.2: Link Budget.

The required small-scale fading margin is given by (since the propagation path loss model gives a median loss)

$$M_{\text{median|dB}} = M_{\text{mean|dB}} - 1.58 \text{ dB} \tag{5.70}$$

where

$$\begin{aligned} M_{\text{mean|dB}} &= -10 \log_{10} \left(\ln \left(\frac{1}{1 - P_{\text{out}}} \right) \right) \\ &= -10 \log_{10} \left(\ln \left(\frac{1}{1 - 0.05} \right) \right) \\ &= 12.9 \text{ dB}. \end{aligned} \tag{5.71}$$

Thus, the required small-scale margin is $M_{\text{median|dB}} = 12.9 - 1.58 = 11.3$ dB.

(c) For 95% boundary coverage, the system can have a maximum outage probability of $P_{\text{out}} = 0.05$ due to the large-scale fading at the maximum distance $d_{\max}$. Since the large-scale fading is log-normally distributed with $\sigma_F = 5$ dB, the outage probability due to large-scale fading is given by (the tail probability of the normal distribution in dB)

$$P_{\text{out}} = Q \left(\frac{M_{F|\text{dB}}}{\sigma_F} \right). \tag{5.72}$$

Thus,

$$\begin{aligned} \frac{M_{F|\text{dB}}}{\sigma_F} &= Q^{-1} \left(P_{\text{out}} \right) \\ M_{F|\text{dB}} &= \sigma_F \cdot Q^{-1} \left(P_{\text{out}} \right), \end{aligned} \tag{5.73}$$

which results in a large-scale fading margin of $M_{F|\text{dB}} = 5 \text{ dB} \cdot 1.64 = 8.2$ dB.

(d) The total fading margin obtained by adding the margins for small-scale and large-scale fading is

$$\begin{aligned} M_{|\text{dB}} &= M_{\text{median|dB}} + M_{F|\text{dB}} \\ &= 11.3 \text{ dB} + 8.2 \text{ dB} \\ &= 19.5 \text{ dB}. \end{aligned} \tag{5.74}$$

Note that the small-scale fading margin has been given relative to the median path loss, since the propagation path loss model gives a median loss. The total transmit power required is

$$\begin{aligned} P_{\text{TX|dB}} &= C_{\text{min|dB}} - G_{\text{BS}} + L_{0|\text{dB}} - G_{\text{MS}} + M_{|\text{dB}} \\ &= -122 - 2.15 + 139.4 - 2.15 + 19.5 \\ &= 32.6 \text{ dBm}. \end{aligned} \tag{5.75}$$

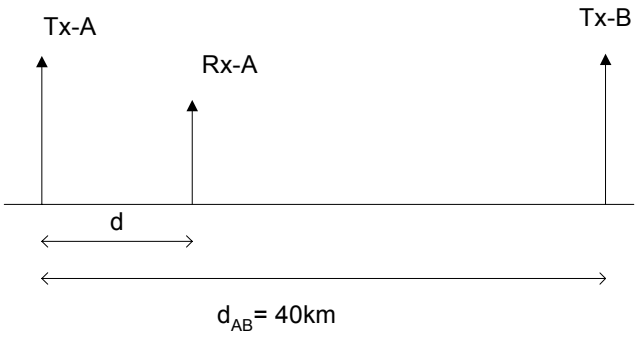

Figure 5.3: Scenario: Tx-B interferes with the reception of Rx-A.

11. The scenario is shown in Fig. 5.3.

(a) Since both the useful and the interfering signals are independent and log-normally distributed we can calculate the corresponding standard deviation of the received $(C/I)_{|\mathrm{dB}}$ as

$$\sigma_{F,\mathrm{tot}} = \sqrt{\sigma_{F,\mathrm{A}}^2 + \sigma_{F,\mathrm{B}}^2} = 9\sqrt{2} = 12.7 \text{ dB}. \tag{5.76}$$

The received $(C/I)_{|\mathrm{dB}}$ is required to stay above $(C/I)_{\mathrm{min}|\mathrm{dB}}$ with a probability of 0.99, i.e., a maximum outage probability P_{out} of 0.01. We have

$$P_{\mathrm{out}} = Q\left(\frac{M_{|\mathrm{dB}}}{\sigma_{F,\mathrm{tot}}}\right) \tag{5.77}$$

which results in

$$\begin{aligned} M_{|\mathrm{dB}} &= \sigma_{F,\mathrm{tot}} \cdot Q^{-1}\left(P_{\mathrm{out}}\right) \\ &= 12.7 \cdot 2.33 \\ &= 29.6 \text{ dB}. \end{aligned} \tag{5.78}$$

(b) With the specified propagation exponent we can calculate the deterministic path loss as a function of distance as

$$L_{0|\mathrm{dB}}(d) = L_{0|\mathrm{dB}}(1) + \eta \cdot 10\log_{10}(d)\,. \tag{5.79}$$

The mean received useful power at Rx-A, at a distance d from Tx-A is

$$C_{\mathrm{A}|\mathrm{dB}} = P_{\text{Tx-A}|\mathrm{dB}} + G_{\text{Tx-A}} - L_{0|\mathrm{dB}}(d) + G_{\text{Rx-A}}\,. \tag{5.80}$$

The mean received interfering power from Tx-B is

$$I_{\mathrm{A}|\mathrm{dB}} = P_{\text{Tx-B}|\mathrm{dB}} + G_{\text{Tx-B}} - L_{0|\mathrm{dB}}(d_{\mathrm{AB}} - d) + G_{\text{Rx-A}}\,. \tag{5.81}$$

Since Tx-A and Tx-B use the same transmit power and the same type of antennas, $(C/I)_{|\mathrm{dB}}$ is calculated as

$$\begin{aligned} (C/I)_{|\mathrm{dB}} &= C_{\mathrm{A}|\mathrm{dB}} - I_{\mathrm{A}|\mathrm{dB}} \\ &= -L_{0|\mathrm{dB}}(d) + L_{0|\mathrm{dB}}(d_{\mathrm{AB}} - d) \\ &= -L_{0|\mathrm{dB}}(1) - 36\log_{10}(d) + L_{0|\mathrm{dB}}(1) + 36\log_{10}(d_{\mathrm{AB}} - d) \\ &= 36\log_{10}\left(\frac{d_{\mathrm{AB}} - d}{d}\right) \\ &= 36\log_{10}\left(\frac{d_{\mathrm{AB}}}{d} - 1\right). \end{aligned} \tag{5.82}$$

Since

$$(C/I)_{|\mathrm{dB}} = (C/I)_{\mathrm{min}|\mathrm{dB}} + M_{|\mathrm{dB}} \tag{5.83}$$

we obtain, with the specified value on $(C/I)_{\mathrm{min}|\mathrm{dB}}$, the maximum distance $d_{\max}$ from

$$\begin{aligned}
(C/I)_{\mathrm{min}|\mathrm{dB}} &= 36\log_{10}\left(\frac{d_{\mathrm{AB}}}{d_{\max}} - 1\right) - M_{|\mathrm{dB}} \qquad (5.84)\\
10^{\frac{(C/I)_{\mathrm{min}|\mathrm{dB}} + M_{|\mathrm{dB}}}{36}} &= \frac{d_{\mathrm{AB}}}{d_{\max}} - 1\\
d_{\max} &= \frac{d_{\mathrm{AB}}}{10^{\frac{(C/I)_{\mathrm{min}|\mathrm{dB}} + M_{|\mathrm{dB}}}{36}} + 1}\\
&= \frac{40 \cdot 10^3}{10^{(7+29.6)/36} + 1}\\
d_{\max} &= 3.51 \text{ km.}
\end{aligned}$$

(c) If the separation distance d_{AB} between Tx-A and Tx-B is reduced from 40 km to 20 km, $d_{\max}$ will also be reduced to half.

Chapter 6

Wideband and directional channel characterization

1. Both the spreading and scattering functions describe the channel's delay and Doppler characteristics. However, the respective underlying models for the channel are different. In the case of the spreading function, the channel is viewed as a *deterministic* function. In contrast, in deriving the scattering function we have assumed a *statistical* model for the channel.

2. This function can be useful mainly for two applications:

   (a) if one wishes to estimate the channel quality of the downlink based on the quality of the uplink, or vice versa. This applies to both time division multiplex and frequency division multiplex systems since $R_H(\Delta t, \Delta f)$ depends on both the time and frequency separation. In general, it is desirable that the correlation between the channels in the uplink and the downlink is high, so that channel estimates from one can be used for the adaptive transmission in the other. More details about this aspect can also be found in Sec. 20.1

   (b) for the design of diversity systems: again, the information can be used for both temporal and frequency diversity. Details about diversity systems can be found in Chapter 13, but the basic principle is that the signal is transmitted on independent paths, so that there is a low probability that all signal paths are in a fading dip simultaneously. In this case, it is desirable that the correlation coefficient is as low as possible. The information about the required spacing in time or frequency can be found from $P_H(\Delta t, \Delta f)$.

3. Correcting for a misprint in the problem formulation, we write the power delay profile as

$$P(\tau) = \begin{cases} a_1 e^{-b_1 \tau} & 0 \le \tau \le 20\ \mu\text{s} \\ a_2 e^{-b_2\left[t - 55\cdot 10^{-6}\right]} & 55\ \mu\text{s} \le \tau \le 65\ \mu\text{s} \\ 0 & \text{elsewhere} \end{cases} \tag{6.1}$$

   (a) With

$$\begin{aligned} P(0) &= 10^{-13}\ \text{W} \\ P\left(2\cdot 10^{-5}\right) &= 10^{-17}\ \text{W} \\ P\left(55\cdot 10^{-6}\right) &= 10^{-15}\ \text{W} \\ P\left(65\cdot 10^{-6}\right) &= 10^{-17}\ \text{W} \end{aligned} \tag{6.2}$$

   we find that

$$\begin{aligned} a_1 &= 10^{-13} \\ b_1 &= 4.61\cdot 10^5 \\ b_2 &= 4.61\cdot 10^5 \\ a_2 &= 10^{-15}. \end{aligned} \tag{6.3}$$

The time-integrated power is

$$\begin{aligned} P_m &= \int_{-\infty}^{\infty} P(\tau)\, d\tau \\ &= 2.2 \cdot 10^{-19}. \end{aligned} \tag{6.4}$$

The average mean delay is

$$\begin{aligned} T_m &= \frac{\int_{-\infty}^{\infty} P(\tau)\, \tau d\tau}{P_m} \\ &= 2.9\ \mu s. \end{aligned} \tag{6.5}$$

The rms delay spread is

$$\begin{aligned} S &= \sqrt{\frac{\int_{-\infty}^{\infty} P(\tau)\, \tau^2 d\tau}{P_m} - T_m^2} \\ &= 6.5\ \mu s \end{aligned} \tag{6.6}$$

(b) Estimating the coherence bandwidth with $1/2\pi S$ yields $B_c \approx 25$ kHz, and the channel should thus be frequency-selective according to this approximation. The Fourier transform of $P(\tau)$ is

$$\begin{aligned} R_H(0, \Delta f) &= \int_{-\infty}^{\infty} P(\tau)\, e^{-j2\pi\Delta f \tau} d\tau \\ &= a_1 \frac{1 - e^{-(j2\pi\Delta f + b_1)t_1}}{j2\pi\Delta f + b_1} \\ &\quad + a_2 e^{b_2\tau_2} \frac{e^{-(j2\pi\Delta f + b_2)t_2} - e^{-(j2\pi\Delta f + b_2)t_3}}{j2\pi\Delta f + b_2}, \end{aligned} \tag{6.7}$$

where $t_1 = 20\ \mu$s, $t_2 = 55\ \mu$s, and $t_3 = 65\ \mu$s. The normalized magnitude of $R_H(0, \Delta f)$ is plotted below and we see that coherence bandwidth is approximately 125 kHz, which clearly does not agree with the estimate $1/2\pi S$. With a coherence bandwidth of 125 kHz, the channel is regarded as approximately frequency-flat.

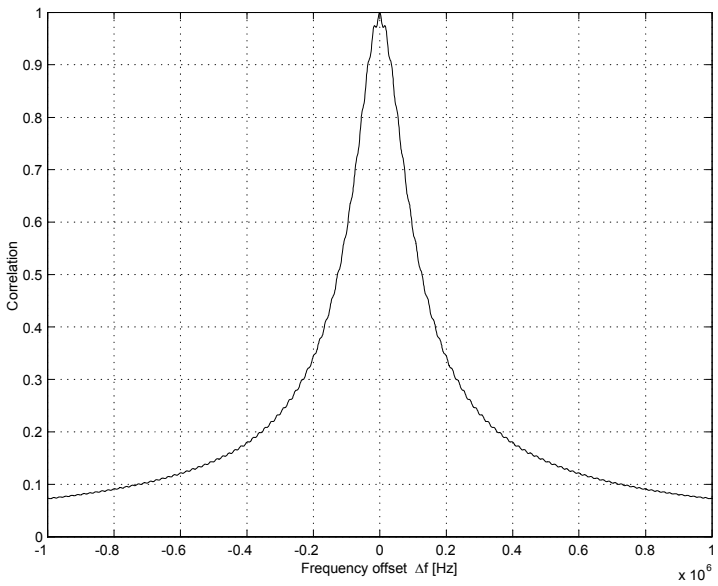

4. The interference quotient Q_{16} with $t_0 = 0$ is

$$\begin{aligned} Q_{16} &= \frac{\int_0^{16\cdot 10^{-6}} P(\tau)\, d\tau}{P_m - \int_0^{16\cdot 10^{-6}} P(\tau)\, d\tau} \\ &= \frac{\int_0^{16\cdot 10^{-6}} a_1 e^{-b_1\tau} d\tau}{\int_0^{65\cdot 10^{-6}} P(\tau)\, d\tau - \int_0^{16\cdot 10^{-6}} a_1 e^{-b_1\tau} d\tau} \\ &= 1.95 \cdot 10^{-3}. \end{aligned} \tag{6.8}$$

Let the PDP that is terminated after 20 μs be $P'(\tau)$, i.e.,

$$P'(\tau) = \begin{cases} a_1 e^{-b_1\tau}, & 0 \le \tau \le 20\ \mu\text{s} \\ 0, & \text{otherwise} \end{cases}, \tag{6.9}$$

and thus the time-integrated power is

$$\begin{aligned} P'_m &= \int_{-\infty}^{\infty} P'(\tau)\, d\tau \\ &= \int_0^{20\cdot 10^{-6}} a_1 e^{-b_1\tau} d\tau \\ &= 2.2 \cdot 10^{-19}. \end{aligned} \tag{6.10}$$

Then the interference quotient becomes

$$\begin{aligned} Q'_{16} &= \frac{\int_0^{16\cdot 10^{-6}} P'(\tau)\, d\tau}{P'_m - \int_0^{16\cdot 10^{-6}} P'(\tau)\, d\tau} \\ &= 1.89 \cdot 10^{3}. \end{aligned} \tag{6.11}$$

5. From Figure 6.7 we see that the range over which the spreading function has non-zero components is approximately symmertric, and extending from -10 Hz to 10 Hz. A rough estimate of the coherence time is given as

$$T_{\text{coh}} = \frac{1}{2\pi S_\nu} \tag{6.12}$$

and for a Jakes spectrum, the rms Doppler spread is $0.7\nu_{\max}$. Thus, the coherence time is therefore approximately 25 ms.

6. As outlined in the previous exercise,

$$T_{\text{coh}} = \frac{1}{2\pi 0.7\nu_{\max}} \tag{6.13}$$

$$\frac{1}{4.4 f_c \frac{\text{v}}{c_0}} > 4.6 \cdot 10^{-3}, \tag{6.14}$$

which gives that the maximum velocity is 16 m/s $\approx$ 60 km/h for $f_c = 900$ MHz and 7.4 m/s $\approx$ 26 km/h for $f_c = 2$ GHz.

7. As discussed in Sec. 6.1.2, we can segment the impulse response into delay bins, where the width of a delay bin is approximately the inverse of the bandwidth. Therefore the number of delay bins becomes the ratio between the excess delay and the chip duration. We obtain five delay bins in the case of 1.3 μs excess delay and one delay bin for 100 ns excess delay. The system can be considered wideband in the former case, but not in the latter.

Chapter 7

Channel models

1. Assume that the transmitted signal is reflected at several reflection points before arriving at the receiver. The attenuation and phase change of the reflected signal is assumed to be independent and random at each reflection point, hence the received signal is the transmitted signal multiplied with a number of complex random variables as
$$r = t \cdot X_1 \cdot X_2 \cdot \cdots \cdot X_L \tag{7.1}$$
the attenuation is
$$h = \frac{r}{t} = X_1 \cdot X_2 \cdot \cdots \cdot X_L \tag{7.2}$$
By taking the logarithm of h we have
$$h_{|\mathrm{dB}} = X_{1|\mathrm{dB}} + X_{2|\mathrm{dB}} + \cdots + X_{L|\mathrm{dB}} \tag{7.3}$$
From the Central Limit Theorem (sum of equally distributed random variables), $h_{|\mathrm{dB}}$ is Gaussian distributed. Hence the linear, h, is log-normal distributed. NOTE: A rule of thumb is that the sum should consist of at least 10 random variables, hence that requires 10 reflection points. After 10 reflections there is not much power left. For this reason, this process for the justification of a lognormal distribution is still under discussion in the literature.

2. We are considering propagation in a medium-sized city where we have got the following parameters.

Parameters	
h_b	$= 40$ m
h_m	$= 2$ m
f_c	$= 900$ MHz
d	$= 2$ km

   (a) By using Okumura's measurements, the total propagation loss can be written as the free-space path loss corrected by the 3 correction terms in the excess loss, A_exc: due to carrier frequency, correction due to BS height, H_cb, and correction due to MS height, H_cm. The resulting Okumura path-loss is:
$$L_\mathrm{Oku} = L_\mathrm{free} + A_\mathrm{exc} - H_\mathrm{cb} - H_\mathrm{cm}. \tag{7.4}$$
   The free-space attenuation between isotropic antennas is given by:
$$L_\mathrm{free} = 20\log_{10}\left(\frac{4\pi d}{\lambda}\right) = 20\log_{10}\left(\frac{4\pi df}{c}\right) = 97.5 \text{ dB}. \tag{7.5}$$
   The excess loss as taken from Fig. 7.12 in App. 7.A is:
$$A_\mathrm{exc} = 23.5 \text{ dB}, \tag{7.6}$$
   for the specified carrier frequency and BS-MS separation. Note that this value is only correct for a base station height of 200 m and a mobile station height of 3 m. For other antenna heights the

excess loss must be corrected using the correction factors of Figures 7.13 and 7.14. For the given BS height we get a correction factor of:

$$H_{\mathrm{cb}} = -10 \text{ dB}. \tag{7.7}$$

and for the MS height:

$$H_{\mathrm{cm}} = -2 \text{ dB}. \tag{7.8}$$

Finally,

$$L_{\mathrm{Oku}} = 97.5 + 23.5 - (-10) - (-2) = 133 \text{ dB}. \tag{7.9}$$

(b) Table 7.1 shows that f, h_{b}, h_{m}, and d are in the range of validity for the Okumura-Hata model. Hence, the total propagation loss can be written as:

$$L_{\text{O-H}} = A + B\log_{10}(d) + C, \tag{7.10}$$

where d is specified in km, and where,

$$A = 69.5 + 26.16\log_{10}(f) - 13.82\log_{10}(h_b) - a(h_m), \tag{7.11}$$

and

$$B = 44.9 - 6.55\log_{10}(h_b), \tag{7.12}$$

where f is specified in MHz and h_b and h_m are given in meters. Furthermore,

$$a(h_m) = (1.1\log_{10}(f) - 0.7)h_m - (1.56\log_{10}(f) - 0.8), \tag{7.13}$$

and

$$C = 0. \tag{7.14}$$

Thus,

$$a(h_m) = (1.1\log_{10}(900) - 0.7)2 - (1.56\log_{10}(900) - 0.8) = 1.3, \tag{7.15}$$

which results in

$$A = 69.55 + 26.16\log_{10}(900) - 13.82\log_{10}(40) - 1.3 = 123.4, \tag{7.16}$$

and

$$B = 44.9 - 6.55\log_{10}(40) = 34.4. \tag{7.17}$$

This leads to a total loss of

$$L_{\text{O-H}} = 123.4 + 34.4\log_{10}(2) + 0 = 133.7 \text{ dB}. \tag{7.18}$$

(c) The results from the two different path loss calculations agree within one dB, which is not a significant difference. That they agree well is not too surprising, since the latter calculation (Okumura-Hata) is based on a parameterization of the first (Okumura).

3. (a) The model validity is given by Table 7.2 where it can be seen that $800 < f_{\mathrm{c}} < 2000$ MHz, $4 < h_{\mathrm{b}} < 50$ m (both for $h_b = 19$ and 23 m), $1 < h_{\mathrm{m}} < 3$ m, and $0.02 < d < 5$ km. Consequently the model is valid.

(b) The base station antenna is located 3 m above the rooftops, i.e., $h_b = 23$ m. The total path loss of the COST 231-Walfish-Ikegami model is given by

$$L = L_0 + L_{\mathrm{rts}} + L_{\mathrm{msd}}, \tag{7.19}$$

where

$$\begin{aligned} L_0 &= 32.4 + 20\log_{10}(d) + 20\log_{10}(f_0) \\ &= 32.4 + 20\log_{10}(0.8) + 20\log_{10}(1800) = 95.56 \text{ dB}, \end{aligned} \tag{7.20}$$

is the free-space path loss (with d specified in km and f_0 in MHz). The rooftop-to-street diffraction and scatter loss is given by

$$L_{\text{rts}} = -16.9 - 10\log_{10}(w) + 10\log_{10}(f_0) + 20\log_{10}(\Delta h_m) + L_{\text{ori}}, \tag{7.21}$$

with w in meters and f_0 in MHz. Here,

$$\Delta h_m = h_{\text{Roof}} - h_m = 20 - 1.8 = 18.2, \tag{7.22}$$

and

$$L_{\text{ori}} = 4.0 + 0.114(\varphi - 55), \tag{7.23}$$

with φ in deg. for $55° \leq \varphi \leq 90°$. Hence,

$$L_{\text{ori}} = 4.0 + 0.114(90 - 55) = 7.99, \tag{7.24}$$

which results in

$$L_{\text{rts}} = -16.9 - 10 + 32.6 + 25.2 + 7.99 = 38.84 \text{ dB}. \tag{7.25}$$

The multiscreen loss is given by

$$L_{\text{msd}} = L_{\text{bsh}} + k_a + k_d\log_{10}(d) + k_f\log_{10}(f_0) - 9\log_{10}(b), \tag{7.26}$$

where d is specified in km, f_0 in MHz and b in meters. For base station heights $h_b > h_{\text{Roof}}$ we have:

$$\begin{aligned} L_{\text{bsh}} &= -18\log_{10}(1 + \Delta h_b) \\ &= -18\log_{10}(1 + h_b - h_{\text{Roof}}) \\ &= -18\log_{10}(1 + 3) = -10.8. \end{aligned} \tag{7.27}$$

and

$$\begin{aligned} k_a &= 54, \\ k_d &= 18, \end{aligned} \tag{7.28}$$

For a medium-sized city, we have

$$k_f = -4 + 0.7\left(\frac{f_0}{925} - 1\right) = -3.34 \tag{7.29}$$

where f_0 is specified in MHz. Consequently,

$$\begin{aligned} L_{\text{msd}} &= -10.8 + 54 + 18\log_{10}(0.8) + (-3.34)\log_{10}(1800) - 9\log_{10}(30) \\ &= 17.26 \text{ dB}, \end{aligned} \tag{7.30}$$

which results in a total loss

$$L = 95.6 + 38.9 + 17.3 = 151.7 \text{ dB}. \tag{7.31}$$

(c) Here the base station antenna is located 1 m below the rooftops, i.e., $h_b = 19$ m. Since only h_b has changed, L_0 and L_{rts} are the same. The multiscreen loss is given by

$$L_{\text{msd}} = L_{\text{bsh}} + k_a + k_d\log_{10}(d) + k_f\log_{10}(f_0) - 9\log_{10}(b), \tag{7.32}$$

where d is specified in km, f_0 in MHz and b in meters. Since $h_b < h_{\text{Roof}}$ we have

$$L_{\text{bsh}} = 0 \tag{7.33}$$

and

$$\begin{aligned} k_a &= 54 - 0.8\Delta h_b \\ &= 54 - 0.8\,(h_b - h_{\text{Roof}}) \\ &= 54 - 0.8(-1) = 54.8. \end{aligned} \tag{7.34}$$

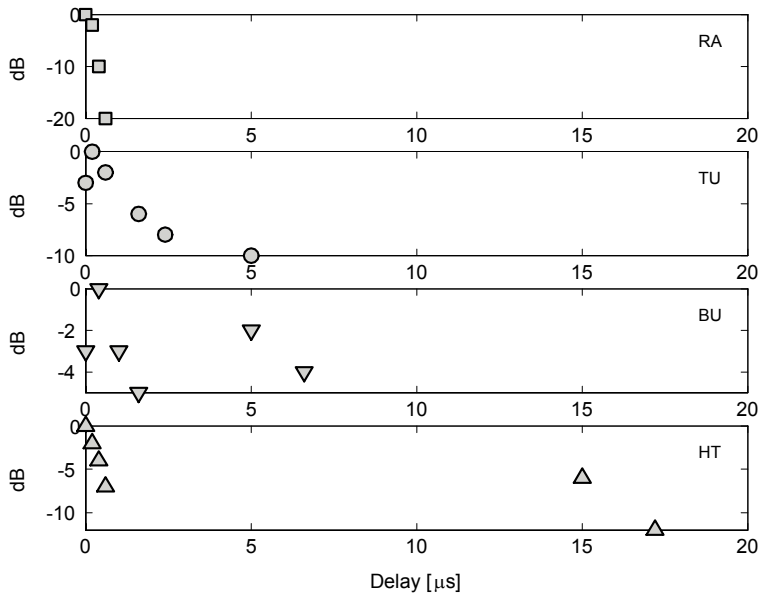

Figure 7.1: PDPs as a function of the time delay for the RA, TU, BU and HT scenarios, respectively.

where in latter case we have noted that $d > 0.5$ km. Furthermore,

$$k_d = 18 - 15\frac{\Delta h_b}{h_{\text{Roof}}} = 18 - 15\frac{(-1)}{20} = 18.75 \tag{7.35}$$

k_f is the same as in the previous problem, i.e., $k_f = -3.34$. Consequently,

$$\begin{aligned} L_{\text{msd}} &= 0 + 54.8 + 18.79\log_{10}(0.8) + (-3.34)\log_{10}(1800) - 9\log_{10}(30) \\ &= 28.82 \text{ dB}, \end{aligned} \tag{7.36}$$

which results in a total loss

$$L = 95.6 + 38.9 + 28.8 = 163.2 \text{ dB}. \tag{7.37}$$

With a BS below rooftops the attenuation due to multiscreen loss (L_{msd}) is higher than for a BS above rooftops. This is reasonable since high surrounding buildings shadow the transmissions from a low BS resulting in higher path loss.

4. We are considering the COST 207 wideband model.

   (a) Tables 7.3-7.6 are used to plot the PDPs for the four different terrain types, rural area (RA), typical urban (TU), bad urban (BU) and hilly terrain (HT). The result is displayed in Figure 7.1.

   (b) Figure 7.1 is redrawn with values of the path length (by using $d = c\tau$; where c is the speed of light and τ the time delay) on the x-axis instead. The result is shown in Figure 7.2.

   RA - The rural area does not contain many reflection points in terms of buildings and other obstacles, which results in a quite short delay spread (echos) of the signal.

   TU - In the urban (city) area there are a large number of scattering points, resulting in a larger delay spread compared to RA.

   BU - In the urban area there might also be some high rise builidings, resulting in strong reflections delayed a few μs relative to the first peak and occurring at a delay such that the first peak has not fully decayed.

   HT - In hilly terrain, the direct path first arrives with a little delay spread. No power is received for a considerable amount of delay followed by strong reflections from far-away hills (delay = 15 μs).

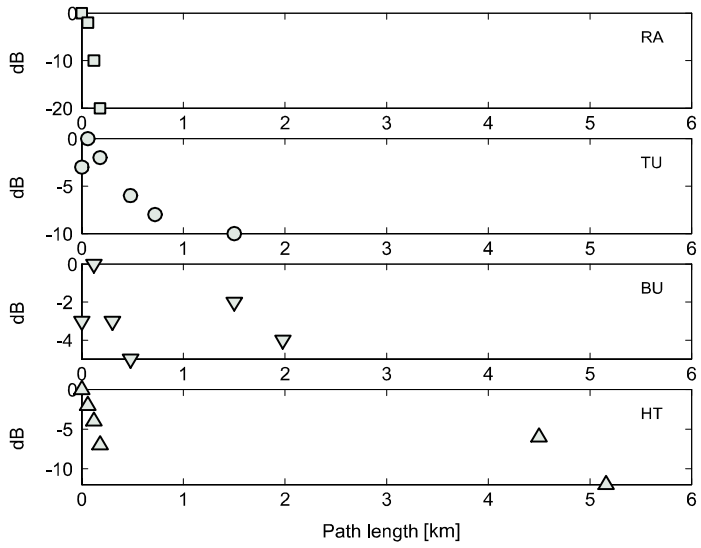

Figure 7.2: PDPs as a function of the path length for the RA, TU, BU and HT scenarios, respectively.

5. The power delay profile can be obtained from the complex impulse response, $h(t,\tau)$ as

$$P_h(\tau) = \int_{t=-\infty}^{\infty} |h(t,\tau)|^2 \, dt \tag{7.38}$$

if ergodicity holds.

(a) The normalized second-order central moment is known as *average RMS delay spread* and defined as

$$S_\tau = \sqrt{\frac{\int_{\tau=-\infty}^{\infty} P_h(\tau)\,\tau^2 d\tau}{P_m} - T_m^2} \tag{7.39}$$

where P_m is the time integrated power (total energy)

$$P_m = \int_{\tau=-\infty}^{\infty} P_h(\tau)\, d\tau \tag{7.40}$$

and T_m is the average mean delay (normalized first-order central moment) defined as

$$T_m = \frac{\int_{\tau=-\infty}^{\infty} P_h(\tau)\,\tau d\tau}{P_m} \tag{7.41}$$

The normalizations and the "$-T_m^2$" are done to keep the *average RMS delay spread* independent of the propagation delay but dependent on the excess delay and independent on the total energy. Hence, it is only a measure of the spread of the channel. For the RA environment of the COST 207 we have (see App. 7.C)

$$P_h(\tau) = e^{-9.2\cdot 10^6\cdot\tau} \tag{7.42}$$

$$S_{\tau,\mathrm{RA}} = \sqrt{\frac{\int_0^{0.0000007} e^{-9.2\cdot 10^6\cdot\tau}\tau^2 d\tau}{\int_0^{0.0000007} e^{-9.2\cdot 10^6\cdot\tau} d\tau} - \left(\frac{\int_0^{0.0000007} e^{-9.2\cdot 10^6\cdot\tau}\tau d\tau}{\int_0^{0.0000007} e^{-9.2\cdot 10^6\cdot\tau} d\tau}\right)^2} = 1.1\times 10^{-7} \tag{7.43}$$

Note, however, that the RA has a Rician-fading first component. Thus, while the rms delay spread can be mathematically defined and computed as above, great care must be taken when interpreting the result and applying it, e.g., to BER computations (see also Chapter 12).
For the TU environment

$$P_h(\tau) = e^{-9.2\cdot 10^6\cdot\tau}$$

$$S_{\tau,\mathrm{TU}} = \sqrt{\frac{\int_0^{0.000007} e^{-10^6\cdot\tau}\tau^2 d\tau}{\int_0^{0.000007} e^{-10^6\cdot\tau} d\tau} - \left(\frac{\int_0^{0.000007} e^{-10^6\cdot\tau}\tau d\tau}{\int_0^{0.000007} e^{-10^6\cdot\tau} d\tau}\right)^2} = 9.8\times 10^{-7} \tag{7.44}$$

(b) The coherence bandwidth is the correlation function exceeding the threshold. The rms delay spread S_τ and the coherence bandwidth B_{coh} are obviously related: S_τ is derived from the PDP $P_h(\tau)$ while B_{coh} is obtained from the frequency correlation function, which is the Fourier transform of the PDP. Based on this insight, an "uncertainty relationship" could be derived

$$B_{\mathrm{coh}} \geq \frac{1}{2\pi S_\tau} \quad [rad/s] \tag{7.45}$$

hence the coherence band is often approximated as

$$B_{\mathrm{coh}} \approx \frac{1}{S_\tau} \quad [Hz] \tag{7.46}$$

hence

$$B_{\mathrm{coh,RA}} \approx 1/1.1\times 10^{-7} = 9.1\times 10^{-8} \tag{7.47}$$
$$B_{\mathrm{coh,TU}} \approx 1/9.8\times 10^{-7} = 1.0\times 10^{-8} \tag{7.48}$$

(c) Yes, two very different PDPs could have the same RMS delay spread. RMS delay spread is not enough to describe the channel PDP.

6. (a) The amplitude, α_n, of each the N MPC is i.i.d, hence the received signal at element 1 and 2 is then

$$h_1 = C\sum_{n=1}^{N}\alpha_n \tag{7.49}$$
$$h_2 = C\sum_{n=1}^{N}\alpha_n e^{j\frac{2\pi}{\lambda}d\sin(\Omega)} \tag{7.50}$$

where C is a normalization factor making the correlation, r, range between 0 and 1. The correlation between element 1 and 2, r, is then

$$\begin{aligned}\rho &= E\left[h_1^*\cdot h_2\right] = E\left[C^2\sum_{n=1}^{N}\alpha_n^*\cdot\sum_{n=1}^{N}\alpha_n e^{j\frac{2\pi}{\lambda}d\sin(\Omega)}\right] \\ &= C^2E\left[\sum_{n=1}^{N}\alpha_n^*\cdot\sum_{n=1}^{N}\alpha_n e^{j\frac{2\pi}{\lambda}d\sin(\Omega)}\right] \underset{\alpha_n \text{ and } \alpha_{n+1} \text{ independent}}{=} C^2E\left[\sum_{n=1}^{N}\alpha_n^*\alpha_n e^{j\frac{2\pi}{\lambda}d\sin(\Omega)}\right] \\ &= C^2E\left[\sum_{n=1}^{N}|\alpha_n|^2 e^{j\frac{2\pi}{\lambda}d\sin(\Omega)}\right]\end{aligned} \tag{7.51}$$

The expectation is for an angular distribution of $f_\phi(\phi)$

$$\begin{aligned}\rho &= C^2\int_{-\infty}^{\infty} f_\phi(\phi)\sum_{n=1}^{N}|\alpha_n|^2 e^{j\frac{2\pi}{\lambda}d\sin(\phi)}d\phi \\ &= C^2\sum_{n=1}^{N}|\alpha_n|^2\cdot\int_{-\infty}^{\infty} f_\phi(\phi)e^{j\frac{2\pi}{\lambda}d\sin(\phi)}d\phi\end{aligned} \tag{7.52}$$

(b) The correlation simulated coefficient is plotted in Fig. 7.3. For another distribution of the APS the correlation will change.

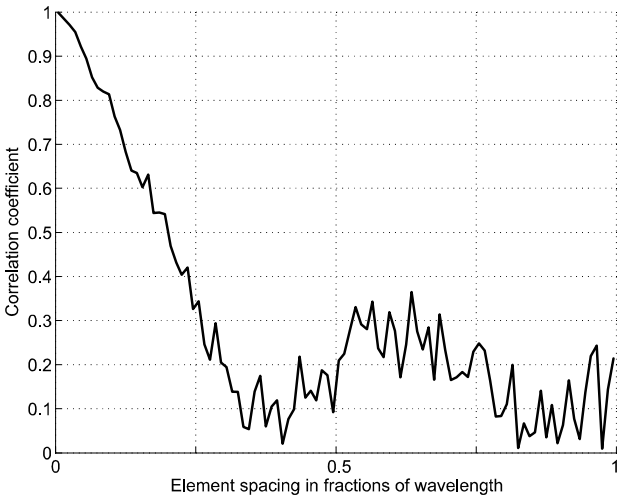

Figure 7.3: Simulation results for the correlation in Exercise 7.6.

```
function RadioSys_Corr()
noMPC = 100;
sigma = 2*pi;
counter = 0;
noSnap = 500;
dVec = [0.01:0.02:2];
for d = dVec
 counter = counter + 1;
 R(counter) = Corr(sigma, noMPC, d, noSnap);
end;
h = plot(dVec, R, 'k-', 'LineWidth', 2)
set(gca, 'FontSize', 14);
xlabel('Element spacing in fractions of wavelength', 'FontSize', 14)
ylabel('Correlation coefficient', 'FontSize', 14)
box off;
grid
function R = Corr(sigma, noMPC, d, noSnap)
alfa = sigma*randn(noMPC, 1);
alfa = sigma*rand(noMPC, 1);
R = 0;
for k = 1 :  noSnap
 a = (randn(noMPC, 1) + j*randn(noMPC, 1))/sqrt(2);
 h1 = sum(a); % received signal at antenna 1
 h2 = sum(a.*exp(j*2*pi*d*sin(alfa))); % received signal at antenna 2
 normal = sqrt(abs(h1)^2 + abs(h2)^2)/sqrt(2); % normalization factor E[abs(h1)] = E[abs(h1)]
= 1.  Results in a correlation between 0 and 1.
 h1 = h1/normal;
 h2 = h2/normal;
 R = R + h1*h2';
end;
R = abs(R/noSnap);
```

Chapter 8

Channel sounding

1. (a) The minimum measurable difference in time delay between the multipath components is determined as
$$\Delta\tau_{\min} = t_{\text{on}} = 50 \text{ ns}. \tag{8.1}$$
(b) The maximum time delay which can be measured unambiguously is determined by the pulse repetition period as
$$\tau_{\max} = T_{\text{rep}} = 20 \ \mu\text{s}. \tag{8.2}$$

2. According to the theory of linear systems, if white noise $n(t)$ is applied at the input of a linear system and the output $r(t)$ is cross-correlated with a delayed replica of the input $n(t-\tau)$, then the resulting cross-correlation is proportional to the impulse response of the system evaluated at the delay τ, $h(t)|_{t=\tau}$. From the definition of the cross-correlation
$$E\left[r(t)\, n^*(t-\tau)\right] = E\left[\int_{-\infty}^{\infty} n(t-x)\, h(x)\, n^*(t-\tau)\, dx\right], \tag{8.3}$$
where the output $r(t)$ is represented as the convolution relationship $r(t) = \int_{-\infty}^{\infty} n(t-x)\, h(x)\, dx$. Interchanging the order of the expectation and integral operators
$$\begin{aligned} &= \int_{-\infty}^{\infty} h(x)\, E\left[n(t-x)\, n^*(t-\tau)\right] dx \qquad (8.4)\\ &= \int_{-\infty}^{\infty} h(x)\, R_n(\tau - x)\, dx \\ &= N_0 \int_{-\infty}^{\infty} h(x)\, \delta(\tau - x)\, dx \end{aligned}$$
where $R_n(\tau) = E\left[n(t)\, n^*(t-\tau)\right] = N_0\delta(\tau)$ is the auto-correlation function of the white noise process, N_0 is the single-sided noise power spectral density. Using the properties of the convolution integral
$$\begin{aligned} &= N_0 \int_{-\infty}^{\infty} \delta(x)\, h(\tau - x)\, dx \\ &= N_0\left[\delta(\tau) * h(\tau)\right] = N_0 h(\tau). \qquad (8.5) \end{aligned}$$

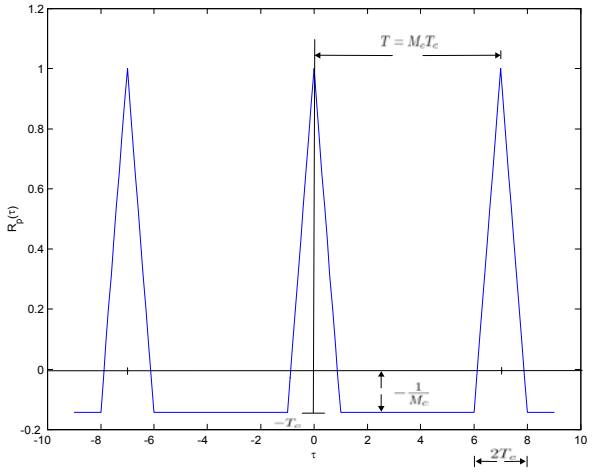

Figure 8.1: Auto correlation function for the code waveform is periodic.

Consequently, the impulse response of a linear system such as the wireless propagation channel can be evaluated using white noise and some form of correlation processing. In practice it is not possible to generate true white noise so channel sounding systems use deterministic waveforms with noise like properties. The most widely used example of such waveforms are the pseudo-random binary maximal-length sequences (m-sequences, PN-sequences).

3. (a) The period M_c of the sequence is determined as

$$M_c = 2^m - 1 = 2^3 - 1 = 7 \tag{8.6}$$

(b) Considering the feedback connections, the sequence $\{a_k\}$ is generated according to the formula

$$a_k = a_{k-2} + a_{k-3}. \tag{8.7}$$

For the initial conditions, $a_{k-3} = 1, a_{k-2} = a_{k-1} = 0$, the generated sequence is

$$a_k = \{1001011, 1001011, 1001011, ...\} \qquad k \geqslant 0 \tag{8.8}$$

This sequence is periodic with period 7.

4. This spreading waveform has the autocorrelation function

$$R_p(\tau) = R_{\acute{C}_m}(l)\left(1 - \frac{\delta}{T_c}\right) + R_{\acute{C}_m}(l+1)\frac{\delta}{T_c} \tag{8.9}$$

where

$$\begin{aligned} \tau &= lT_c + \delta \\ l &= \left\lfloor \frac{\tau}{T_c} \right\rfloor \\ 0 &\leq \delta < T_c \end{aligned} \tag{8.10}$$

(a) The plot is shown in Fig. 8.1.

(b) The dynamic range of the system determines how large a difference can be observed between the strongest and the weakest measured multipath components. Ignoring the effect of system noise, the dynamic range is purely a function of the m-sequence period and equals

$$\text{dynamic range} = 20\log_{10}(M_c). \tag{8.11}$$

Note, however, that better dynamic range can be achieved with nonlinear evaluation methods, e.g., interference cancellation schemes (compare also Sec. 18.4).

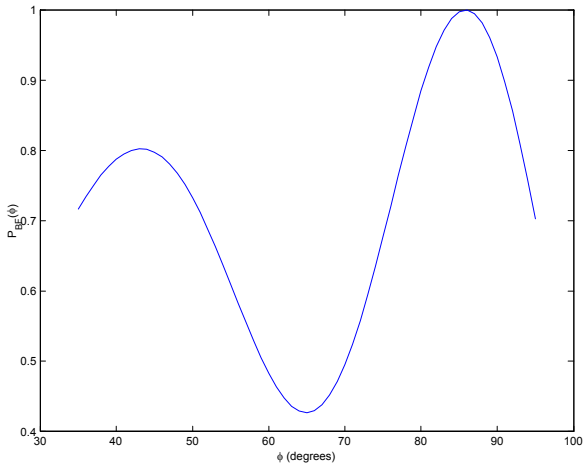

Figure 8.2: Normalized beam forming spectrum versus DOA for sufficiently separated angles.

5. :

(a) The maximum Doppler shift experienced by a MS moving with velocity v is given as

$$\upsilon_{\max} = \frac{\mathrm{v}}{\lambda},$$

thus

$$\begin{aligned} \mathrm{v} &= \frac{c_0}{2K_{\mathrm{scal}} M_c T_c f_c} \\ \mathrm{v} &= \frac{3 \cdot 10^8}{2 \cdot 5000 \cdot 31 \cdot 0.1 \cdot 900} = 10.8 \text{ m/s} \end{aligned} \tag{8.12}$$

(b) The maximum unambiguous time delay which an STDCC system can measure is given as

$$\begin{aligned} \tau_{\max} &= M_c T_c \\ &= 31 \cdot 0.1 \ \mu s = 3.1 \ \mu s \end{aligned} \tag{8.13}$$

(c) According to B-8.2, $\upsilon_{\max}$ is inversely proportional to M_c, provided that all other parameters are fixed. If we increase the m-sequence period by the factor $\frac{63}{31} \approx 2$, the maximum Doppler shift which the receiver can handle is reduced by half. Thus the maximum permissible mobile velocity will be reduced by half, e.g., re-calculating part (a) with $M_c = 63$ gives a maximum permissible velocity of 5.4 m/s. An increase in M_c by a factor 2 will increase the maximum measurable delay of the multipath components by the same factor.

6. :

(a) We plot the angular spectrum for the conventional beamformer given in Eq. (B-8.39)

$$P_{\mathrm{BF}}(\phi) = \frac{\alpha^{\dagger}(\phi) \mathbf{R}_{rr} \alpha(\phi)}{\alpha^{\dagger}(\phi) \alpha(\phi)} \tag{8.14}$$

The angles at which peaks occur in the spectrum are the estimates for the angles of arrival. The results are shown in Fig. 8.2. The matlab code is provided below.

```
nr=4; % No of elements in ULA
d_r=0.5; % element spacing in wavelengths
```

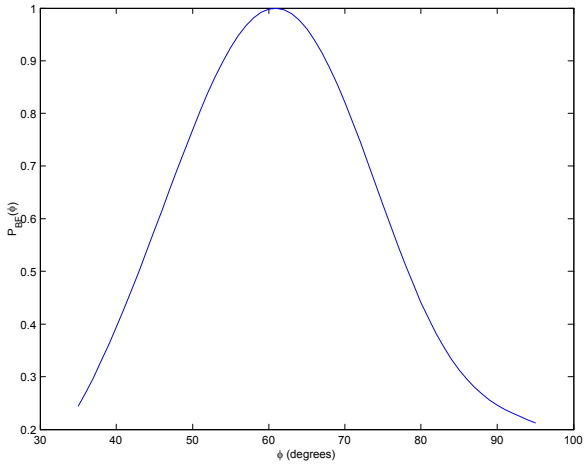

Figure 8.3: Normalized beam forming spectrum versus DOA for angle separation less than angle resolution of beamformer.

```
steer_vector=inline('exp(-j*2*pi*d_r*transpose(0:nr-1)*cos(DOA))');
% steer_vector is an inline function for the steering vector
theta=(35:95)*pi/180; % plot spectrum over this range of angles
for inx=1:length(theta)
x=steer_vector(theta(inx),d_r,nr);
P_spectrum(inx)=x'*R_rr*x/(x'*x);
end
P_spectrum=P_spectrum/max(abs(P_spectrum)); % Normalize
plot(theta*180/pi,abs(P_spectrum))
xlabel('\theta (degrees)')
ylabel('P_B_F(\phi)')
```

The true values for the two angles of arrival in this example were 45° and 85°. Reading the angles coresponding to the spectrum peaks gives 43° and 86° as the respective estimates.

(b) The procedure described in part (a) is repeated. However, the spectrum as shown in Fig. 8.3 shows only one DOA, estimated at 61°. The explanation comes from the true DOAs in this example which are 60° and 85°. These DOAs correspond to an electrical angle separation of $\frac{2\pi}{\lambda} \cdot d\_r \left(\cos\left(\phi_1\right) - \cos\left(\phi_2\right)\right) = \pi \left(\cos\left(45°\right) - \cos\left(85°\right)\right) = 1.95$ radians, which is less than the resolution limit of the beamformer given by $\frac{2\pi}{L} = \frac{2\pi}{1.5} = 4.2$ radians. Hence some super resolution algorithm has to be used to estimate both angles.

7. Following the steps outlined in App. 8.A, the DOAs are estimated as 44.99° and 85.01° which are identical to their true values. The matlab implementation is provided below:

```
[U,D] = eig(R_rr); % eigen value decomposition of Cov. matrix
U=U(:,end-(MPC-1):end); % select eigen vectors corresponding to the 2(source order) dominant eigen-
values
J_1=eye(nr);
J_1=J_1(1:nr-1,:);
J_2=eye(nr);
J_2=J_2(2:nr,:);
PSI=(J_1*U)\J_2*U;
PHI_EIG=eig(PSI);
DOA_ESPRIT=180/pi*acos(angle(PHI_EIG)/(-2*pi*d_r))
```

(a) Repeating the same procedure for scenario (b) , where the beamformer did not work, we get DOA estimates of 60.0° and 85.1° which match their respective true values.

8. The m-th sample of the impulse response is given by

$$h_{\mathrm{m}} = s_{\mathrm{m}} + n_{\mathrm{m}} \tag{8.15}$$

where n_{m} = noise amplitude in the m-th sample. The SNR in the m-th sample is given by

$$SNR_m = \frac{s_m^2}{\sigma^2}. \tag{8.16}$$

By averaging over the M snapshots, we define the following two new variables

$$\begin{aligned} Y &= \frac{1}{M}\sum_{m=1}^{M} s_m, \\ N &= \frac{1}{M}\sum_{m=1}^{M} n_m. \end{aligned}$$

The mean SNR is given by

$$SNR = \frac{E\left[Y^2\right]}{E\left[N^2\right]} \tag{8.17}$$

where the expectation is with respect to realizations of the channel, during t_{meas}. Inserting Y and N into Eq. (8.17) gives

$$SNR = \frac{E\left[\left(\frac{1}{M}\sum_{m=1}^{M} s_m\right)^2\right]}{E\left[\left(\frac{1}{M}\sum_{m=1}^{M} n_m\right)^2\right]} = \frac{E\left[\sum_{m=1}^{M} s_m \sum_{k=1}^{M} s_k\right]}{E\left[\sum_{m=1}^{M} n_m \sum_{k=1}^{M} n_k\right]} \tag{8.18}$$

Since the channel is invariant during t_{meas}, $s_m = s_k$ is deterministic, hence

$$SNR = \frac{M^2 s_m^2}{E\left[\sum_{m=1}^{M} n_m^2\right] + E\left[\sum_{m=1}^{M} n_m \sum_{k=1,k\neq m}^{M} n_k\right]}. \tag{8.19}$$

Due to statistical independence of the noise samples, $E\left[\sum_{m=1}^{M} n_m \sum_{k=1,k\neq m}^{M} n_k\right] = 0$, and $E\left[\sum_{m=1}^{M} n_m^2\right] = M\sigma^2$. Hence

$$SNR = \frac{M^2 s_m^2}{M\sigma^2} = M \cdot SNR_m \tag{8.20}$$

It is to be noted that the factor M improvement in SNR is achieved only on the average; in individual realizations the improvement can be less.

Chapter 9

Antennas

1. When we place the handset to the head the total attenuation is increased by 6 dB, which corresponds to a factor 4 on a linear scale. The distance that can be covered thus decreases by a factor

$$4^{1/3.2} = 1.54 \tag{9.1}$$

so that the covered distance is

$$d = 24 \text{ km}. \tag{9.2}$$

2. As a first step, we need to compute the size of a patch antenna. It follows from elementary considerations that

$$\begin{aligned} \lambda_0 &= \frac{c_0}{2.4 \text{ GHz}} = 0.125 \text{ m} \\ \lambda_{\text{substrate}} &= \frac{\lambda_0}{\sqrt{\varepsilon_\text{r}}} = 0.079 \text{ m} \\ L &= 0.5\lambda_{\text{substrate}} = 0.04 \text{ m} = 4 \text{ cm} \end{aligned} \tag{9.3}$$

Thus, the patch is rather large, and will tend to extend to an area gripped by the hand. Placement along the top of the PDA is preferable. One of the solutions found in commercial products is to have a WiFi card partly protruding from the top of the PDA, thus minimizing the risk of having it covered by the hand. Placement within the casing is often difficult, as the casing can be essentially a Faraday cage.

3. From

$$1 = \frac{2\lambda d}{(\pi D)^2} \tag{9.4}$$

it follows straightforwardly that

$$D = 1.26 \text{ cm} \tag{9.5}$$

4. As a first step, find the direction of the maximum of the pattern

$$\begin{aligned} G(\phi,\theta) &= \sin^n\left(\frac{\theta}{\theta_0}\right)\cos\left(\frac{\theta}{\theta_0}\right) \\ \frac{d}{d\theta}\sin^n\left(\frac{\theta}{\theta_0}\right)\cos\left(\frac{\theta}{\theta_0}\right) &= 0 \\ \frac{d}{d\theta}\sin^n\left(\frac{\theta}{\theta_0}\right)\cos\left(\frac{\theta}{\theta_0}\right) &= n\sin^{n-1}\left(\frac{\theta}{\theta_0}\right)\cos^2\left(\frac{\theta}{\theta_0}\right) - \sin^n\left(\frac{\theta}{\theta_0}\right)\sin\left(\frac{\theta}{\theta_0}\right) = \\ \sin^{n-1}\left(\frac{\theta}{\theta_0}\right)\left(n\cos^2\left(\frac{\theta}{\theta_0}\right) - \sin^2\left(\frac{\theta}{\theta_0}\right)\right) &= 0 \end{aligned} \tag{9.6}$$

Trivial solutions (n-1 of them) are $\theta = 0$. As $G(\phi,\theta) = 0$ for these, this angle gives a minimum. Additional solutions are the solutions to:

$$n\cos^2\left(\frac{\theta}{\theta_0}\right) - \sin^2\left(\frac{\theta}{\theta_0}\right) = 0 \tag{9.7}$$

so that

$$\theta = \theta_0 \arctan(\sqrt{n}) \ . \tag{9.8}$$

The gain in the direction of the maximum is then

$$\sin^n\left(\arctan(\sqrt{n})\right)\cos\left(\arctan(\sqrt{n})\right) \tag{9.9}$$

which becomes after some trigonometric manipulations

$$\frac{n^{n/2}}{(1+n)^{(1+n)/2}} \tag{9.10}$$

(a) We then have to find the $x = \cos(\frac{\theta}{\theta_0})$ so that

$$x\left(1-x^2\right)^{n/2} = \frac{1}{2}\frac{n^{n/2}}{(1+n)^{(1+n)/2}} \ . \tag{9.11}$$

(b) similarly, for the 10 dB attenuation, find the solution to

$$x\left(1-x^2\right)^{n/2} = \frac{1}{10}\frac{n^{n/2}}{(1+n)^{(1+n)/2}} \tag{9.12}$$

(c) For the directivity,

$$\begin{aligned} D(\phi_d,\theta_d) &= \frac{G(\phi_d,\theta_d)}{\frac{1}{4\pi}\iint G(\phi,\theta)\sin\theta d\phi d\theta} \\ D(\phi_d,\theta_d) &= \frac{\sin^n\left(\frac{\theta_d}{\theta_0}\right)\cos\left(\frac{\theta_d}{\theta_0}\right)}{\frac{1}{4\pi}\iint \sin^n\left(\frac{\theta}{\theta_0}\right)\cos\left(\frac{\theta}{\theta_0}\right)\sin\theta d\phi d\theta} \end{aligned} \tag{9.13}$$

Using the result for the maximum value of $G(x)$, we get

$$\frac{\frac{n^{n/2}}{(1+n)^{(1+n)/2}}}{\frac{1}{2}\int \sin^n\left(\frac{\theta}{\theta_0}\right)\cos\left(\frac{\theta}{\theta_0}\right)\sin\theta d\theta} \tag{9.14}$$

which can be evaluated analytically.

(d) The numerical result are: for the 3 dB bandwidth: 1.341 rad; for the 10 dB bandwidth, 2.151. The directivity is 2.2.

5. The impedance of the corresponding full wavelength wire antenna is

$$\begin{aligned} Z_A &= 80\pi^2\left(\frac{L_a}{\lambda}\right)^2 \\ Z_A &= 20\pi^2 = 197\Omega \end{aligned} \tag{9.15}$$

which gives the impedance of the slot antenna

$$\begin{aligned} Z_B &= \frac{{Z_0}^2}{4Z_A} \\ Z_B &= \frac{377^2}{788}\Omega = 180\Omega \end{aligned} \tag{9.16}$$

6. (a) The equations for the radiation resistance at TX and RX are

$$\begin{aligned} R_{TX} &= \frac{1}{4}80\pi^2\left(\frac{\lambda/2}{\lambda}\right)^2 \\ R_{TX} &= 50\Omega \\ R_{RX} &= 80\pi^2\left(\frac{\lambda/20}{\lambda}\right)^2 \\ R_{RX} &= 2\Omega \end{aligned} \tag{9.17}$$

(b) The radiation efficiency is computed from

$$\eta = \frac{R_{rad}}{R_{rad} + R_{ohmic}} \tag{9.18}$$

so that at the transmitter it is

$$\eta_{TX} = \frac{50}{50+10} = 83\% \tag{9.19}$$

and at the receiver it is

$$\eta_{RX} = \frac{2}{2+10} = 17\% \quad . \tag{9.20}$$

7. (a) The array factor is

$$|M(\phi,\theta)| = \left| \frac{\sin\left[\frac{N_r}{2}\left(\frac{2\pi}{\lambda}d_a\cos\phi - \Delta\right)\right]}{\sin\left[\frac{1}{2}\left(\frac{2\pi}{\lambda}d_a\cos\phi - \Delta\right)\right]} \right| \tag{9.21}$$

Inserting Δ we get:

$$\begin{aligned} |M(\phi,\theta)| &= \left| \frac{\sin\left[\frac{N}{2}\left(\frac{2\pi}{\lambda}d_a\cos\phi + \frac{2\pi}{\lambda}d_a\right)\right]}{\sin\left[\frac{1}{2}\left(\frac{2\pi}{\lambda}d_a\cos\phi + \frac{2\pi}{\lambda}d_a\right)\right]} \right| \\ &= \left| \frac{\sin\left[\frac{N}{2}\frac{2\pi}{\lambda}d_a\left(\cos\phi + 1\right)\right]}{\sin\left[\frac{1}{2}\frac{2\pi}{\lambda}d_a\left(\cos\phi + 1\right)\right]} \right| \end{aligned} \tag{9.22}$$

Endfire direction: $\phi = 0$

$$\begin{aligned} |M(\phi,\theta)| &= \left| \frac{\sin\left[\frac{N}{2}\left(\frac{2\pi}{\lambda}d_a + \frac{2\pi}{\lambda}d_a\right)\right]}{\sin\left[\frac{1}{2}\left(\frac{2\pi}{\lambda}d_a + \frac{2\pi}{\lambda}d_a\right)\right]} \right| \\ &= \left| \frac{\sin\left[N\frac{2\pi}{\lambda}d_a\right]}{\sin\left[\frac{2\pi}{\lambda}d_a\right]} \right| \end{aligned} \tag{9.23}$$

(b) Inserting Δ we get:

$$|M(\phi,\theta)| = \left| \frac{\sin\left[\frac{N}{2}\left(\frac{2\pi}{\lambda}d_a\cos\phi + \frac{2\pi}{\lambda}d_a + \frac{\pi}{N}\right)\right]}{\sin\left[\frac{1}{2}\left(\frac{2\pi}{\lambda}d_a\cos\phi + \frac{2\pi}{\lambda}d_a + \frac{\pi}{N}\right)\right]} \right| \tag{9.24}$$

Endfire direction: $\phi = 0$

$$\begin{aligned} |M(\phi,\theta)| &= \left| \frac{\sin\left[\frac{N}{2}\left(\frac{2\pi}{\lambda}d_a + \frac{2\pi}{\lambda}d_a + \frac{\pi}{N}\right)\right]}{\sin\left[\frac{1}{2}\left(\frac{2\pi}{\lambda}d_a + \frac{2\pi}{\lambda}d_a + \frac{\pi}{N}\right)\right]} \right| \\ &= \left| \frac{\sin\left[N\frac{2\pi}{\lambda}d_a + \frac{\pi}{2}\right]}{\sin\left[\frac{2\pi}{\lambda}d_a + \frac{\pi}{2N}\right]} \right| \end{aligned} \tag{9.25}$$

If we instead use

$$\Delta = -\left[\frac{2\pi}{\lambda}d_a + \frac{\pi}{N}\right] \tag{9.26}$$

we obtain the "Hansen–Woodyard" endfire antenna, which shows an increased directivity in the endfire direction. For the gain of the whole array, we would also have to take the gain of the antenna elements into account.

Chapter 10

Structure of a wireless communication link

1. The structure of the directional coupler is sketched in Fig. 10.1.

   (a) Identifying the S matrix. the directivity is defined in terms of S-matrix elements as

   $$D = -20 \log \frac{|S_{14}|}{|S_{13}|} \tag{10.1}$$

   so that in this example

   $$\frac{|S_{13}|}{|S_{14}|} = 0.1 \ . \tag{10.2}$$

   The insertion attenuation is defined as

   $$A = -20 \log |S_{12}| \tag{10.3}$$

   so that here

   $$|S_{12}| = 0.89 \ . \tag{10.4}$$

   Finally, the coupling attenuation is defined as

   $$|C = -20 \log |S_{13}| \tag{10.5}$$

   so that

   $$|S_{13}| = 0.1 \ . \tag{10.6}$$

   Since the reflection coefficients are identical to $|S_{ii}|$, we find that

   $$|S_{ii}| = 0.12 \tag{10.7}$$

   The phase shifts are usually zero, except for the coupled paths, so that

   $$\arg(S_{13}) = \arg(S_{42}) = \pi/2 \ . \tag{10.8}$$

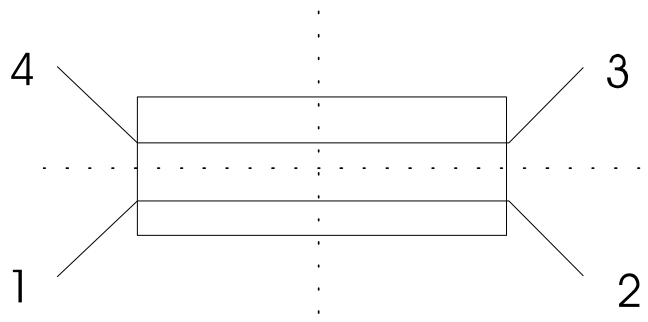

Figure 10.1: Directional coupler for Exercise 10.1.

(b) The device is passive, reciprocal, and symmetrical with respect to two planes (dotted lines in Fig. 10.1).

2. For the computations, it is convenient to normalize the impedance with a reference impedance of 50 Ω

$$Z_A = \frac{70 - 85j}{50} = 1.4 - 1.7j \ . \tag{10.9}$$

(a) The normalized impedance of the inductance is

$$jX = j\frac{\omega L}{Z_0} = j\frac{2\pi \cdot 250 \cdot 10^6 \cdot 85 \cdot 10^{-9}}{50} = 2.67j \tag{10.10}$$

The total impedance thus becomes

$$Z_{\text{tot,norm}} = \frac{Z_{\text{tot}}}{Z_0} = 1.4 - j1.7 + j2.67 = 1.4 + j0.97 \tag{10.11}$$

and the reflection coefficient becomes

$$\rho = 0.41 \exp(j\frac{\pi}{180}45.5) \ . \tag{10.12}$$

(b) In order for the impedance to become real, we require that

$$-1.7 + \frac{\omega L}{Z_0} = n\pi \tag{10.13}$$

This is achieved, e.g., by

$$L = \frac{50 \cdot 1.7}{2\pi \cdot 250 \cdot 10^6} = 54.1 \text{ nH} \quad . \tag{10.14}$$

3. As we have seen in Chapter 3, Eq. (B-3.6), the equivalent noise figure of a cascade of two amplifiers is

$$F_{\text{eq}} = F_1 + \frac{F_2 - 1}{G_1} \ . \tag{10.15}$$

Let us now prove that M is the correct criterion for placing an amplifier first. The statement to be proved is that the following should be fulfilled:

$$M_1 = \frac{F_1 - 1}{1 - 1/G_1} < M_2 = \frac{F_2 - 1}{1 - 1/G_2} \ . \tag{10.16}$$

This can be rewritten as

$$(F_1 - 1)(1 - 1/G_2) < (F_2 - 1)(1 - 1/G_1) \tag{10.17}$$

which can be expanded to

$$F_1 - 1 - \frac{F_1}{G_2} + \frac{1}{G_2} < F_2 - 1 - \frac{F_2}{G_1} + \frac{1}{G_1} \tag{10.18}$$

which is identical to

$$F_1 + \frac{F_2 - 1}{G_1} < F_2 + \frac{F_1 - 1}{G_2} \tag{10.19}$$

Quod erat demonstrandum.

4. The diode current is

$$i = i_s \left[\exp\left(\frac{u}{u_{\text{t}}}\right) - 1\right] \tag{10.20}$$

(a) Using a Taylor expansion of the exponential function

$$\exp(x) = 1 + \frac{x}{1!} + \frac{x^2}{2!} + \frac{x^3}{3!} + \frac{x^4}{4!}.... \tag{10.21}$$

we find that to a first approximation, the normalized output current $y = i/i_s$ is

$$i = x + \frac{x^2}{2} \tag{10.22}$$

where $x = u/u_\mathrm{t} = x_1 \cos(\omega t)$. Substituting this, we obtain

$$y = x_1 \cos(\omega t) + \frac{x_1^2}{2} \cos^2(\omega t) \tag{10.23}$$

which can be further expanded into

$$y = x_1 \cos(\omega t) + \frac{x_1^2}{4} \left[1 + \cos(2\omega t)\right]. \tag{10.24}$$

This demonstrates that the output signal has a DC component that is proportional to the squared amplitude of the signal, and thus to the power.

(b) The measurement error stems from the difference between the exact value of the exponential function and the approximation Eq. (10.21). The main source of discrepancy is the term $x^4/4!$ (note that the odd terms do not contribute to the DC component. A 5% error occurs if the fourth-order term becomes 0.05 times the desired second-order term

$$\frac{1}{24} x_1^4 = 0.05 \frac{1}{4} x_1^2 \tag{10.25}$$

which occurs at

$$x_1 \approx 0.9 \longrightarrow u_1 \approx 0.9 u_\mathrm{t} \ . \tag{10.26}$$

5. The amplifier gain is 26 dB; the power of the desired output components is thus related to that of the input components (both written on a dB scale)

$$y = x + 26 \ . \tag{10.27}$$

The intermodulation products have the general property that

$$\widetilde{y} = 3x + k \tag{10.28}$$

because they represent the cubic terms in the input-output relationship. If the strength of the input signals is -6 dBm, the power of the intermodulation products is

$$-10 = 3 \cdot (-6) + k \tag{10.29}$$

so that $k = 8$ dBm. For the intercept point, i.e., $y = \widetilde{y}$, we then require

$$x + 26 = 3x + 8 \tag{10.30}$$

so that the intercept point lies at 9 dBm input power, which is equivalent to 35 dB output power.

6. For notational convenience, we assume that the signal varies between -1 and $+1$. Thus, the quantization interval is $a = 2/2^n$, where n is the number of bits of the ADC.

(a) Within the quantization interval, the error is uniformly distributed, and thus has a variance of $a^2/12$. The average power of the total signal is 1/3. In order for the relative variance to stay below a treshold of K dB, we thus require that

$$\frac{\frac{1}{12}\left(\frac{1}{2^{n-1}}\right)^2}{1/3} < 10^{-K/10} \tag{10.31}$$

which can be simplified to

$$n > 0.5 \log_2(K) \tag{10.32}$$

which translates to 2, 4, and 6 bits for $K = 10, 20, 30$ dB.

(b) If the maximum amplitude decreases by a factor of 2, the quantization interval becomes $1/2^n$ of the peak amplitude. The required number of bits thus doubles.

Chapter 11

Modulation formats

1. The advantage of a smoother filter is that the spectral efficiency becomes higher. The drawback is that the signal does not always reach the ideal MSK signal points. Therefore the smoother filter implies a higher sensitivity to noise and other disturbances.

2. Writing the transmit signal as

$$g_m(t) = \cos\left[(2\pi f_c + b_m 2\pi f_{\text{mod}}(t))t\right] \tag{11.1}$$

we solve for

$$\int_0^T \cos\left[(2\pi f_c - 2\pi f_1)t\right] \cos\left[(2\pi f_c + 2\pi f_1)t\right] dt = 0 \tag{11.2}$$

$$\begin{aligned} & \int_0^T \cos\left[(2\pi f_c - 2\pi f_1)t\right] \cos\left[(2\pi f_c + 2\pi f_1)t\right] dt \\ = & \int_0^T \frac{1}{2}\cos 4\pi f_1 t + \frac{1}{2}\cos 4\pi t f_c dt \end{aligned} \tag{11.3}$$

The second term is the integral of the carrier frequency, which is not of interest. Solve for the first term

$$\int_0^T \frac{1}{2}\cos 4\pi f_1 t dt = \left[\frac{1}{8\pi f_1}\sin 4\pi t f_1\right]_0^T = 0 \tag{11.4}$$

which is 0 when $f_1 = \frac{1}{4T}$, i.e., a separation of $\frac{1}{2T}$. One should however note that this requires coherent demodulation with full knowledge of the phase. For non-coherent demodulation, the minimum separation is $\frac{1}{T}$.

3. The minimum value of the envelope is, e.g., achieved when going from the point e^{j0} to the point $e^{j7\pi/8}$. Trigonometric calculations give the minimum distance to origin as $1 \cdot \sin(\pi/16) \approx 0.195$. Since the mean envelope is unity, the requested ratio becomes 0.195.

   With $\frac{\pi}{4} - 8$ PSK, the constellation points are $n\pi/4$, $n = 0, 1, ..7$ for the original constellation as well as for the rotated constellation. Therefore, there are no advantages of such a modulation compared to "normal" 8-PSK.

4. In App. 11.A, we found that

$$\text{Re}\left\{s(t)\right\} = \sqrt{2E_{\text{B}}/T_{\text{B}}} \sin\left[\varphi_{\text{prev}}\left(k-1\right)\right] b_k \sin\left[\boldsymbol{\omega}_{\text{mod}}\left(t - kT_{\text{B}}\right)\right] \tag{11.5}$$

$$\text{Im}\left\{s(t)\right\} = \sqrt{2E_{\text{B}}/T_{\text{B}}} \cos\left[\varphi_{\text{prev}}(k)\right] b_{k+1} \sin\left[\boldsymbol{\omega}_{\text{mod}}\left(t - (k+1)\,T_{\text{B}}\right)\right] \tag{11.6}$$

   Omitting multiplicative factors, and recognizing that

$$\sin\left[\varphi_{\text{prev}}\left(k-1\right)\right] b_k = \pm 1 \tag{11.7}$$

$$\cos\left[\varphi_{\text{prev}}(k)\right] b_{k+1} = \pm 1 \tag{11.8}$$

the total signal is

$$\begin{aligned} s(t) &= \pm\sin(\omega_{\mathrm{mod}}(t-kT_B)) \pm j\sin(\omega_{\mathrm{mod}}(t-(k+1)T_B)) = \\ &= \pm\sin(\omega_{\mathrm{mod}}(t-kT_B)) \pm j\sin(\omega_{\mathrm{mod}}(t-kT_B)-\omega_{\mathrm{mod}}T_B) \end{aligned} \tag{11.9}$$

Since

$$\omega_{\mathrm{mod}}T_B = \frac{\pi}{2} \tag{11.10}$$

$s(t)$ can be rewritten as

$$s(t) = \pm\sin(\omega_{\mathrm{mod}}(t-kT_B)) \pm j\cos(\omega_{\mathrm{mod}}(t-kT_B)) \tag{11.11}$$

Since

$$\sqrt{\sin^2(x)+\cos^2(x)} = 1, \tag{11.12}$$

Eq. (11.11) is a constant-envelope signal.

5. (a) As a first step, we use a normalized version of the function $g(t)$ as the first expansion function. In order to ensure unit energy,

$$\phi_1(t) = \sqrt{3}\,[1-(t/T)] \tag{11.13}$$

Next, we need to project the function $f(t)$ onto $\phi_1(t)$:

$$a_2 = \int f(t)\phi_1(t)dt = \frac{\sqrt{3}}{8} \tag{11.14}$$

and the second basis function is

$$\phi_2(t) = 0.638\left[-\frac{3}{8}\,[1-(t/T)] + \left\{ \begin{array}{cc} 1 & 0<t<T/2 \\ -2 & T/2<t<T \end{array} \right.\right] \tag{11.15}$$

(b) The points in the signal constellation diagram can now be easily found by taking

$$\int_0^1 f(g)\phi_i(t)dt \qquad i=1,2 \tag{11.16}$$

and similarly for the other functions. We get the following expansions:

$$f(t) = (0.217, 1.565) \tag{11.17}$$

$$g(t) = (0.577, 0) \tag{11.18}$$

and the function that is constant for 0<t<1 has the expansion (0.866, 0.439) for the expansion functions ϕ_1 and ϕ_2. Note, however, that this function cannot be represented completely as a linear combination of the two expansion functions.

6. $p_{\mathrm{D}}(t)$ is given by the sequence $\{+1-1+1-1,-1,-1,-1,+1,+1\}$

7. Due to the symmetry of the problem, it is sufficient to consider only one quadrant in the signal-space diagram. The points in this diagram are

$$1{+}j, 3{+}j, 5{+}j, 7{+}j, 1{+}3j, 3{+}3j, 5{+}3j, 7{+}3j, 1{+}5j, 3{+}5j, 5{+}5j, 7{+}5j, 1{+}7j, 3{+}7j, 5{+}7j, 7{+}7j \tag{11.19}$$

times d, if the distance between two points is $2d$. The average signal energy is thus

$$\begin{aligned} \overline{E_s} &= \frac{d^2}{16}(1+1+9+1+25+1+49+1+1+9+9+9+25+9 \\ &\quad +49+9+1+25+9+25+25+25+49+25+1+49 \\ &\quad +9+49+25+49+49+49) \end{aligned} \tag{11.20}$$

$$= 42d^2 \tag{11.21}$$

8. A transmit power of 20 W means 43 dBm, so we need an attenuation of 93 dB for the out-of-band emissions. For BPSK modulation using raised cosine pulses the signal has no power outside $|f| > \frac{1+\alpha}{2T}$, so the data rate can be at least 741 kbps. For MSK, on the other hand, the out-of-band power is attenuated only by 33 dB for $fT_B = 1.35$, since

$$S(f) = \frac{16T_\mathrm{B}}{\pi^2}\left(\frac{\cos(2\pi f T_\mathrm{B})}{1-16f^2T_\mathrm{B}^2}\right)^2. \tag{11.22}$$

Thus, BPSK is therefore the better choice.

Chapter 12

Demodulation

1. (a) The parameters given in the problem statement are

Antenna gain	$G_a = 30$ dB
Distance attenuation	$L_{\mathrm{PL}} = 150$ dB
Receiver noise figure	$F_{\mathrm{sys}} = 7$ dB
Symbol rate	$d_s = 2 \cdot 10^7$ symb/s
Maximum BER	$p_{b,\max} = 10^{-5}$
Nyquist signalling	

Using the receiver noise figure (converted to linear scale!) the power spectral density of the noise, N_0, is calculated as

$$\begin{aligned} N_0 &= k_B(F_{\mathrm{sys}} - 1)T_0 \\ &= 1.38 \cdot 10^{-23} \cdot (10^{7/10} - 1) \cdot 290 \\ &= 1.606 \cdot 10^{-20} \text{ W/Hz}. \end{aligned} \tag{12.1}$$

The BER as functions of E_b/N_0 for the modulation schemes are

Coherent BPSK	$p_b = \frac{1}{2}\operatorname{erfc}\left(\sqrt{\frac{E_b}{N_0}}\right)$
Coherent FSK	$p_b = \frac{1}{2}\operatorname{erfc}\left(\sqrt{\frac{E_b}{2N_0}}\right)$
Differential BPSK	$p_b = \frac{1}{2}\exp\left(-\frac{E_b}{N_0}\right)$
Non-coherent FSK	$p_b = \frac{1}{2}\exp\left(-\frac{E_b}{2N_0}\right)$.

Note that

$$Q(z) = \frac{1}{2}\operatorname{erfc}\left(\frac{z}{\sqrt{2}}\right) \tag{12.2}$$

for $z \geq 0$. Using the BER requirement and the above expressions, minimum required E_b/N_0 quantities are

Coherent BPSK	$\left(\frac{E_b}{N_0}\right)_{\min} = \left(\operatorname{erfc}^{-1}(2p_{b,\max})\right)^2 = 9.09$
Coherent FSK	$\left(\frac{E_b}{N_0}\right)_{\min} = 2\left(\operatorname{erfc}^{-1}(2p_{b,\max})\right)^2 = 18.19$
Differential BPSK	$\left(\frac{E_b}{N_0}\right)_{\min} = \ln\left(\frac{1}{2p_{b,\max}}\right) = 10.82$
Non-coherent FSK	$\left(\frac{E_b}{N_0}\right)_{\min} = 2\ln\left(\frac{1}{2p_{b,\max}}\right) = 21.64.$

Since the power spectral density of the noise is known, the required bit energy is calculated as

$$E_{b,\min} = \left(\frac{E_b}{N_0}\right)_{\min} \cdot N_0 \text{ J} \tag{12.3}$$

for each modulation scheme. Then the minimum received power at the antenna output is

$$\begin{aligned} C_{\min} &= E_{b,\min} d_b \\ &= E_{b,\min} d_s \text{ W}, \end{aligned} \tag{12.4}$$

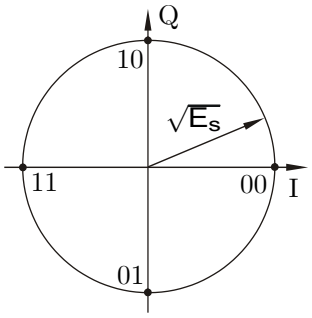

Figure 12.1: QPSK signal constellation.

since the modulation schemes are all binary. This results in

Coherent BPSK	$C_{\min} = -115.3$ dBW
Coherent FSK	$C_{\min} = -112.3$ dBW
Differential BPSK	$C_{\min} = -114.6$ dBW
Non-coherent FSK	$C_{\min} = -111.6$ dBW.

Then, the link budget provides the required transmit power as

$$\begin{aligned} C &= P_{TX} + G_a - L_{\text{PL}} + G_a \\ P_{TX,\min} &= C_{\min} - 2G_a + L_{\text{PL}} \end{aligned} \tag{12.5}$$

which results in

Coherent BPSK	$P_{TX,\min} = -25.3$ dBW
Coherent FSK	$P_{TX,\min} = -22.3$ dBW
Differential BPSK	$P_{TX,\min} = -24.6$ dBW
Non-coherent FSK	$P_{TX,\min} = -21.6$ dBW.

(b) The four-phase QPSK signal can be written as

$$s(t) = \sqrt{\frac{2E_s}{T_s}} \cos\left(2\pi f_c t + (i-1)\frac{\pi}{2}\right) \tag{12.6}$$

for $i = 1, 2, 3, 4$, in the symbol interval $0 \le t \le T_s$. Here, E_s is the symbol energy, T_s the symbol length and f_c the carrier frequency. Note that the total symbol energy is twice the bit energy since two bits are transmitted per symbol. Using

$$\cos(A + B) = \cos(A)\cos(B) - \sin(A)\sin(B), \tag{12.7}$$

the QPSK signal can be rewritten as

$$\begin{aligned} s(t) = &\sqrt{\frac{2E_s}{T_s}} \cos\left((i-1)\frac{\pi}{2}\right) \cos\left(2\pi f_c t\right) - \\ &\sqrt{\frac{2E_s}{T_s}} \sin\left((i-1)\frac{\pi}{2}\right) \sin\left(2\pi f_c t\right). \end{aligned} \tag{12.8}$$

Thus, with the two orthogonal basis functions

$$\begin{aligned} \phi_1 &= \sqrt{\frac{2}{T_s}} \cos\left(2\pi f_c t\right) \\ \phi_2 &= \sqrt{\frac{2}{T_s}} \sin\left(2\pi f_c t\right), \end{aligned} \tag{12.9}$$

it can be seen that the signal $s(t)$ can be viewed as two binary antipodal signals in quadrature, each carrying one bit, as illustrated in Figure 12.1. There is no interference between the signals

in quadrature, which means that each quadrature signal has the bit error probability of BPSK. Therefore,

$$p_{b,\mathrm{QPSK}} = p_{b,\mathrm{BPSK}} = \frac{1}{2}\operatorname{erfc}\left(\sqrt{\frac{E_b}{N_0}}\right). \tag{12.10}$$

Note that the BER of QPSK is the same as that of BPSK even though two bits are conveyed per QPSK symbol. The data rate can thus be doubled without sacrificing BER performance or increasing transmission bandwidth.

In the case of BPSK, the symbol error probability is the same as the bit error probability. For QPSK, the probability of correct decision of one symbol (i.e., two symbol bits) is $(1 - p_{b,\mathrm{QPSK}})^2$. Thus, the symbol error probability is

$$\begin{aligned} p_{s,\mathrm{QPSK}} &= 1 - (1 - p_{b,\mathrm{BPSK}})^2 \\ &= 1 - \left(1 - \frac{1}{2}\operatorname{erfc}\left(\sqrt{\frac{E_b}{N_0}}\right)\right)^2 \\ &= \operatorname{erfc}\left(\sqrt{\frac{E_b}{N_0}}\right)\left(1 - \frac{1}{4}\operatorname{erfc}\left(\sqrt{\frac{E_b}{N_0}}\right)\right). \end{aligned} \tag{12.11}$$

(c) Since QPSK has the same BER as BPSK, the required transmit power is the same as obtained for coherently detected BPSK in a), i.e., $P_{TX,\min} = -25.3$ dBW.

(d) Differentially detected QPSK has a BER of

$$p_{b,\mathrm{DQPSK}} = Q_1(a,b) - \frac{1}{2}I_0(ab)\exp\left(-\frac{1}{2}\left(a^2 + b^2\right)\right), \tag{12.12}$$

where

$$a = \sqrt{2\frac{E_b}{N_0}\left(1 - \frac{1}{\sqrt{2}}\right)}, \tag{12.13}$$

$$b = \sqrt{2\frac{E_b}{N_0}\left(1 + \frac{1}{\sqrt{2}}\right)}, \tag{12.14}$$

$Q_1(a,b)$ is Marcum's Q-function for $M = 1$, and $I_0(ab)$ is the zero order modified Bessel function of the first kind. The required E_b/N_0 used in (c) was calculated in (a) to be $E_b/N_0 = 9.09$, which is now used to calculate a and b. Thus,

$$a = \sqrt{2 \cdot 9.09\left(1 - \frac{1}{\sqrt{2}}\right)} = 2.31 \tag{12.15}$$

and

$$b = \sqrt{2 \cdot 9.09\left(1 + \frac{1}{\sqrt{2}}\right)} = 5.57. \tag{12.16}$$

Using these values of a and b, $Q_1(a,b) = 8.81 \cdot 10^{-4}$ and $I_0(ab) = 4.33 \cdot 10^4$, which results in

$$\begin{aligned} p_{b,\mathrm{DQPSK}} &= 8.81 \cdot 10^{-4} - \frac{1}{2} \cdot 4.33 \cdot 10^4 \cdot \exp\left(-\frac{1}{2}\left(a^2 + b^2\right)\right) \\ &= 6.08 \cdot 10^{-4}. \end{aligned} \tag{12.17}$$

Recall that the original requirement on maximum BER was 10^{-5}, which means that the BER has been degraded by a factor of 60. However, coherent detection of the QPSK symbols is no longer needed.

2 .

(a) Before using the upper bound we go through the problem in somewhat more detail. In general, for an M-ary modulation format, the average bit error probability can be written as

$$p_b = \sum_{i=1}^{M} \Pr\{s = s_i\} \Pr\{e|s = s_i\}, \tag{12.18}$$

where $\Pr\{s = s_i\}$ is the probability of transmitting the signal s_i out of the M alternatives, and $\Pr\{e|s = s_i\}$ is the average bit error probability given that the signal s_i was transmitted. By considering all the possible symbol errors we have

$$\Pr\{e|s = s_i\} = \sum_{j=1, j\neq i}^{M} \Pr\{\hat{s} = s_j|s = s_i\} \frac{n_{ij}}{\log_2(M)}, \tag{12.19}$$

where $\Pr\{\hat{s} = s_j|s = s_i\}$ is the probability of detecting signal s_j given that the signal s_i was transmitted, n_{ij} is the number of bit errors that occurs, and $\log_2(M)$ is the total number of bits per symbol. Assuming that all M signals have equal probability of being transmitted,

$$p_b = \frac{1}{M \log_2(M)} \sum_{i=1}^{M} \sum_{j=1, j\neq i}^{M} \Pr\{\hat{s} = s_j|s = s_i\} n_{ij}. \tag{12.20}$$

The problem is to determine $\Pr\{\hat{s} = s_j|s = s_i\}$ for all combinations of signal alternatives.
The "full" union bound is obtained by using

$$\Pr\{\hat{s} = s_j|s = s_i\} \leq Q\left(\sqrt{\frac{d_{ij}^2}{2N_0}}\right), \tag{12.21}$$

where d_{ij} is the distance between signals s_i and s_j. Thus, the bounded BER expression is

$$p_b \leq \frac{1}{M \log_2(M)} \sum_{i=1}^{M} \sum_{j=1, j\neq i}^{M} Q\left(\sqrt{\frac{d_{ij}^2}{2N_0}}\right) n_{ij}. \tag{12.22}$$

Using this expression, the bounded BER for Gray coded QPSK is

$$\begin{aligned} p_{b,\mathrm{QPSK}} &\leq \frac{1}{8} \cdot 4 \cdot \left(Q\left(\sqrt{\frac{2E_s}{2N_0}}\right) \cdot 1 + Q\left(\sqrt{\frac{4E_s}{2N_0}}\right) \cdot 2 + Q\left(\sqrt{\frac{2E_s}{2N_0}}\right) \cdot 1 \right) \\ &= Q\left(\sqrt{\frac{E_s}{N_0}}\right) + Q\left(\sqrt{\frac{2E_s}{N_0}}\right) \\ &= Q\left(\sqrt{\frac{2E_b}{N_0}}\right) + Q\left(\sqrt{\frac{4E_b}{N_0}}\right). \end{aligned} \tag{12.23}$$

(b) The exact BER expression is

$$p_{b,\mathrm{QPSK}} = Q\left(\sqrt{\frac{2E_b}{N_0}}\right), \tag{12.24}$$

which means that we overestimate the BER using the full union bound, especially for low E_b/N_0. With the specified amount of difference we have

$$Q\left(\sqrt{\frac{4E_b}{N_0}}\right) = 10^{-5} \tag{12.25}$$

which results in

$$\frac{E_b}{N_0} = 6.58 \text{ dB}. \tag{12.26}$$

For E_b/N_0 above 6.58 dB the difference in error probability between the bound and the exact expression is less than 10^{-5}.

3 Firstly, we calculate the average symbol energy. From the symmetry of the constellation shown in Figure B-25.4, it can be seen that three different groups of constellation points must be treated separately since the points in each groups have the same distance to the origin. The first group is $\{000, 111\}$, the second is $\{101, 011, 001, 010\}$, and the third is $\{100, 110\}$. Since the signal alternatives are equally probable, the average symbol energy is

$$\begin{aligned}
\bar{E}_s &= \frac{1}{M}\sum_{i=1}^{M} d_i^2 \qquad (12.27)\\
&= \frac{1}{8}\left(2\left(\frac{d_{\min}}{2}\right)^2 + 4\left(\sqrt{\left(\frac{d_{\min}}{2}\right)^2 + d_{\min}^2}\right)^2 + 2\left(\frac{3d_{\min}}{2}\right)^2\right)\\
&= \frac{d_{\min}^2}{8}\left(\frac{1}{2} + 5 + \frac{9}{2}\right)\\
&= \frac{5}{4}d_{\min}^2.
\end{aligned}$$

where the d_i is the distance from origo to constellation point i, and $d_{\min}$ is the minimum distance between constellation points, as shown in Figure B-25.4. With 3 bits per symbol, the average energy per bit is $\bar{E}_b = \bar{E}_s/3 = \frac{5}{12}d_{\min}^2$.

The full union bound is given by

$$p_b \leq \frac{1}{M\log_2(M)}\sum_{i=1}^{M}\sum_{j=1, j\neq i}^{M} Q\left(\sqrt{\frac{d_{ij}^2}{2N_0}}\right) n_{ij}\ . \qquad (12.28)$$

If the sum over j, i.e., all the possible erroneous signal alternatives, is reduced to include only the nearest neighbor signal alternatives in the constellation, the nearest neighbor union bound is obtained. Note that this is not a true bound, but rather an approximation of the BER. Thus, to calculate the nearest neighbor union bound we must evaluate

$$p_b \approx \frac{1}{M\log_2(M)}\sum_{i=1}^{M}\sum_{j\in A_i} Q\left(\sqrt{\frac{d_{ij}^2}{2N_0}}\right) n_{ij}, \qquad (12.29)$$

where A_i is the set of nearest neighbors to signal alternative i. In this case, taking the number of bit errors that occur into account, we have

$$\begin{aligned}
p_b &\approx \frac{1}{24}\left(2\cdot Q\left(\sqrt{\frac{d_{\min}^2}{2N_0}}\right) + 2\cdot Q\left(\sqrt{\frac{d_{\min}^2}{2N_0}}\right)(1+1+1+2)\right. \qquad (12.30)\\
&\quad \left. +2\cdot Q\left(\sqrt{\frac{d_{\min}^2}{2N_0}}\right)(2+2) + 2\cdot Q\left(\sqrt{\frac{d_{\min}^2}{2N_0}}\right)(1+2)\right)\\
&= \frac{13}{12}Q\left(\sqrt{\frac{d_{\min}^2}{2N_0}}\right)\\
&= \frac{13}{12}Q\left(\sqrt{\frac{6\bar{E}_b}{5N_0}}\right).
\end{aligned}$$

4 .

(a) In Figure B-25.5, it can be seen that the minimum distance is $d_{\min} = 2\sqrt{E_s}\sin(\pi/8)$. The nearest

neighbor union bound is given by

$$\begin{aligned} p_b &\approx \frac{1}{M\log_2(M)} \sum_{i=1}^{M} \sum_{j \in A_i} Q\left(\sqrt{\frac{d_{ij}^2}{2N_0}}\right) n_{ij} \qquad (12.31) \\ &= \frac{1}{24} \cdot ((2+1)+(1+2)+(2+2)+(2+2)+(2+1) \\ &\quad +(1+2)+(2+2)+(2+2)) \cdot Q\left(\frac{d_{\min}}{\sqrt{2N_0}}\right) \\ &= \frac{7}{6} Q\left(\frac{2\sqrt{E_s}\sin(\pi/8)}{\sqrt{2N_0}}\right) \\ &= \frac{7}{6} Q\left(\sqrt{\frac{6E_b}{N_0}}\sin(\pi/8)\right). \end{aligned}$$

(b) When Gray coding is used, only one bit changes between adjacent constellation points. Thus, the nearest neighbor union bound is given by

$$\begin{aligned} p_b &\approx \frac{1}{24} \cdot 8 \cdot 2 \cdot Q\left(\sqrt{\frac{6E_b}{N_0}}\sin(\pi/8)\right) \qquad (12.32) \\ &= \frac{2}{3} Q\left(\sqrt{\frac{6E_b}{N_0}}\sin(\pi/8)\right). \end{aligned}$$

The approximative gain from the Gray coding at a BER of 10^{-5} is the ratio of the required E_b/N_0 with and without Gray coding. In this case we have

$$\begin{aligned} G_{\text{Gray}} &= \frac{\left(\frac{E_b}{N_0}\right)}{\left(\frac{E_b}{N_0}\right)_{\text{Gray}}} \qquad (12.33) \\ &= \frac{\frac{1}{6}\left(\frac{Q^{-1}\left(\frac{6}{7}\cdot 10^{-5}\right)}{\sin(\pi/8)}\right)^2}{\frac{1}{6}\left(\frac{Q^{-1}\left(\frac{3}{2}\cdot 10^{-5}\right)}{\sin(\pi/8)}\right)^2} \\ &= \left(\frac{Q^{-1}\left(\frac{6}{7}\cdot 10^{-5}\right)}{Q^{-1}\left(\frac{3}{2}\cdot 10^{-5}\right)}\right)^2 \\ &= 0.26 \text{ dB}. \end{aligned}$$

5 Three different methods are used for detecting the symbol errors in the following MATLAB$^{\text{TM}}$ program. In the first case, where BPSK is analyzed, Gaussian noise samples are generated and a threshold is used for determining if a noise sample would have generated a symbol error.

In the second case, where QPSK is analyzed, complex noise samples are generated and added to the transmitted signal constellation point. Then, the angles in the complex plane are used to determine which of the symbols are in error.

Finally, in the case of 8-PSK, complex noise samples are generated and added to the transmitted symbol just as in the QPSK case above, but Euclidean distances are then calculated to all signal alternatives and used for detecting symbol errors.

Simulated BER for coherently detected BPSK, QPSK and 8-PSK can be obtained using the following code:

```
snrstart_dB = 0; % Start Eb/N0 [dB]
snrstop_dB = 15; % Stop Eb/N0 [dB]
snrdelta_dB = 0.5; % Step size [dB]
```

```
samples = 1e6; % Number of samples per Eb/N0 point

% Results (estimated bit error probabilities)
result_antip = [];
result_QPSK = [];
result_8PSK = [];

% Start a loop over the specified Eb/N0 values.
for snr_dB = [snrstart_dB:snrdelta_dB:snrstop_dB]

% Print out current SNR.
snr_dB

% Non-dB Eb/N0
snr = 10^(snr_dB/10);

% Assume that the same symbol is transmitted all the time.
% Note that this is not always a valid assumption.

% ------------------------------------------------------------------
% First, binary antipodal signalling:

% Create zero mean Gaussian noise variables with unit variance.
noise = randn(1,samples);

% snr = Eb/N0
% var = N0/2 = 1
% => N0 = 2
% => Eb = snr*2
% Detection threshold = sqrt(Eb)

% If a (zero mean) noise sample is larger than sqrt(Eb),
% a wrong decision is made.

% How many errors?
error_vector = noise > sqrt(snr*2);
error_antip = sum(error_vector);

% Store results.
result_antip = [result_antip error_antip/samples];

% ------------------------------------------------------------------
% Coherent Gray coded QPSK signalling:
% Note: two bits per symbol.

% snr = Eb/N0
% var = N0/2 = 1 (on both I and Q channels)
% => N0 = 2
% => Eb = snr*2
% Es = 2*Eb => Es = 4*snr

% A correct decision is made if the constellation point angle
% is within pi/4 and -pi/4.

% Create the transmitted signal (at sqrt(Es)).
t = sqrt(4*snr);
```

```
% Create the I and Q noise samples (zero mean, unit variance).
noiseI = randn(1,samples);
noiseQ = randn(1,samples);

% The received signals:
r = t + noiseI + noiseQ*i;

% Angles for all samples:
phi = angle(r);

% How many errors?

% One bit error:
error_vector = phi > pi/4 & phi < 3*pi/4;
error_QPSK = sum(error_vector);
error_vector = phi < -pi/4 & phi > -3*pi/4;
error_QPSK = error_QPSK + sum(error_vector);

% Two bit errors:
error_vector = phi > 3*pi/4 | phi < -3*pi/4;
error_QPSK = error_QPSK + 2*sum(error_vector);
% Store results (two bits per sample).
result_QPSK = [result_QPSK error_QPSK/(samples*2)];

% ------------------------------------------------------------
% Coherent Gray coded 8-PSK signalling:
% Note: three bits per symbol.

% snr = Eb/N0
% var = N0/2 = 1 (on both I and Q channels)
% => N0 = 2
% => Eb = snr*2
% Es = 3*Eb => Es = 6*snr

% A correct decision is made if constellation point angle is
% within pi/8 and -pi/8. Calculate distances to all signal
% alternatives.

% Create signal alternatives.
s = sqrt(6*snr)*exp([0:pi/4:7*pi/4]'*i);

% Create the transmitted signal.
t = sqrt(6*snr);

% Create the I and Q noise samples (zero mean, unit variance).
noiseI = randn(1,samples);
noiseQ = randn(1,samples);

% The received signals:
r = t + noiseI + noiseQ*i;

% Squared distances to all signal alternatives...
% How many errors?

% Difference vector to signal alternative i: r-s(i)
```

```
diff = [];
diff = [diff; abs(r-s(1))];
diff = [diff; abs(r-s(2))];
diff = [diff; abs(r-s(3))];
diff = [diff; abs(r-s(4))];
diff = [diff; abs(r-s(5))];
diff = [diff; abs(r-s(6))];
diff = [diff; abs(r-s(7))];
diff = [diff; abs(r-s(8))];

% Get the indices of the signal alternatives with the minimum
% (squared) distance for each sample.
[MinVal,Index] = min(diff);

% One bit errors:
error_vector = Index == 2; % s(2)
error_8PSK = sum(error_vector);
error_vector = Index == 6; % s(6)
error_8PSK = error_8PSK + sum(error_vector);
error_vector = Index == 8; % s(8)
error_8PSK = error_8PSK + sum(error_vector);

% Two bit errors:
error_vector = Index == 3; % s(3)
error_8PSK = error_8PSK + 2*sum(error_vector);
error_vector = Index == 5; % s(5)
error_8PSK = error_8PSK + 2*sum(error_vector);
error_vector = Index == 7; % s(7)
error_8PSK = error_8PSK + 2*sum(error_vector);

% Three bit errors:
error_vector = Index == 4; % s(4)
error_8PSK = error_8PSK + 3*sum(error_vector);

% Store results (three bits per sample).
result_8PSK = [result_8PSK error_8PSK/(samples*3)];

end

% The Eb/N0 values:
snr_dB = [snrstart_dB:snrdelta_dB:snrstop_dB];

% Plot the results.
figure;
semilogy(snr_dB,Q(sqrt(2*10.^(snr_dB/10))),'-');
hold on;
semilogy(snr_dB,result_antip,'+');
semilogy(snr_dB,result_QPSK,'o');
semilogy(snr_dB,2/3*Q(sqrt(6*10.^(snr_dB/10))*sin(pi/8)),':');
semilogy(snr_dB,result_8PSK,'d');
ylabel('BER');
xlabel('E_b/N_0 [dB]');
legend('Exact BPSK and QPSK','Sim BPSK','Sim QPSK',...
'NNUB 8-PSK','Sim 8-PSK');
```

The code provided above can be used to generate Figure 12.2. It can be seen in Figure 12.2 that the

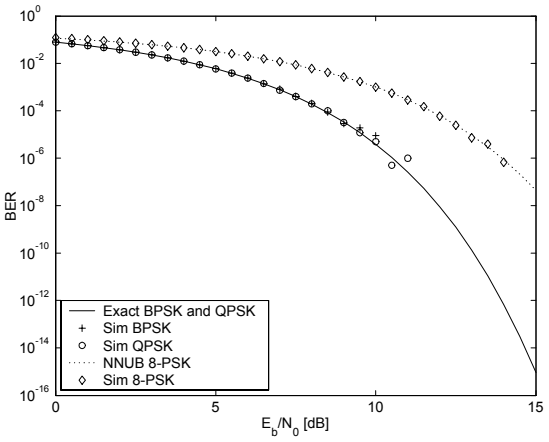

Figure 12.2: Exact and simulated BER for BPSK and QPSK. Nearest neighbor union bound (NNUB) BER and simulated BER for 8-PSK.

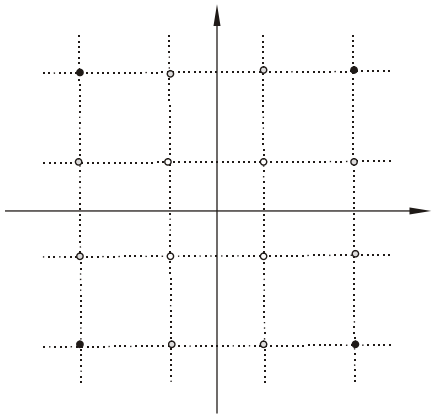

Figure 12.3: 16-QAM signal constellation.

statistics get weaker as the E_b/N_0 is increased since fewer and fewer error events occur. It is however hard to determine in which region the union bound appears to be tight for 8-PSK.

6. We start by calculating nearest neighbor union bound on BER for the 16-QAM modulation scheme, expressed as a function of minimum distance $d_{\min}$. Since the constellation is Gray coded only one bit error occurs when a nearest neighbor constellation point is selected. Due to the symmetry of the 16-QAM constellation, there are three groups of constellation points, where the points in each group have the same distances to the origin and the same numbers of nearest neighbor constellation points (see Figure 12.3). We have

$$\begin{aligned} p_b &\approx \frac{1}{M\log_2(M)} \sum_{i=1}^{M} \sum_{j\in A_i} Q\left(\sqrt{\frac{d_{ij}^2}{2N_0}}\right) n_{ij} \qquad (12.34) \\ &= \frac{1}{64}\left(4\cdot 2 + 8\cdot 3 + 4\cdot 4\right) Q\left(\sqrt{\frac{d_{\min}^2}{2N_0}}\right) \\ &= \frac{3}{4} Q\left(\sqrt{\frac{d_{\min}^2}{2N_0}}\right). \end{aligned}$$

Next, replace $d_{\min}$ with the average bit energy. The average symbol energy (assuming equally probable symbols) is

$$\begin{aligned} \bar{E}_s &= \frac{1}{M}\sum_{i=1}^{M} d_i^2 \\ &= \frac{1}{16}\left(4\cdot\frac{1}{2}+4\cdot\frac{9}{2}+8\cdot\frac{5}{2}\right)d_{\min}^2 \\ &= \frac{5}{2}d_{\min}^2, \end{aligned} \tag{12.35}$$

which means that the average bit energy is $\bar{E}_b = \bar{E}_s/4 = \frac{5}{8}d_{\min}^2$. Thus,

$$\begin{aligned} p_b &\approx \frac{3}{4}Q\left(\sqrt{\frac{d_{\min}^2}{2N_0}}\right) \\ &= \frac{3}{4}Q\left(\sqrt{\frac{4\bar{E}_b}{5N_0}}\right). \end{aligned} \tag{12.36}$$

For the BER not to exceed 10^{-5}, the E_b/N_0 must be above

$$\begin{aligned} \frac{\bar{E}_b}{N_0} &= \frac{5}{4}\left(Q^{-1}\left(\frac{4}{3}\cdot 10^{-5}\right)\right)^2 \\ &= 13.4 \text{ dB} \end{aligned} \tag{12.37}$$

in the case of 16-QAM, and above

$$\begin{aligned} \frac{\bar{E}_b}{N_0} &= \frac{1}{2}\left(Q^{-1}\left(10^{-5}\right)\right)^2 \\ &= 9.6 \text{ dB} \end{aligned} \tag{12.38}$$

in the case of QPSK. Consequently, the useful range of E_b/N_0 for the QPSK mode of operation is between 9.6 and 13.4 dB and above 13.4 dB for the 16-QAM scheme.

7 In general, for M-ary signalling, the probability of symbol error is

$$\begin{aligned} p_s &= \Pr\{e|s=s_i\} \\ &= \sum_{j=1,j\neq i}^{M} \Pr\{\hat{s}=s_j|s=s_i\}, \end{aligned} \tag{12.39}$$

where $\Pr\{\hat{s}=s_j|s=s_i\}$ is the probability for detecting signal alternative j, given that alternative i has been transmitted. Upper bounding this expression using the pairwise probabilities for binary orthogonal signaling, we have

$$\begin{aligned} p_s &= \sum_{j=1,j\neq i}^{M} \Pr\{\hat{s}=s_j|s=s_i\} \\ &\leq (M-1)\cdot Q\left(\sqrt{\frac{E_s}{N_0}}\right) \\ &< M\cdot Q\left(\sqrt{\frac{E_s}{N_0}}\right) \\ &< M\cdot e^{-\frac{E_s}{2N_0}}. \end{aligned} \tag{12.40}$$

This can be rewritten as

$$\begin{aligned} p_s &< M \cdot e^{-\frac{E_s}{2N_0}} \\ &= 2^k \cdot e^{-\frac{kE_b}{2N_0}} \\ &= e^{k\ln 2 - \frac{kE_b}{2N_0}} \\ &= e^{\frac{k}{2}\left(2\ln 2 - \frac{E_b}{N_0}\right)}, \end{aligned} \tag{12.41}$$

and consequently, $p_s \to 0$ as $M \to \infty$ if $E_b/N_0 > 2\ln 2 = 1.42$ dB.

8 .

(a) The BER as functions of $\bar{\gamma}_b = \bar{E}_b/N_0$ for the modulation schemes when the channel is Rayleigh fading and the average bit energy is $\bar{E}_b$, are

Coherent BPSK	$p_b = \frac{1}{2}\left(1 - \sqrt{\frac{\bar{\gamma}_b}{1+\bar{\gamma}_b}}\right)$
Coherent FSK	$p_b = \frac{1}{2}\left(1 - \sqrt{\frac{\bar{\gamma}_b}{2+\bar{\gamma}_b}}\right)$
Differential BPSK	$p_b = \frac{1}{2(1+\bar{\gamma}_b)}$
Non-coherent FSK	$p_b = \frac{1}{2+\bar{\gamma}_b}$.

Using the BER requirement and the above expressions, minimum required $\bar{E}_b/N_0$ are

Coherent BPSK	$\left(\frac{\bar{E}_b}{N_0}\right)_{\min} = \frac{(1-2p_{b,\max})^2}{1-(1-2p_{b,\max})^2} = 2.50 \cdot 10^4$
Coherent FSK	$\left(\frac{\bar{E}_b}{N_0}\right)_{\min} = \frac{2(1-2p_{b,\max})^2}{1-(1-2p_{b,\max})^2} = 5.00 \cdot 10^4$
Differential BPSK	$\left(\frac{\bar{E}_b}{N_0}\right)_{\min} = \frac{1}{2p_{b,\max}} - 1 = 5.00 \cdot 10^4$
Non-coherent FSK	$\left(\frac{\bar{E}_b}{N_0}\right)_{\min} = \frac{1}{p_{b,\max}} - 2 = 10.00 \cdot 10^4$.

With the new required values of $\bar{E}_b/N_0$, the transmit power must be increased with factors of 34.4 dB in the case of coherent detection and 36.6 dB in case of non-coherent detection, i.e., with factors of about 3000. E.g., if DPSK is used, the transmit power must be increased to $P_{TX,\min} = 12$ dBW = 15.8 W to fulfill the requirements on BER.

(b) The BER for DPSK in a Rician channel is given by

$$p_b = \frac{1+K_r}{2\left(\bar{\gamma}_b + 1 + K_r\right)} \exp\left(-\frac{K_r\bar{\gamma}_b}{\bar{\gamma}_b + 1 + K_r}\right). \tag{12.42}$$

This expression can be numerically solved for $p_b = 10^{-5}$ and $K_r = 10$, and the solution is $\bar{\gamma}_b = 76.623$. Thus, the transmit power must be increased by a factor of $10 \cdot \log_{10}(76.623/10.82) = 8.5$ dB. As $K_r \to 0$, the power in the dominating component (direct path) is reduced to zero, which means that the results from the Rayleigh fading channel are expected (use $K_r = 0$ in the expression above).

9 Note that there is a misprint in the formulation of the problem: the noise figure should be 10 dB.

(a) Firstly, we determine the required minimum E_b/N_0 to achieve the required BER of 10^{-4}. The BER of differentially detected MSK is given by

$$p_b = \frac{1}{2\left(1 + \frac{E_b}{N_0}\right)}, \tag{12.43}$$

and thus,

$$\begin{aligned} \left(\frac{E_b}{N_0}\right)_{\min} &= \frac{1}{2p_{b,\max}} - 1 \\ &= 5 \cdot 10^3. \end{aligned} \tag{12.44}$$

The power spectral density of the noise, N_0, is calculated using the receiver noise figure, $F_{\text{sys}} = 10$ dB (converted to linear scale!) as

$$\begin{aligned} N_0 &= k_B(F_{\text{sys}} - 1)T_0 \\ &= 1.38 \cdot 10^{-23} \cdot (10^{10/10} - 1) \cdot 290 \\ &= 3.60 \cdot 10^{-20} \text{ W/Hz}. \end{aligned} \tag{12.45}$$

The required bit energy is then calculated as

$$\begin{aligned} E_{b,\min} &= \left(\frac{E_b}{N_0}\right)_{\min} \cdot N_0 \text{ J} \\ &= 1.8 \cdot 10^{-16} \text{ J}, \end{aligned} \tag{12.46}$$

and the minimum received power at the antenna output is

$$\begin{aligned} C_{\min} &= E_{b,\min} d_b \\ &= 1.8 \cdot 10^{-16} \cdot 3 \cdot 10^3 \\ &= 5.4 \cdot 10^{-13} \text{ W} \\ &= -122.7 \text{ dBW}. \end{aligned} \tag{12.47}$$

Using the transmit power $P_{\text{TX}} = 10$ dBm $= -20$ dBW (EIRP) and the antenna gain of $G_a = 5$ dB, the link budget gived a received power of

$$C = P_{\text{TX}} - L_{\text{PL}} + G_a, \tag{12.48}$$

where L_{PL} is the path loss in dB. Then,

$$\begin{aligned} L_{\text{PL,max}} &= P_{\text{TX}} + G_a - C_{\min} \\ &= -20 + 5 - (-122.7) \\ &= 107.7 \text{ dB} \end{aligned} \tag{12.49}$$

is the maximum tolerable path loss in the system. Using the Okumura-Hata path loss model and the specified carrier frequency and base station and mobile station heights, the maximum distance can be calculated. We have

$$L = A + B \log_{10}(d) + C, \tag{12.50}$$

where d is the cell radius in km. Finally, with

$$\begin{aligned} B &= 44.9 - 6.55 \log_{10}(30) \\ &= 35.2, \end{aligned} \tag{12.51}$$

$$\begin{aligned} C &= -2(\log_{10}(1200/28))^2 - 5.4 \\ &= -10.7, \end{aligned} \tag{12.52}$$

$$\begin{aligned} a &= 3(1.1 \log_{10}(1200) - 0.7)) - (1.56 \log_{10}(1200) - 0.8) \\ &= 4.1, \end{aligned} \tag{12.53}$$

and

$$\begin{aligned} A &= 69.55 + 26.16 \log_{10}(1200) - 13.82 \log_{10}(30) - a \\ &= 125.6, \end{aligned} \tag{12.54}$$

the maximum cell radius can be calculated as

$$\begin{aligned} d_{\max} &= 10^{\frac{L_{\text{PL,max}} - A - C}{B}} \\ &= 0.62 \text{ km}. \end{aligned} \tag{12.55}$$

However, it should be noted that shadow fading has not been considered.

(b) Using

$$\mathrm{BER}_{\mathrm{Doppler}} = \frac{1}{2}\pi^2 (f_{D,\max} T_B)^2, \tag{12.56}$$

where $f_{D,\max}$ is the maximum doppler frequency and T_B is the bit time, we have for an irreducable BER due to frequency dispersion of $\mathrm{BER}_{\mathrm{Doppler}} = 10^{-5}$

$$\begin{aligned} f_{D,\max} &= \frac{\sqrt{2\mathrm{BER}_{\mathrm{Doppler}}}}{\pi T_B} \\ &= 4.27 \text{ Hz} \end{aligned} \tag{12.57}$$

Then, from

$$f_{D,\max} = f_c \frac{v}{c}, \tag{12.58}$$

where v is the terminal velocity and c the speed of light, we obtain a maximum terminal velocity of

$$\begin{aligned} v &= \frac{f_{D,\max} c}{f_c} \\ &= 1.07 \text{ m/s} \\ &= 3.8 \text{ km/h}. \end{aligned} \tag{12.59}$$

10 .

(a) With a BER of p_b, the probability that all 8000 bits in an IP packet are correctly received is $(1-p_b)^{8000}$. The probability that one or more of the bits are in error (i.e., packet error) is then $1-(1-p_b)^{8000}$. Hence, this quantity must not exceed the specified packet error rate $p_p = 10^{-3}$. Thus,

$$\begin{aligned} p_{b,\max} &= 1-(1-p_p)^{1/8000} \\ &= 1.25 \cdot 10^{-7}. \end{aligned} \tag{12.60}$$

With this requirement on BER, the maximum average delay spread S_τ, in the case of MSK over a Rayleigh faded channel, is calculated from

$$p_b = \frac{4}{9}\left(\frac{S_\tau}{T_B}\right)^2, \tag{12.61}$$

which results in

$$\begin{aligned} S_\tau &= \frac{3}{2}\sqrt{p_{b,\max}} T_B \\ &= 5.3 \text{ ns}, \end{aligned} \tag{12.62}$$

where T_B is the bit time given by the specified data rate.

(b) Typical delay spreads in indoor environments are $5-50$ ns, in urban environments $100-800$ ns, and in hilly terrain delay spread can be up to 18 μs, as can be seen from Chapter 7.

Chapter 13

Diversity

1. Equation (B-13.35) is

$$\overline{BER} \approx \left(\frac{1}{4\bar{\gamma}}\right)^{N_\mathrm{r}} \binom{2N_\mathrm{r}-1}{N_\mathrm{r}}. \tag{13.1}$$

   (a) For $N_\mathrm{r} = 1$ and $\bar{\gamma} = 20$ dB we obtain $\overline{BER} \approx 1/4\bar{\gamma} = 2.5 \cdot 10^{-3}$.

   (b) For $N_\mathrm{r} = 3$ and $\bar{\gamma} = 20$ dB we obtain $\overline{BER} \approx \left(\frac{1}{4 \cdot 10^2}\right)^3 \binom{5}{3} \approx 1.6 \cdot 10^{-7}$. The result in (a) is approximately 15000 times larger than in (b).

   (c) In order to achieve $1.6 \cdot 10^{-7}$ with a single-antenna system, we would require $4\bar{\gamma} = 1/1.6 \cdot 10^{-7}$, so that $\bar{\gamma} = 1.6 \cdot 10^6$, which corresponds to 62 dB.

2. Consider RSSI-driven selection diversity and maximum-ratio combining (MRC) diversity.

   (a) The requirement is that the instantaneous SNR, $\gamma = E_b/N_0$, cannot fall below a certain value more than 1% of the time. Figure B-13.10 gives the cdf of the normalized SNR, $\gamma/\bar{\gamma}$, for the two different diversity schemes and different numbers of antenna elements. Outage will occur whenever the SNR goes below a specified value. The probability for such an event can be read out directly from the figure since it is the cdf of the normalized SNR that is shown in the figure. For example, we read out $\gamma/\bar{\gamma} = -20$ dB for 1% outage and one antenna. This means that 1% of the time, $\gamma_{|\mathrm{dB}} = \bar{\gamma}_{|\mathrm{dB}} - 20$ dB, or in other words, γ is 20 dB below the mean, which is also the fading margin.

N_r	RSSI	MRC
1	20 dB	20 dB
2	10 dB	8 dB
3	6 dB	4 dB

(13.2)

   The corresponding diversity gains, D, for RSSI-driven diversity are given by

$$\begin{aligned} D_{\mathrm{RSSI},M=2} &= 20 - 10 = 10 \text{ dB} \\ D_{\mathrm{RSSI},M=3} &= 20 - 6 = 14 \text{ dB} \end{aligned} \tag{13.3}$$

   and for MRC diversity

$$\begin{aligned} D_{\mathrm{MRC},M=2} &= 20 - 8 = 12 \text{ dB} \\ D_{\mathrm{MRC},M=2} &= 20 - 4 = 16 \text{ dB} \end{aligned} \tag{13.4}$$

   (b) For a BER of 10^{-3}, Figure B-13.11 gives the following requirements on the SNR

N_r	RSSI	MRC
1	26 dB	26 dB
2	15 dB	13 dB
3	11 dB	9 dB

The corresponding diversity gains for RSSI-driven diversity are given by

$$\begin{aligned} D_{\mathrm{RSSI},M=2} &= 26-15=11 \text{ dB} \\ D_{\mathrm{RSSI},M=3} &= 26-11=15 \text{ dB} \end{aligned} \tag{13.5}$$

and for MRC diversity

$$\begin{aligned} D_{\mathrm{MRC},M=2} &= 26-13=13 \text{ dB} \\ D_{\mathrm{MRC},M=3} &= 26-9=17 \text{ dB}. \end{aligned} \tag{13.6}$$

(c) With 10 % probability of outage, Figure B-13.10 gives

N_r	RSSI	MRC
1	10 dB	10 dB
2	4 dB	5 dB
3	2 dB	0 dB

(13.7)

with corresponding values on the diversity gain given by

$$\begin{aligned} D_{\mathrm{RSSI},M=2} &= 10-4=6 \text{ dB} \\ D_{\mathrm{RSSI},M=3} &= 10-2=8 \text{ dB} \\ D_{\mathrm{MRC},M=2} &= 10-5=5 \text{ dB} \\ D_{\mathrm{RSSI},M=3} &= 10-0=10 \text{ dB} \end{aligned} \tag{13.8}$$

With a new BER of 10^{-2}, Figure B-13.11 gives

N_r	RSSI	MRC
1	16 dB	16 dB
2	9 dB	7 dB
3	6 dB	5 dB

(13.9)

The corresponding diversity gains are given by

$$\begin{aligned} D_{\mathrm{RSSI},M=2} &= 16-9=7 \text{ dB} \\ D_{\mathrm{RSSI},M=3} &= 16-6=10 \text{ dB} \\ D_{\mathrm{MRC},M=2} &= 16-7=9 \text{ dB} \\ D_{\mathrm{RSSI},M=3} &= 16-5=11 \text{ dB} \end{aligned} \tag{13.10}$$

It is evident that the diversity gain increases when the specified values of BER and outage probability are small.

3. Let the average SNR be Γ.

(a) When only one antenna is used the probability that the SNR is below a threshold γ_t, i.e., the probability that an outage occurs, is

$$P_\mathrm{out} = 1 - e^{-\gamma_\mathrm{t}/\Gamma}. \tag{13.11}$$

The fading margin is thus

$$M_1 = \frac{\Gamma}{\gamma_\mathrm{t}} = -\frac{1}{\ln\left(1-P_\mathrm{out}\right)}. \tag{13.12}$$

(b) When two antennas are used, the probability that the SNR after the selection device is below a threshold γ_t is

$$P_\mathrm{out} = \left(1 - e^{-\gamma_\mathrm{t}/\Gamma}\right)^2. \tag{13.13}$$

The fading margin is thus

$$M_2 = \frac{\Gamma}{\gamma_\mathrm{t}} = -\frac{1}{\ln\left(1-\sqrt{P_\mathrm{out}}\right)}. \tag{13.14}$$

(c) The diversity gain is the decrease in fading margin that is obtained when going from one to two antennas. This decrease is

$$\begin{aligned}\frac{M_1}{M_2} &= \frac{-\frac{1}{\ln(1-P_{\text{out}})}}{-\frac{1}{\ln\left(1-\sqrt{P_{\text{out}}}\right)}} = \frac{\ln\left(1-\sqrt{P_{\text{out}}}\right)}{\ln\left(1-P_{\text{out}}\right)} \\ &= \frac{\ln\left(1-\sqrt{0.01}\right)}{\ln\left(1-0.01\right)} \approx 10 \text{ dB}.\end{aligned} \tag{13.15}$$

4. The BER of BPSK on AWGN is given by

$$\text{BER}\left(\gamma\right) = \frac{1}{2}\text{erfc}\left(\sqrt{\gamma}\right). \tag{13.16}$$

If the BER requirement is BER_{t}, this gives the SNR threshold as

$$\gamma_{\text{t}} = \left[\text{erfc}^{-1}\left(2\text{BER}_{\text{t}}\right)\right]^2, \tag{13.17}$$

where $\text{erfc}^{-1}\left(x\right)$ is the inverse of the complementary error function. Equation (B-13.17) gives the pdf of the output SNR of an $N_{\text{r}}-$th order maximal ratio combiner. However, the total energy in the power delay profile is fixed; in other words, increasing N_{r} does not change the mean SNR. Thus we must replace $\bar{\gamma}$ in Eq. (B-13.17) with $\bar{\gamma}_c/N_{\text{r}}$. We require that the probability that the instantaneous SNR is less than γ_{t} is less than P_{out}, which gives the following inequality

$$\int_0^{\gamma_{\text{t}}} \frac{1}{(N_{\text{r}}-1)!}\frac{\gamma^{N_{\text{r}}-1}}{\left(\frac{\bar{\gamma}_c}{N_{\text{r}}}\right)^{N_{\text{r}}}}e^{-\gamma N_{\text{r}}/\bar{\gamma}_c}d\gamma < P_{\text{out}} \tag{13.18}$$

We then substitute $t = \gamma N_{\text{r}}/\bar{\gamma}_c$, which gives

$$\begin{aligned}&\int_0^{\gamma_{\text{t}} N_{\text{r}}/\bar{\gamma}_c} \frac{1}{(N_{\text{r}}-1)!}\frac{\left(\frac{t\bar{\gamma}_c}{N_{\text{r}}}\right)^{N_{\text{r}}-1}}{\left(\frac{\bar{\gamma}_c}{N_{\text{r}}}\right)^{N_{\text{r}}}}e^{-t}\frac{\bar{\gamma}_c}{N_{\text{r}}}dt \\ &= \int_0^{\gamma_{\text{t}} N_{\text{r}}/\bar{\gamma}_c} \frac{1}{(N_{\text{r}}-1)!}t^{N_{\text{r}}-1}e^{-t}dt \\ &= \Gamma\left(\frac{\gamma_{\text{t}} N_{\text{r}}}{\bar{\gamma}_c}, N_{\text{r}}\right),\end{aligned} \tag{13.19}$$

where $\Gamma(.,.)$ is the incomplete Gamma function. We now need to find numerically the smallest N_{r} for which

$$\Gamma\left(\frac{\left[\text{erfc}^{-1}\left(2\text{BER}_{\text{t}}\right)\right]^2 N_{\text{r}}}{\bar{\gamma}_c}, N_{\text{r}}\right) < P_{\text{out}}, \tag{13.20}$$

which using $\text{BER}_{\text{t}} = 10^{-3}$, $\bar{\gamma}_c = 15$ dB, and $P_{\text{out}} = 1\%$ produces the following values

N_{r}	$\Gamma\left(\cdot,\cdot\right)$
1	0.1401
2	0.0374
3	0.0111
4	0.0034

(13.21)

Thus, four resolvable multipaths reduce the fluctuations of the combiner, or Rake, output sufficiently to achieve the BER requirement.

5. The mean SNR with H-S/MRC is given by Eq. (B-13.29) as

$$\Gamma_{\text{H-S/MRC}} = L\left(1 + \sum_{n=L+1}^{N}\frac{1}{n}\right)\bar{\Gamma}, \tag{13.22}$$

where $\bar{\Gamma}$ is the branch SNR. Using the equation above with $L = N = 5$, the mean SNR for "full" MRC becomes

$$\Gamma_{\text{MRC}} = N\left(1 + \sum_{n=N+1}^{N} \frac{1}{n}\right)\bar{\Gamma} = N\bar{\Gamma} = 5\bar{\Gamma}. \tag{13.23}$$

For H-S/MRC where the $L = 3$ strongest out of $N = 5$ diversity branches are chosen, we obtain

$$\Gamma_{\text{H-S/MRC}} = 3\left(1 + \sum_{n=3+1}^{5} \frac{1}{n}\right)\bar{\Gamma} = 4.35\bar{\Gamma}. \tag{13.24}$$

The loss in mean SNR is therefore

$$\frac{\Gamma_{\text{H-S/MRC}}}{\Gamma_{\text{MRC}}} = \frac{4.35\bar{\Gamma}}{5\bar{\Gamma}} = 0.87 = -0.6 \text{ dB}. \tag{13.25}$$

6. The scheme in this problem is called the *Alamouti scheme* (see also Chapter 20).

   (a) The outputs become

$$\begin{aligned} r_1 &= s_1 h_1 + s_2 h_2 + n_1 \\ r_2 &= s_2^* h_1 - s_1^* h_2 + n_2. \end{aligned} \tag{13.26}$$

   (b) We compute $\hat{s}_1$ and $\hat{s}_2$

$$\begin{aligned} \hat{s}_1 &= h_1^* r_1 - h_2 r_2^* \\ &= h_1^*\left(s_1 h_1 + s_2 h_2 + n_1\right) - h_2\left(s_2 h_1^* - s_1 h_2^* + n_2^*\right) \\ &= s_1|h_1|^2 + s_2 h_1^* h_2 + h_1^* n_1 - s_2 h_1^* h_2 + s_1|h_2|^2 - h_2 n_2^* \\ &= s_1\left(|h_1|^2 + |h_2|^2\right) + h_1^* n_1 - h_2 n_2^* \\ &= s_1\left(\alpha_1^2 + \alpha_2^2\right) + h_1^* n_1 - h_2 n_2^* \\ \hat{s}_2 &= h_2^* r_1 + h_1 r_2^* \\ &= h_2^*\left(s_1 h_1 + s_2 h_2 + n_1\right) + h_1\left(s_2 h_1^* - s_1 h_2^* + n_2^*\right) \\ &= s_1 h_1 h_2^* + s_2|h_2|^2 + h_2^* n_1 + s_2|h_1|^2 - s_1 h_1 h_2^* + h_1 n_2^* \\ &= s_2\left(\alpha_1^2 + \alpha_2^2\right) + h_1 n_2^* + h_2^* n_1. \end{aligned} \tag{13.27}$$

   For the single antenna case, let the transmitted symbol be s, the attenuation $h = \alpha e^{-j\phi}$, and the noise n. The SNR then becomes

$$\gamma_{\text{s-a}} = \frac{E\left(|hs|^2\right)}{E\left(|n|^2\right)} = \frac{|h|^2 E\left(|s|^2\right)}{N_0} = \frac{\alpha^2 E_s}{N_0}, \tag{13.28}$$

   where E_s is the signal energy and N_0 is the AWGN variance. For the two transmit antenna case, the SNR becomes

$$\gamma_{\text{t-a}} = \frac{E\left(|s_1\left(\alpha_1^2 + \alpha_2^2\right)|^2\right)}{E\left(|h_1^* n_1 - h_2 n_2^*|^2\right)} = \frac{\left(\alpha_1^2 + \alpha_2^2\right)^2 E\left(|s_1|^2\right)}{\left(\alpha_1^2 + \alpha_2^2\right) N_0} = \frac{\left(\alpha_1^2 + \alpha_2^2\right)}{2}\frac{E_s}{N_0}. \tag{13.29}$$

   We see that the scheme can be viewed as an addition of two single antenna SNRs, although a 3 dB penalty is paid since the power per antenna must be halved.

7. Let the instantaneous SNR at the kth antenna, or branch, be given by the random variable Γ_k, with mean value $\bar{\gamma}_k$. The output of a maximal ratio combiner consists of a sum of the individual branch SNR's, i.e.,

$$\Gamma_{\text{MRC}} = \sum_{k=1}^{N_{\text{r}}} \Gamma_k. \tag{13.30}$$

If the fading is Rayleigh, the branch SNRs are exponentially distributed, and therefore

$$pdf_{\Gamma_k}(\gamma) = \frac{1}{\bar{\gamma}_k} e^{-\gamma/\bar{\gamma}_k}. \tag{13.31}$$

To derive the pdf of the combiner output $\Gamma_{\rm MRC}$, we can perform an $N_{\rm r}$-fold convolution of the branch pdf's. Another approach is to utilize a transform. Let the moment generating function (MGF) of a random variable X be defined as

$$\psi_X(s) = E\left[e^{-sX}\right]. \tag{13.32}$$

Then the MGF of $\Gamma_{\rm MRC}$ is

$$\psi_{\Gamma_{\rm MRC}}(s) = \prod_{k=1}^{N_{\rm r}} \psi_{\Gamma_k}(s). \tag{13.33}$$

In our case the MGF of a branch SNR is given by

$$\begin{aligned} \psi_{\Gamma_k}(s) &= E\left[e^{-s\Gamma_k}\right] \\ &= \int_0^\infty e^{-s\gamma} pdf_{\Gamma_k}(\gamma)\, d\gamma \\ &= \int_0^\infty e^{-s\gamma} \frac{1}{\bar{\gamma}_k} e^{-\gamma/\bar{\gamma}_k} d\gamma \\ &= \frac{1}{1+\bar{\gamma}_k s}. \end{aligned} \tag{13.34}$$

The inverse of $\psi_{\Gamma_{\rm MRC}}(s)$ is then found by table look-up.

(a) For the case of equal branch powers we have that

$$\begin{aligned} \psi_{\Gamma_{\rm MRC}}(s) &= \prod_{k=1}^{N_{\rm r}} \psi_{\Gamma_k}(s) \\ &= \left(\frac{1}{1+\bar{\gamma}s}\right)^{N_{\rm r}}. \end{aligned} \tag{13.35}$$

Table look-up will reveal that

$$\int_0^\infty \frac{t^{n-1}e^{-at}}{(n-1)!} e^{-st} dt = \left(\frac{1}{s+a}\right)^n, \tag{13.36}$$

which gives that

$$pdf_{\Gamma_{\rm MRC}}(\gamma) = \left(\frac{1}{\bar{\gamma}}\right)^{N_{\rm r}} \frac{\gamma^{N_{\rm r}-1} e^{-\gamma/\bar{\gamma}}}{(N_{\rm r}-1)!}, \quad \gamma \geq 0. \tag{13.37}$$

(b) For the case of distinct branch powers, the MGF of $\Gamma_{\rm MRC}$ is given by

$$\psi_{\Gamma_{\rm MRC}}(s) = \prod_{k=1}^{N_{\rm r}} \frac{1}{1+\bar{\gamma}_k s}. \tag{13.38}$$

By using partial fraction expansion this expression can also be written as

$$\psi_{\Gamma_{\rm MRC}}(s) = \sum_{k=1}^{N_{\rm r}} \frac{\mu_k}{1+\bar{\gamma}_k s}, \tag{13.39}$$

where

$$\mu_k = \prod_{\substack{\ell=1 \\ \ell \neq k}}^{N_{\rm r}} \frac{\bar{\gamma}_k}{\bar{\gamma}_k - \bar{\gamma}_\ell}. \tag{13.40}$$

We can therefore again utilize (13.36), with $n=1$, to obtain the answer

$$pdf_{\Gamma_{\rm MRC}}(\gamma) = \sum_{k=1}^{N_{\rm r}} \frac{\mu_k}{\bar{\gamma}_k} e^{-\gamma/\bar{\gamma}_k}. \tag{13.41}$$

8. The $k-$th matched filter correlates the received signal with a complex-conjugate replica of the wideband transmitted signal. The replica is delayed τ_k, and before combining the output of the $k-$th matched filter is weighed with the complex-conjugate of the fading gain of the $k-$th multipath, h_k. At the output of the $k-$th matched filter we thus have

$$\begin{aligned} q_k &= h_k^* \int_0^T \xi^*\left(t-\tau_k\right) r\left(t\right) dt \\ &= h_k^* \int_0^T \xi^*\left(t-\tau_k\right) \left[\sum_{m=1}^{N_{\mathrm{r}}} h_m \xi\left(t-\tau_m\right) + n\left(t\right)\right] dt \\ &= h_k^* \sum_{m=1}^{N_{\mathrm{r}}} h_m \int_0^T \xi^*\left(t-\tau_k\right) \xi\left(t-\tau_m\right) dt + h_k^* \int_0^T \xi^*\left(t-\tau_k\right) n\left(t\right) dt. \end{aligned} \tag{13.42}$$

We now use the assumption that the wideband transmitted signal has perfect autocorrelation properties. This is equivalent to

$$\int_0^T \xi^*\left(t-\tau_k\right) \xi\left(t-\tau_m\right) dt = \left\{ \begin{array}{ll} E_s, & k=m \\ 0, & k \neq m \end{array} \right. , \tag{13.43}$$

which simplifies the expression for q_k to

$$\begin{aligned} q_k &= h_k^* h_k E_s + h_k^* \int_0^T \xi\left(t-\tau_k\right) n\left(t\right) dt \\ &= |h_k|^2 E_s + h_k^* n_k. \end{aligned} \tag{13.44}$$

Here n_k is the noise term with variance $E_s N_0$, which is equal for all n_k. The SNR at the output of the kth matched filter is

$$\begin{aligned} \Gamma_k &= \frac{E_s^2 \left(|h_k|^2\right)^2}{|h_k^*|^2 E\left(|n_k|^2\right)} = \frac{E_s^2 \alpha_k^2}{E_s N_0} \\ &= \frac{E_s \alpha_k^2}{N_0}. \end{aligned} \tag{13.45}$$

The combiner adds the outputs of the matched filters to obtain

$$\begin{aligned} q_{\mathrm{tot}} &= \sum_{k=1}^{N_{\mathrm{r}}} q_k \\ &= \sum_{k=1}^{N_{\mathrm{r}}} \left(E_s |h_k|^2 + h_k^* n_k\right). \end{aligned} \tag{13.46}$$

The SNR of q_{tot} is

$$\begin{aligned} \Gamma &= \frac{E_s^2 \left(\sum_{k=1}^{N_{\mathrm{r}}} |h_k|^2\right)^2}{E\left(\left|\sum_{k=1}^{N_{\mathrm{r}}} h_k^* n_k\right|^2\right)} \\ &= \frac{E_s^2 \left(\sum_{k=1}^{N_{\mathrm{r}}} |h_k|^2\right)^2}{\sum_{k=1}^{N_{\mathrm{r}}} |h_k|^2 E(|n_k|^2)} \\ &= \frac{E_s \left(\sum_{k=1}^{N_{\mathrm{r}}} \alpha_k^2\right)^2}{N_0}, \end{aligned} \tag{13.47}$$

and, finally, we have

$$\begin{aligned} \Gamma &= \frac{E_s \sum_{k=1}^{N_{\mathrm{r}}} \alpha_k^2}{N_0} \\ &= \sum_{k=1}^{N_{\mathrm{r}}} \Gamma_k. \end{aligned} \tag{13.48}$$

This result shows that the Rake functions as a maximum ratio combiner since the SNRs of the multipaths are added.

9. Let the mean SNR on both branches be $\bar{\gamma}$.

   (a) Since we have Rayleigh fading, the SNRs for the individual branches are exponentially distributed with mean $\bar{\gamma}$. The cdf is therefore given by

$$\begin{aligned} cdf_{\Gamma_s}(\gamma) &= \begin{cases} \Pr(\Gamma_1 \le \gamma_T \text{ and } \Gamma_2 \le \gamma), & \text{for } \gamma < \gamma_t \\ \Pr(\gamma_t \le \Gamma_1 \le \gamma \text{ or } [\Gamma_1 \le \gamma_t \text{ and } \Gamma_2 \le \gamma]), & \text{for } \gamma \ge \gamma_t \end{cases} \\ &= \begin{cases} \left(1 - e^{-\gamma_t/\bar{\gamma}}\right)\left(1 - e^{-\gamma/\bar{\gamma}}\right), & \text{for } \gamma < \gamma_t \\ e^{-\gamma_t/\bar{\gamma}} - e^{-\gamma/\bar{\gamma}} + \left(1 - e^{-\gamma_t/\bar{\gamma}}\right)\left(1 - e^{-\gamma/\bar{\gamma}}\right), & \text{for } \gamma \ge \gamma_t \end{cases}. \end{aligned} \tag{13.49}$$

   The pdf is found by differentiation of the cdf as

$$\begin{aligned} pdf_{\Gamma_s}(\gamma) &= \frac{d}{d\gamma} cdf_{\Gamma_s}(\gamma) \\ &= \begin{cases} \left(1 - e^{-\gamma_t/\bar{\gamma}}\right)\frac{1}{\bar{\gamma}} e^{-\gamma/\bar{\gamma}}, & \text{for } \gamma < \gamma_t \\ \left(2 - e^{-\gamma_t/\bar{\gamma}}\right)\frac{1}{\bar{\gamma}} e^{-\gamma/\bar{\gamma}}, & \text{for } \gamma \ge \gamma_t \end{cases}. \end{aligned} \tag{13.50}$$

   (b) The mean SNR is given by

$$\begin{aligned} E(\Gamma_s) &= \int_0^\infty \gamma pdf_{\Gamma_s}(\gamma)\, d\gamma \\ &= \int_0^{\gamma_t} \gamma \left(1 - e^{-\gamma_t/\bar{\gamma}}\right)\frac{1}{\bar{\gamma}} e^{-\gamma/\bar{\gamma}} d\gamma \\ &\quad + \int_{\gamma_t}^\infty \gamma \left(2 - e^{-\gamma_t/\bar{\gamma}}\right)\frac{1}{\bar{\gamma}} e^{-\gamma/\bar{\gamma}} d\gamma \\ &= \bar{\gamma} + \gamma_t e^{-\gamma_t/\bar{\gamma}}. \end{aligned} \tag{13.51}$$

   The switching threshold γ_t^* that maximizes the mean SNR is found by differentiating $E(\Gamma_s)$

$$\frac{d}{d\gamma_t} E(\Gamma_s) = \left(1 - \frac{\gamma_t}{\bar{\gamma}}\right) e^{-\gamma_t/\bar{\gamma}}. \tag{13.52}$$

   The optimum threshold is therefore $\gamma_t^* = \bar{\gamma}$, and for this case the mean SNR becomes

$$E(\Gamma_s) = \left(1 + e^{-1}\right)\bar{\gamma}. \tag{13.53}$$

   Thus we have a 1.4 dB increase in the mean SNR compared to using a single antenna. For two-branch MRC the gain would be 3 dB and for two-branch selection diversity the gain would be 1.8 dB.

   (c) The average BER is given by

$$\begin{aligned} \overline{\text{BER}} &= \int_0^\infty \text{BER}(\gamma)\, pdf_{\Gamma_s}(\gamma)\, d\gamma \\ &= \int_0^{\gamma_t} \frac{1}{2} e^{-\gamma} \left(1 - e^{-\gamma_t/\bar{\gamma}}\right)\frac{1}{\bar{\gamma}} e^{-\gamma/\bar{\gamma}} d\gamma \\ &\quad + \int_{\gamma_t}^\infty \frac{1}{2} e^{-\gamma} \left(2 - e^{-\gamma_t/\bar{\gamma}}\right)\frac{1}{\bar{\gamma}} e^{-\gamma/\bar{\gamma}} d\gamma \\ &= \frac{1}{2(1+\bar{\gamma})}\left(1 - e^{-\gamma_t/\bar{\gamma}} + e^{-\left(1+\frac{1}{\bar{\gamma}}\right)\gamma_t}\right). \end{aligned} \tag{13.54}$$

   The optimum (with respect to the average BER) threshold is given by differentiating with respect to γ_t

$$\begin{aligned} &\frac{d}{d\gamma_t}\frac{1}{2(1+\bar{\gamma})}\left(1 - e^{-\gamma_t/\bar{\gamma}} + e^{-\left(1+\frac{1}{\bar{\gamma}}\right)\gamma_t}\right) \\ &= \frac{1}{2(1+\bar{\gamma})}\left(\frac{1}{\bar{\gamma}} e^{-\gamma_t/\bar{\gamma}} - \frac{1}{1+\frac{1}{\bar{\gamma}}} e^{-\left(1+\frac{1}{\bar{\gamma}}\right)\gamma_t}\right). \end{aligned} \tag{13.55}$$

Setting the derivative to zero yields

$$\gamma_{\mathrm{t}}^{*} = \ln\left(\frac{\bar{\gamma}}{1+\frac{1}{\bar{\gamma}}}\right). \tag{13.56}$$

The average BER with the optimum threshold can now be expressed as

$$\begin{aligned}\overline{\mathrm{BER}} &= \frac{1}{2\left(1+\bar{\gamma}\right)}\left(1-e^{-\gamma_{\mathrm{t}}^{*}/\bar{\gamma}}+e^{-\left(1+\frac{1}{\bar{\gamma}}\right)\gamma_{\mathrm{t}}^{*}}\right) \qquad (13.57)\\ &= \frac{1}{2\left(1+\bar{\gamma}\right)}\left[1-\left(\frac{1+\frac{1}{\bar{\gamma}}}{\bar{\gamma}}\right)^{1/\bar{\gamma}}+\left(\frac{1+\frac{1}{\bar{\gamma}}}{\bar{\gamma}}\right)^{\left(1+\frac{1}{\bar{\gamma}}\right)}\right].\end{aligned}$$

For an average branch SNR of $\bar{\gamma} = 15$ dB, we obtain $\overline{\mathrm{BER}} = 2\cdot 10^{-3}$.

10. The SNR pdf of an N_{r}-branch ideal maximal ratio combiner is

$$pdf_{\gamma}\left(\gamma\right) = \frac{\gamma^{N_{\mathrm{r}}-1}}{(N_{\mathrm{r}}-1)!\Gamma^{N_{\mathrm{r}}}}e^{-\gamma/\Gamma}. \tag{13.58}$$

Rearranging the terms in the pdf that is given in the problem gives

$$pdf_{\gamma}\left(\gamma\right) = \sum_{n=0}^{N_{\mathrm{r}}-1}\binom{N_{\mathrm{r}}-1}{n}\frac{\left(1-\rho^{2}\right)^{N_{\mathrm{r}}-1-n}\rho^{2n}}{n\left(n-1\right)!}\frac{\gamma^{n}}{\Gamma^{n+1}}e^{-\gamma/\Gamma}, \tag{13.59}$$

and substituting $n = s-1$ gives

$$\begin{aligned}pdf_{\gamma}\left(\gamma\right) &= \sum_{s=1}^{N_{\mathrm{r}}}\binom{N_{\mathrm{r}}-1}{s-1}\frac{\left(1-\rho^{2}\right)^{N_{\mathrm{r}}-s}\rho^{2(s-1)}}{(s-1)!}\frac{\gamma^{s-1}}{\Gamma^{s}}e^{-\gamma/\Gamma} \qquad (13.60)\\ &= \sum_{s=1}^{N_{\mathrm{r}}}A\left(s\right)\frac{\gamma^{s-1}}{(s-1)!\Gamma^{s}}e^{-\gamma/\Gamma},\end{aligned}$$

where

$$A\left(s\right) = \binom{N_{\mathrm{r}}-1}{s-1}\left(1-\rho^{2}\right)^{N_{\mathrm{r}}-s}\rho^{2(s-1)}. \tag{13.61}$$

(a) When $\rho = 0$, all the terms in the pdf become zero except when $s = 1$, and we thus have

$$pdf_{\gamma}\left(\gamma\right) = \frac{1}{\Gamma}e^{-\gamma/\Gamma}, \quad \rho = 0, \tag{13.62}$$

which is the pdf of the SNR for a single branch.

(b) When $\rho = 1$, all the terms in the pdf become zero except when $s = N_{\mathrm{r}}$, and we thus have

$$pdf_{\gamma}\left(\gamma\right) = \frac{1}{(N_{\mathrm{r}}-1)!}\frac{\gamma^{N_{\mathrm{r}}-1}}{\Gamma^{N_{\mathrm{r}}}}e^{-\gamma/\Gamma}, \quad \rho = 1, \tag{13.63}$$

which is the pdf of the SNR of an N_{r}-branch ideal maximal ratio combiner.

(c) Let the instantaneous error rate be $P\left(\gamma\right)$. The average error rate then becomes

$$\begin{aligned}P_{E} &= \int_{0}^{\infty}P\left(\gamma\right)pdf_{\gamma}\left(\gamma\right)d\gamma \qquad (13.64)\\ &= \int_{0}^{\infty}P\left(\gamma\right)\sum_{s=1}^{N_{\mathrm{r}}}A\left(s\right)\frac{\gamma^{s-1}}{(s-1)!\Gamma^{s}}e^{-\gamma/\Gamma}d\gamma\\ &= \sum_{s=1}^{N_{\mathrm{r}}}A\left(s\right)\int_{0}^{\infty}P\left(\gamma\right)\frac{\gamma^{s-1}}{(s-1)!\Gamma^{s}}e^{-\gamma/\Gamma}d\gamma.\end{aligned}$$

The definition of $P_e(\Gamma, s)$ is

$$P_e(\Gamma, s) = \int_0^\infty P(\gamma) \frac{\gamma^{s-1}}{(s-1)!\Gamma^s} e^{-\gamma/\Gamma} d\gamma, \tag{13.65}$$

and we can thus substitute the integral for $P_e(\Gamma, s)$. This yields

$$P_E = \sum_{s=1}^{N_r} A(s) P_e(\Gamma, s) \tag{13.66}$$

(d) Using the approximate expression for $P_e(\Gamma, s)$ gives the average error rate for large mean SNRs as

$$P_E = \sum_{s=1}^{N_r} A(s) \frac{C(s)}{\Gamma^s}. \tag{13.67}$$

This sum is for large mean SNRs dominated by the first term, and the average error rate approximately becomes

$$P_E = \left(1-\rho^2\right)^{N_r-1} \frac{C(1)}{\Gamma}. \tag{13.68}$$

Note that this corresponds to a system with no diversity.

11. The SNR for the $k-$th branch is given by the useful energy divided by the AWGN variance as

$$\gamma_k = \frac{s_k^2}{N_0}. \tag{13.69}$$

The total AWGN variance after combining is

$$N_t = N_0 \sum_{k=1}^{N_r} \alpha_k^2, \tag{13.70}$$

and the total useful energy after combining is

$$E_t = \left(\sum_{k=1}^{N_r} \alpha_k s_k \right)^2. \tag{13.71}$$

The SNR after combining thus becomes

$$\begin{aligned} \gamma &= \frac{E_t}{N_t} \\ &= \frac{\left(\sum_{k=1}^{N_r} \alpha_k s_k\right)^2}{N_0 \sum_{k=1}^{N_r} \alpha_k^2}. \end{aligned} \tag{13.72}$$

Cauchy's inequality states that

$$\left(\sum_{k=1}^{n} a_k b_k \right)^2 \leq \left(\sum_{k=1}^{n} a_k^2 \right) \left(\sum_{k=1}^{n} b_k^2 \right), \tag{13.73}$$

with equality for $a_k = c b_k$, where c is an arbitrary constant. The maximal SNR after combining is therefore given by

$$\gamma = \frac{\sum_{k=1}^{N_r} \alpha_k^2 \sum_{k=1}^{N_r} \alpha_k^2}{N_0 \sum_{k=1}^{N_r} \alpha_k^2} = \frac{\sum_{k=1}^{N_r} \alpha_k^2}{N_0}, \tag{13.74}$$

which with $\alpha_k = s_k$ gives that

$$\gamma = \sum_{k=1}^{N_r} \gamma_k. \tag{13.75}$$

The maximal ratio combining rule thus corresponds to adding the branch SNRs.

Chapter 14

Channel coding

1. (a) Systematic coding is done by letting the codeword be $X(x) = P(x) + x^{N-K}U(x)$, where $P(x)$ is the remainder when dividing $x^{N-K}U(x)$ by $G(x)$, i.e.

$$x^{N-K}U(x) = x^4(x^2+1) = x^6 + x^4 \tag{14.1}$$

Polynomial division gives $P(x) = x + 1$, and the codeword is

$$X(x) = x^6 + x^4 + x + 1. \tag{14.2}$$

(b) The syndrome is given by the remainder when dividing by $G(x)$. We see that $R(x) = x^6 + x^5 + x^4 + x + 1$ only differs from $X(x)$ (in (a)) by x^5. Using this we can perform a simple polynomial division $x^5/G(x)$ instead of $R(x)/G(x)$. This gives

$$S(x) = x^2 + x + 1. \tag{14.3}$$

(c) First we calculate the syndromes for all single-error patterns and all dual-error patterns, with errors adjacent to each other. If all these syndromes are unique a decoder can distinguish between them and we have proven the claim.

2. Yes, the entire code can be found from the given information. By using the cyclic property and, e.g., shifting the given code word three steps to the left, we get three new codewords (one for each shift). The four codewords are (in vector form):

Codeword	x^6	x^5	x^4	x^3	x^2	x	1
$\mathbf{x}_1$	0	0	1	0	1	1	0
$\mathbf{x}_2$	0	1	0	1	1	0	0
$\mathbf{x}_3$	1	0	1	1	0	0	0
$\mathbf{x}_4$	0	1	1	0	0	0	1

(14.4)

These code words are linerarly independent and span the whole code space. We can create the code words for $U(x) = 1$, x, x^2 and x^3 with the linear combinations $\mathbf{x}_1 + \mathbf{x}_2 + \mathbf{x}_4$, $\mathbf{x}_1$, $\mathbf{x}_1 + \mathbf{x}_4$ or $\mathbf{x}_2 + \mathbf{x}_3 + \mathbf{x}_4$. Using the linear property, all other codewords can easily be calculated.

3. To prove that the generator polynomial $G(x)$ is the only codeword with degree $N - K$ we use two properties of cyclic codes: 1) the sum of two codewords is another codeword and 2) all codewords have $G(x)$ as a factor. First we assume that there exist at least two codewords of degree $N - K$. The first being the gerenerator polynomial itself $G(x) = x^{N-K} + g_{N-K-1}x^{N-K-1} + \ldots + g_0$ and some other codeword $X(x) = x^{N-K} + a_{N-K-1}x^{N-K-1} + \ldots + a_0$. Adding these two words we get another valid codeword $G(x) + X(x)$. Considering that both $G(x)$ and $X(x)$ have degree $N - K$, the sum must have a degree lower than $N - K$. If $G(x)$ is a factor of all codewords, this leads to a contradiction. Hence, there is only one codeword with degree $N - K$ and that is the generator polynomial itself.

4. Since we have the factorization

$$\begin{aligned} x^{15}+1 \quad = \quad & \left(x^4+x^3+1\right)\left(x^4+x^3+x^2+x+1\right) \times \\ & \left(x^4+x+1\right)\left(x^2+x+1\right)(x+1) \end{aligned} \tag{14.5}$$

and want to find all generator polynomials generating binary cyclic (15, 8) codes, we need to find all factors of degree $15 - 8 = 7$. Inspection shows that these are

$$\begin{aligned} &\left(x^4 + x^3 + 1\right)\left(x^2 + x + 1\right)(x + 1), \\ &\left(x^4 + x^3 + x^2 + x + 1\right)\left(x^2 + x + 1\right)(x + 1), \text{ and} \\ &\left(x^4 + x + 1\right)\left(x^2 + x + 1\right)(x + 1). \end{aligned} \tag{14.6}$$

5. (a) Since the code is linear, the remaining 12 codewords are determined by linear combinations of the above. This gives (the "trivial" all-zero codeword last)

Message					Codeword						
1	1	0	0	→	1	0	1	1	1	0	0
1	0	1	0	→	1	1	1	0	0	1	0
1	0	0	1	→	1	1	0	0	1	0	1
0	1	1	0	→	0	1	0	1	1	1	0
0	1	0	1	→	0	1	1	1	0	0	1
0	0	1	1	→	0	0	1	0	1	1	1
1	1	1	0	→	1	0	0	0	1	1	0
1	1	0	1	→	1	0	1	0	0	0	1
1	0	1	1	→	1	1	1	1	0	0	1
0	1	1	1	→	0	1	0	0	0	1	1
1	1	1	1	→	1	0	0	1	0	1	1
0	0	0	0	→	0	0	0	0	0	0	0

(14.7)

(b) Since the code is linear, the minimum distance $d_{\min}$ is given by the smallest Hamming weight of non-zero codewords. Since we have all codewords, inspection gives $d_{\min} = 3$. The corresponding error correcting capability is $t = \left\lfloor \frac{d_{\min}-1}{2} \right\rfloor = 1$, i.e., the code can correct all single errors.

(c) The generator matrix for the non-systematic code above is

$$\mathbf{G}^* = \begin{bmatrix} 1 & 1 & 0 & 1 & 0 & 0 & 0 \\ 0 & 1 & 1 & 0 & 1 & 0 & 0 \\ 0 & 0 & 1 & 1 & 0 & 1 & 0 \\ 0 & 0 & 0 & 1 & 1 & 0 & 1 \end{bmatrix}, \tag{14.8}$$

i.e. the given codewords placed as rows of a matrix. The generator matrix of the corresponding systematic code would look like

$$\mathbf{G} = [\mathbf{I}|\,\mathbf{P}], \tag{14.9}$$

where $\mathbf{P}$ is the parity matrix and $\mathbf{I}$ a 4×4 identity matrix. Gaussian elimination on $\mathbf{G}^*$ gives

$$\mathbf{G} = \left[\begin{array}{cccc|ccc} 1 & 0 & 0 & 0 & 1 & 1 & 0 \\ 0 & 1 & 0 & 0 & 0 & 1 & 1 \\ 0 & 0 & 1 & 0 & 1 & 1 & 1 \\ 0 & 0 & 0 & 1 & 1 & 0 & 1 \end{array}\right] \begin{array}{l} \text{row}_1 + \text{row}_2 + \text{row}_3 \\ \text{row}_2 + \text{row}_3 + \text{row}_4 \\ \text{row}_3 + \text{row}_4 \\ \text{row}_4 \end{array}. \tag{14.10}$$

(d) Knowing $\mathbf{P}$ (above), the parity check matrix becomes

$$\mathbf{H} = \left[\mathbf{P}^T \middle|\, \mathbf{I}\right] = \left[\begin{array}{cccc|ccc} 1 & 0 & 1 & 1 & 1 & 0 & 0 \\ 1 & 1 & 1 & 0 & 0 & 1 & 0 \\ 0 & 1 & 1 & 1 & 0 & 0 & 1 \end{array}\right]. \tag{14.11}$$

(e) By inspection of the above we can see that all cyclic shifts of codewords are also codewords, meaning that the code is cyclic. The codeword corresponding to $\mathbf{u} = [0001]$, i.e., $U(x) = 1$, and $X(x) = x^3 + x + 1$. We know that all codewords are multiples of the generator polynomial, and that it should have degree $N - K = 3$. Since the generator polynomial itself is the only codeword with highest degree 3, we know that $X(x)$ above is the generator polynomial, i.e.

$$G(x) = x^3 + x + 1. \tag{14.12}$$

6. (a) The codeword $\mathbf{x}$ corresponding to the message $\mathbf{m} = [1011]$ is simply determined by the multiplication

$$\mathbf{x} = \mathbf{mG} = [10111000]\,. \tag{14.13}$$

The parity matrix $\mathbf{H}$ can be found by identifying $\mathbf{P}$ in $\mathbf{G} = [\mathbf{I}\,|\mathbf{P}]$ and inserting it in

$$\mathbf{H} = \left[\mathbf{P}^T\,|\mathbf{I}\right] = \begin{bmatrix} 1 & 0 & 1 & 1 & 1 & 0 & 0 & 0 \\ 1 & 1 & 1 & 0 & 0 & 1 & 0 & 0 \\ 0 & 1 & 1 & 1 & 0 & 0 & 1 & 0 \\ 1 & 1 & 0 & 1 & 0 & 0 & 0 & 1 \end{bmatrix}. \tag{14.14}$$

We can verify our $\mathbf{H}$ by calculating the product $\mathbf{HG}^T$ and ensure that it becomes the **all-zero** matrix.

The syndrome corresponding to the received word $\mathbf{y} = [01011111]$ becomes:

$$\mathbf{s} = \mathbf{yH}^T = [0011] \tag{14.15}$$

(b) By removing the 5^{th} column of $\mathbf{G}$ we get

$$\mathbf{G}^* = \begin{bmatrix} 1 & 0 & 0 & 0 & 1 & 0 & 1 \\ 0 & 1 & 0 & 0 & 1 & 1 & 1 \\ 0 & 0 & 1 & 0 & 1 & 1 & 0 \\ 0 & 0 & 0 & 1 & 0 & 1 & 1 \end{bmatrix}. \tag{14.16}$$

generating a (7, 4) code. The last row of $\mathbf{G}^*$ is the codewod corresponding to the message $\mathbf{u} = [1000]$. The polynomial representation of this codeword is

$$X(x) = x^3 + x + 1. \tag{14.17}$$

If we believe the statement that the code, in addition to its linearity, also is a cyclic code we know that the only degree $N - K = 3$ codeword of the code is the generator polynomial itself. Since $X\,(x)$ above has this property, we know that $G\,(x) = X(x) = x^3 + x + 1$.

7. We would like to prove that

$$d_{\min} \leq N - K + 1 \tag{14.18}$$

always holds for linear (N, K) codes. We will use binary codes here, for simplicity, but the proof is easily extended to other bases. We start by listing the 2^K codewords in the code in a table. Then we remove the $d_{\min} - 1$ first symbols from each codeword and get a new set of 2^K words that are still unique (the original codewords differ in at least $d_{\min}$ positions). Since the new set of words contains $N - (d_{\min} - 1)$ bits we also know that there cannot be more than $2^{N-(d_{\min}-1)}$ different ones. Hence, $2^K \leq 2^{N-(d_{\min}-1)}$ or

$$d_{\min} \leq N - K + 1. \tag{14.19}$$

8. When performing syndrome decoding we have syndromes of length $N - K$ bits, meaning that we can at most have 2^{N-K} unique syndromes. On the other hand, to be able to correct t errors in code words of length N, we need our syndromes to uniquely identify all error patterns of Hamming weight up to and including t errors. The number of such patterns is $\sum_{i=0}^{t} \binom{N}{i}$. Combining these two facts we get the following requirement on syndrome decoding

$$2^{N-K} \geq \sum_{i=0}^{t} \binom{N}{i}. \tag{14.20}$$

9. If the Hamming codes are perfect $t = 1$ error-correcting codes, they should meet the Hamming bound with equality for $t = 1$, i.e.

$$2^{N-K} = \sum_{i=0}^{1} \binom{N}{i} = \binom{N}{0} + \binom{N}{1} = N + 1. \tag{14.21}$$

Given that Hamming codes have parameters $N = 2^m - 1$ and $K = 2^m - 1 - m$ we get

$$2^{N-K} = 2^{2^m-1-(2^m-1-m)} = 2^m \tag{14.22}$$

and

$$N + 1 = 2^m - 1 + 1 = 2^m \tag{14.23}$$

which means that the Hamming bound is met with equality!

10. Soft Viterbi decoding

    (a) Replacing ones and zeros with their antipodal signal constellation points in the trellis stage in Figure B-14.5 a) gives:

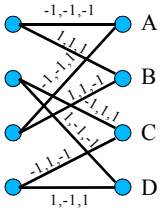

    (b) Executing the Viterbi algorithm for all seven trellis stages gives:

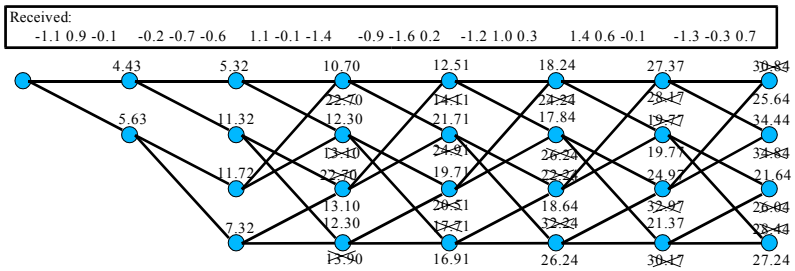

    Keeping only the surviving paths gives the following:

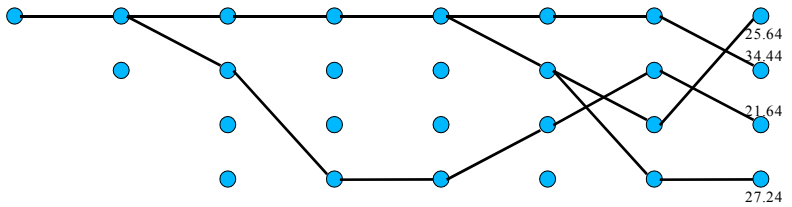

    We should, however, notice that in state B in the second to last trelllis stage there were two equal paths and one was eliminated using the toss of a fair coin. Had the coin given the opposite result, we would have obtained (the equally valid):

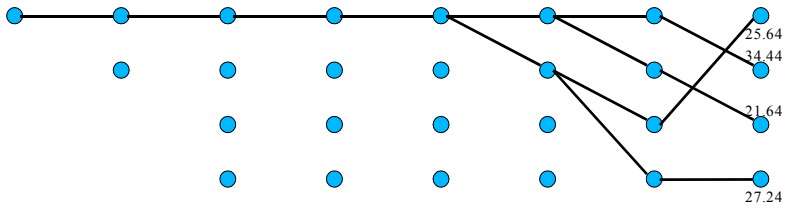

    Neither of the alternatives gave (exactly) the same surviving paths as the hard decoding in Figure B-14.5.

11. Block codes on fading channels

Rewriting the expression against which the BER is proportional, so that we get a $(1/\overline{\gamma}_B)^i$-factor in each term, gives

$$\begin{aligned} & \sum_{i=t+1}^{N} K_i \left(\frac{1}{2+2\overline{\gamma}_B}\right)^i \left(1-\frac{1}{2+2\overline{\gamma}_B}\right)^{N-i} \\ = & \sum_{i=t+1}^{N} K_i \left(1/\overline{\gamma}_B\right)^i \frac{1}{\left(2/\overline{\gamma}_B+2\right)^i} \left(\frac{1/\overline{\gamma}_B+2}{2/\overline{\gamma}_B+2}\right)^{N-i} \end{aligned} \tag{14.24}$$

we can see that the lowest degree $(1/\overline{\gamma}_B)$-term has the asymptote

$$\frac{K_{t+1}}{2^{t+1}} \left(\frac{1}{\overline{\gamma}_B}\right)^{t+1} \tag{14.25}$$

for large $\overline{\gamma}_B$. Hence, with error-correcting capability t we achieve diversity order $t+1$. Since $t = \left\lfloor \frac{d_{\min}-1}{2} \right\rfloor$, we have proven that a code with minimum distance $d_{\min}$ achieves a diversity order of $\left\lfloor \frac{d_{\min}-1}{2} \right\rfloor + 1$.

Chapter 15

Speech coding

1. The two main drawbacks are (i) wasting resources, since the quality of the speech in that case becomes even better than would be necessary for good perception, and (ii) in many cases, the lossless coders result in a variable rate, which is difficult to match to the fixed rate provided by circuit-switched wireless systems.

2. The three main types are (i) *waveform coders,* which use the source model only *implicitly* to design an adaptive dynamical system which maps the original speech waveform on a processed waveform that can be transmitted with fewer bits over the given digital channel, (ii) *model-based coders* or *vocoders,* which rely on an *explicit* source model to represent the speech signal with a small set of parameters which the encoder estimates, quantizes, and transmits over the digital channel, and (iii) *hybrid coders,* which aim at an optimal mix of the two previous designs. They start out with a model-based approach to extract speech signal parameters but still compute the modeling error explicitly on the waveform level.

3. Speech shows a nearly periodic, discrete multi-tone (DMT) signal with a fundamental frequency f_0 in the range of 100 to 150 Hz for male, 190 to 250 Hz for female speakers and 350 to 500 Hz for children. Its spectrum slowly falls off towards higher frequencies and spans a frequency range of several 1000 Hz.

Chapter 16

Equalizers

1. The noise enhancement is a direct result of the filter's construction. For a given channel transfer function $F(z)$, the ZF-filter takes the form $E(z) = F^{-1}(z)$, which provides a strong amplification of the noise at the receiver when $F(z)$ takes a small value. MMSE linear equalizers have lower noise enhancement; DFE and MLSE even less.

2. The main advantage of blind equalization is the improvement of spectral efficiency as compared to conventional equalization that relies on training sequence. The main drawback is the computational complexity and reliability of blind equalization techniques.

   Three established blind techniques are (i) Constant modulus algorithm, (ii) Blind maximum likelihood, (iii) Algorithms based on the cyclostationarity of the received signal.

3. The autocorrelation can be computed as follows:

   (a)

$$\begin{aligned}
\mathbf{R}_{km} &= E\left\{u_k^* u_m\right\} \\
&= E\left\{u_k u_m\right\} \\
&= E\left\{\left[a\sin\left(\omega k\right) + n_k\right]\left[a\sin\left(\omega m\right) + n_m\right]\right\} \\
&= E\left\{\left[a^2 \sin\left(\omega k\right)\sin\left(\omega m\right) + a n_k \sin\left(\omega m\right) + a n_m \sin\left(\omega k\right) + n_k n_m\right]\right\} \\
&= a^2 \sin\left(\omega k\right)\sin\left(\omega m\right) + \sigma_n^2 \delta_{k-m} \\
&= \frac{a^2}{2}\left[\cos\left(\omega k - \omega m\right) - \cos\left(\omega k + \omega m\right)\right] + \sigma_n^2 \delta_{k-m}
\end{aligned} \tag{16.1}$$

   NB. $E\left\{n_k\right\} = 0$ by definition.

   (b) To simplify subsequent notation, let $l = |k - m|$ and thus $\mathbf{R}_{km} = \mathbf{R}_{k,k\pm l} = \mathbf{R}_l$. The difference equation $u_k = b u_{k-1} + n_k$ may be expanded recursively $l - 1$ times as follows.

$$u_k = b^l u_{k-l} + \sum_{q=0}^{l-1} b^q n_{k-q} \tag{16.2}$$

   since

$$\begin{aligned}
u_k &= b u_{k-1} + n_k \\
u_{k-1} &= b u_{k-2} + n_{k-1} \\
&\vdots
\end{aligned} \tag{16.3}$$

   Therefore,

$$\begin{aligned}
R_l &= E\left\{u_k u_{k-l}\right\} \\
&= E\left(b^l u_{k-l}^2 + u_{k-l} \sum_{q=0}^{l-1} b^q n_{k-q}\right) \\
&= b^l E\left\{u_{k-l}^2\right\}
\end{aligned} \tag{16.4}$$

since

$$E\{n_{k-q}u_{k-l}\} = 0,\ l \neq q \tag{16.5}$$

To solve for $E\{u_{k-l}^2\}$, let $l = 0$ in R_l, i.e.,

$$\begin{aligned} E\{u_k^2\} &= E\{(bu_{k-1}+n_k)(bu_{k-1}+n_k)\} = b^2 E\{u_{k-1}^2\} + \sigma_n^2 \\ &\Rightarrow E\{u_k^2\} = \frac{\sigma_n^2}{1-b^2} \end{aligned} \tag{16.6}$$

Finally, substituting into R_l,

$$\mathbf{R}_l = b^l E\{u_{k-l}^2\} = \frac{b^l \sigma_n^2}{1-b^2}. \tag{16.7}$$

4. For a real signal, the MSE is given as

$$\begin{aligned} MSE &= \sigma_S^2 - 2\mathbf{e}^T\mathbf{p} + \mathbf{e}^T\mathbf{R}\mathbf{e} \\ &= 0.7 - 2\begin{bmatrix} e_1 & e_2 & e_3 \end{bmatrix}\begin{bmatrix} 0 \\ 0.278 \\ 0.345 \end{bmatrix} + \begin{bmatrix} e_1 & e_2 & e_3 \end{bmatrix}\begin{bmatrix} 1 & 0.576 & 0.213 \\ 0.576 & 1 & 0.322 \\ 0.213 & 0.322 & 1 \end{bmatrix}\begin{bmatrix} e_1 \\ e_2 \\ e_3 \end{bmatrix} \\ &= 0.7 - 0.556e_2 - 0.69e_3 + e_1^2 + 1.152e_1e_2 + 0.426e_1e_3 + e_2^2 + 0.644e_2e_3 + e_3^2 \end{aligned} \tag{16.8}$$

5. (a) A 5-tap equalizer can only equalize five points in the channel transfer function, i.e., fixing the center position at $n = 0$ to 1 and two positions on each side $n = \pm 1, \pm 2$ to 0. In matrix form, we have

$$\begin{bmatrix} 0 \\ 0 \\ 1 \\ 0 \\ 0 \end{bmatrix} = \begin{bmatrix} 1.0 & 0.2 & -0.02 & 0.1 & 0 \\ -0.1 & 1.0 & 0.2 & -0.02 & 0.1 \\ 0.05 & -0.1 & 1.0 & 0.2 & -0.02 \\ 0.01 & 0.05 & -0.1 & 1.0 & 0.2 \\ 0 & 0.01 & 0.05 & -0.1 & 1.0 \end{bmatrix}\begin{bmatrix} e_{-2} \\ e_{-1} \\ e_0 \\ e_1 \\ e_2 \end{bmatrix} \tag{16.9}$$

Solving for e_n, we obtain

$$\begin{bmatrix} e_{-2} \\ e_{-1} \\ e_0 \\ e_1 \\ e_2 \end{bmatrix} = \begin{bmatrix} 1.0 & 0.2 & -0.02 & 0.1 & 0 \\ -0.1 & 1.0 & 0.2 & -0.02 & 0.1 \\ 0.05 & -0.1 & 1.0 & 0.2 & -0.02 \\ 0.01 & 0.05 & -0.1 & 1.0 & 0.2 \\ 0 & 0.01 & 0.05 & -0.1 & 1.0 \end{bmatrix}^{-1}\begin{bmatrix} 0 \\ 0 \\ 1 \\ 0 \\ 0 \end{bmatrix} = \begin{bmatrix} 0.0442 \\ -0.1812 \\ 0.9567 \\ 0.1113 \\ -0.0349 \end{bmatrix} \tag{16.10}$$

(b) Using Eq.(B-16.43), i.e. $q_n = \sum_{k=-\infty}^{\infty} e_k f_{n-k}$, we obtain the equalizer output as

$$q_n \in \{\ldots, 0, 0.0044, -0.0190, 0.1081, 0, 0, 1, 0, 0, 0.0186, -0.0006, -0.0003, 0, \ldots\}. \tag{16.11}$$

It is observed that the finite-length equalizer enforces the desired response over $n = -2, -1, 0, 1, 2$. However, since the length (or memory) of the channel transfer function is longer than that of the equalizer, residual ISI values exist just outside of the enforced region.

6. (a) If the channel has a transfer function $F(z) = 1 + 0.5z^{-1}$, the ZF-filter must have a transfer function $E(z) = F^{-1}(z) = 1/\left(1 + 0.5z^{-1}\right)$.

(b) The memory of the channel is 1.

(c) The fundamental stage is shown in Figure 16.1.

(d) The trellis representing the equalization process performed by the Viterbi equalizer is shown in Figure 16.2. Tracing the surviving path from the back of the trellis, we end up with the sequence $\{1, 1, -1, 1, -1\}$ which corresponds to the bit sequence $\{1, 1, 0, 1, 0\}$.

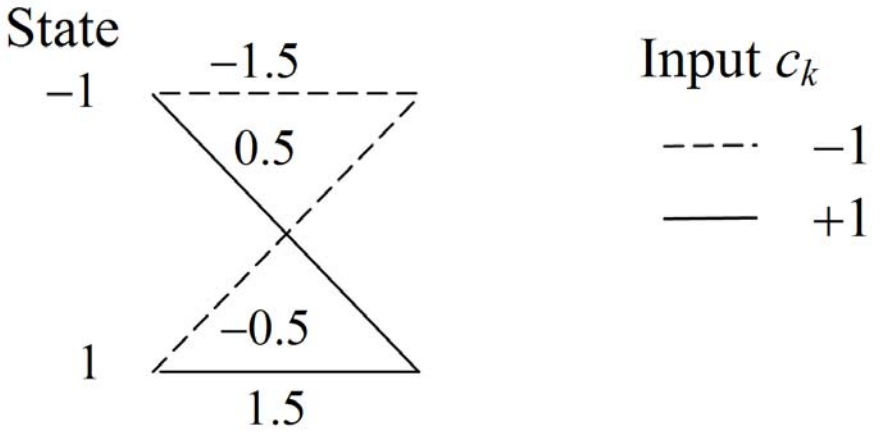

Figure 16.1: One trellis stage.

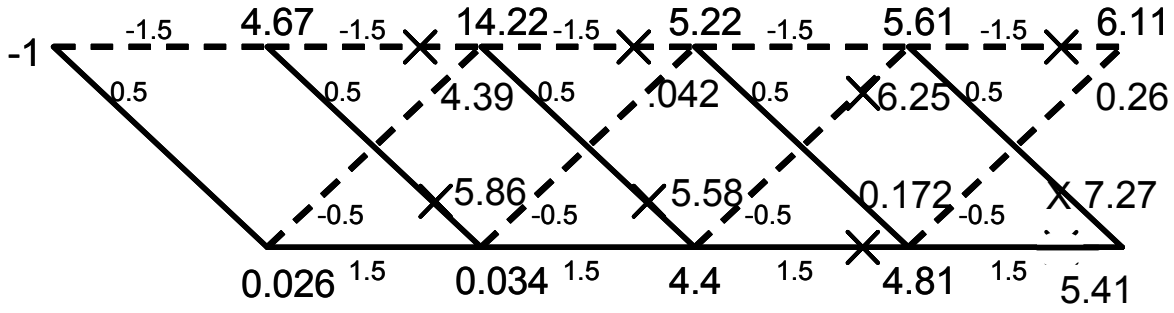

Figure 16.2: Trellis for the equalization performed by the Viterbi equalizer.

7. The MSE equation for this case is given by

$$\begin{aligned} \text{MSE} &= \sigma_S^2 - 2\mathbf{e}^T\mathbf{p} + \mathbf{e}^T\mathbf{R}\mathbf{e} \\ &= 0.6 - 2\begin{bmatrix} e_1 & e_2 \end{bmatrix}\begin{bmatrix} 0.288 \\ 0.113 \end{bmatrix} + \begin{bmatrix} e_1 & e_2 \end{bmatrix}\begin{bmatrix} 1 & 0.651 \\ 0.651 & 1 \end{bmatrix}\begin{bmatrix} e_1 \\ e_2 \end{bmatrix} \\ &= e_1^2 + 1.302e_1e_2 + e_2^2 - 0.576e_1 - 0.226e_2 + 0.3 \end{aligned} \tag{16.12}$$

The presence of the mixed term $1.302e_1e_2$ suggests a rotation of the axes for the parabolic surface with respect to the (e_1, e_2) coordinate system. From a standard calculus textbook, the (anti-clockwise) rotation angle of the axes is given by

$$\begin{aligned} \cot 2\theta &= \frac{A-C}{B} \\ &\Rightarrow \quad \theta = \pi/4 = 45^\circ \end{aligned} \tag{16.13}$$

Therefore,

$$\begin{aligned} e_1 &= \tilde{e}_1\cos\theta - \tilde{e}_2\sin\theta = \frac{\tilde{e}_1}{\sqrt{2}} - \frac{\tilde{e}_2}{\sqrt{2}} \\ e_2 &= \tilde{e}_1\sin\theta + \tilde{e}_2\cos\theta = \frac{\tilde{e}_1}{\sqrt{2}} + \frac{\tilde{e}_2}{\sqrt{2}} \end{aligned} \tag{16.14}$$

where the $(\tilde{e}_1, \tilde{e}_2)$ denotes the rotated coordinate system. Substituting into the MSE equation

$$\begin{aligned} \text{MSE} &= \left(\frac{\tilde{e}_1}{\sqrt{2}} - \frac{\tilde{e}_2}{\sqrt{2}}\right)^2 + 1.302\left(\frac{\tilde{e}_1}{\sqrt{2}} - \frac{\tilde{e}_2}{\sqrt{2}}\right)\left(\frac{\tilde{e}_1}{\sqrt{2}} + \frac{\tilde{e}_2}{\sqrt{2}}\right) + \left(\frac{\tilde{e}_1}{\sqrt{2}} + \frac{\tilde{e}_2}{\sqrt{2}}\right)^2 \\ &= -0.576\left(\frac{\tilde{e}_1}{\sqrt{2}} - \frac{\tilde{e}_2}{\sqrt{2}}\right) - 0.226\left(\frac{\tilde{e}_1}{\sqrt{2}} + \frac{\tilde{e}_2}{\sqrt{2}}\right) + 0.3 \\ &= \frac{\tilde{e}_1^2}{2} - \tilde{e}_1\tilde{e}_2 + \frac{\tilde{e}_2^2}{2} + 1.302\left(\frac{\tilde{e}_1^2}{2} - \frac{\tilde{e}_2^2}{2}\right) + \frac{\tilde{e}_1^2}{2} + \tilde{e}_1\tilde{e}_2 + \frac{\tilde{e}_2^2}{2} - 0.567\tilde{e}_1 + 0.247\tilde{e}_2 + 0.3 \\ &= 1.651\tilde{e}_1^2 + 0.349\tilde{e}_2^2 - 0.567\tilde{e}_1 + 0.247\tilde{e}_2 + 0.3 \\ &= 1.651\left(\tilde{e}_1^2 - 0.343\tilde{e}_1\right) + 0.349\left(\tilde{e}_2^2 + 0.708\tilde{e}_2\right) + 0.3 \\ &= 1.651\left(\tilde{e}_1 - 0.172\right)^2 - 0.049 + 0.349\left(\tilde{e}_2 + 0.354\right)^2 - 0.044 + 0.3 \\ &= 1.651\left(\tilde{e}_1 - 0.172\right)^2 + 0.349\left(\tilde{e}_2 + 0.354\right)^2 + 0.207. \end{aligned} \tag{16.15}$$

To draw the contour plot of the MSE surface, we choose a number of MSE values, i.e., 0.3, 0.5, 1, 1.5, 2. Using the above equation, the elliptical contours can be drawn in the rotated $(\tilde{e}_1, \tilde{e}_2)$ coordinate system (see Fig. 16.3). The contour lines must then be rotated anticlockwise by 45° to the desired MSE contours in (e_1, e_2) coordinate system.

8. (a) With perfect knowledge of $\mathbf{R}$ and $\mathbf{p}$, the LMS algorithm becomes the steepest-descent algorithm. The gradient is known exactly and no longer stochastic as in the case of LMS algorithm. The gradient has been provided as

$$\frac{\partial}{\partial \mathbf{e}_n} = \boldsymbol{\nabla}_n = -2\mathbf{p} + 2\mathbf{R}\mathbf{e}_n. \tag{16.16}$$

The updated equation is thus

$$\mathbf{e}_{n+1} = \mathbf{e}_n - 2\mu\left(\mathbf{R}\mathbf{e}_n - \mathbf{p}\right). \tag{16.17}$$

Using MATLAB, 20 iterations are performed for each of the three cases. The MSE for each of the three cases is given in Fig. 16.4. Since $\mathbf{R}$ and $\mathbf{p}$ are known exactly and fixed, the convergence curve is smooth and monotonic (as opposed to the case in Fig. B-16.5). It is observed that the first two cases $\mu = 0.1/\lambda_{\max}, 0.5/\lambda_{\max}$ converge within 20 iterations, while the third $\mu = 2/\lambda_{\max}$ does not convergence. Indeed, Eq. (B-16.29) states that the condition $0 < \mu < 2/\lambda_{\max}$ is necessary for convergence.

Comparing between $\mu = 0.1/\lambda_{\max}$ and $\mu = 0.5/\lambda_{\max}$, we further confirm that a larger (or properly chosen) μ can drastically speed up convergence.

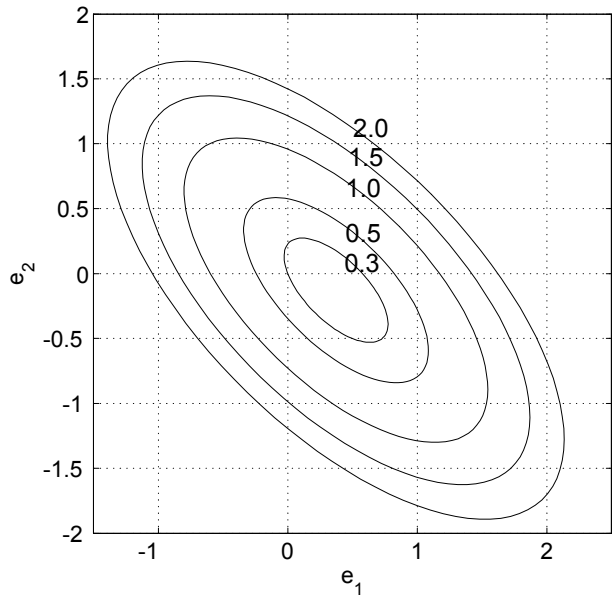

Figure 16.3: MSE contours for the 2-tap equalizer.

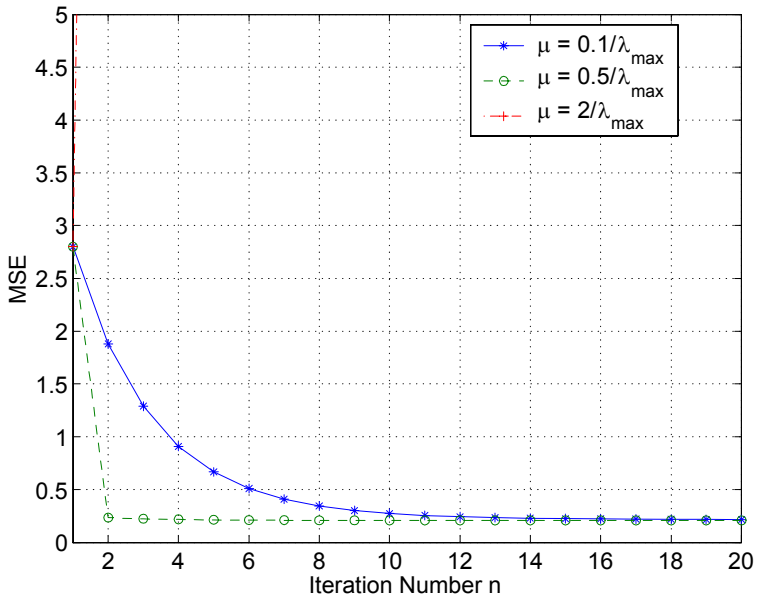

Figure 16.4: MSE curves for different step sizes.

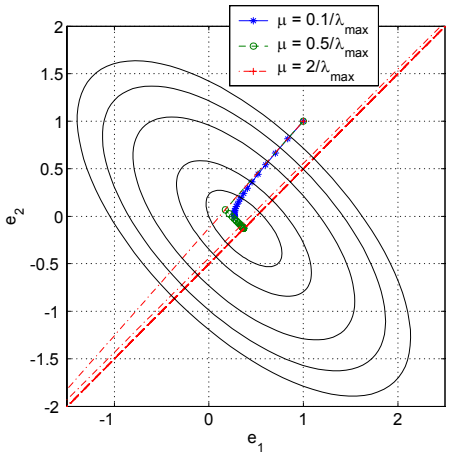

Figure 16.5: Convergence paths for different step sizes.

(b) The convergence paths are given in the Fig. 16.5. The MSE surface contours obtained from Exercise 16.7 is included in the figure.

It is interesting to note that while convergence is observed in the previous figure for $\mu = 0.1/\lambda_{\max}$, its filter coefficients are still not close to the optimal value given by the Wiener solution $\mathbf{e}_{\text{opt}} = \mathbf{R}^{-1}\mathbf{p} = \begin{bmatrix} 0.372 & -0.129 \end{bmatrix}^T$. On the other hand, good convergence is obtained for $\mu = 0.5/\lambda_{\max}$. For $\mu = 2/\lambda_{\max}$, due to the large step size, a large oscillating behavior is observed around the optimal value.

Chapter 17

Multiple access and the cellular principle

1. The number of analog duplex channels are $N_{\text{ch}} = 250$. The ratio between the reuse distance D and the cell radius R must be at least $D/R = 7$. The cell radius is $R = 2$ km. During a busy hour each subscriber generates one call of two minutes on average. The system can be modeled as Erlang B. The required maximum blocking probability is 3%.

   (a) **i.** To find the maximum number of subscribers per cell we first need the cluster size, which can be found using Tab. B-17.2. According to the table the smallest *valid* cluster size of $N_{\text{cluster}} = 19$ is obtained for a $D/R = 7.5$. The number of channels per cell is then

   $$N_{\text{cell}} = \frac{N_{\text{ch}}}{N_{\text{cluster}}} = \frac{250}{19} = 13.1. \tag{17.1}$$

   Figure B-17.2 shows the trunking gain. Since a curve for 13 channels per cell is absent, we have to approximate a value between the curves for $N_{\text{cell}} = 10$ and $N_{\text{cell}} = 15$. A blocking probability of 0.03 would then result in a cell capacity C_{cell} of about 9 Erlang per cell. During a busy hour each subscriber produces an average traffic of $T_{\text{sub}} = 2/60 = 0.033$ Erlang (recall that one Erlang corresponds to one fully used channel). Hence the maximum number of subscribers per cell is

   $$N_{\text{max,cell}} = \frac{C_{\text{cell}}}{T_{\text{cell}}} = \frac{9}{0.033} = 270. \tag{17.2}$$

   ii. From the above, the cell capacity is $C_{\text{cell}} = 9$ Erlang. The area of a cell is

   $$A_{\text{cell}} = \pi R^2 = \pi 2^2 = 12.6 \text{ km}^2. \tag{17.3}$$

   Thus, the network capacity is

   $$C_{\text{net}} = \frac{C_{\text{cell}}}{A_{\text{cell}}} = \frac{9}{12.6} = 0.72 \text{ Erlang/km}^2. \tag{17.4}$$

   (b) With digital transmission the number of duplex channels is reduced to $N_{\text{ch,dig}} = 125$. But at the same time, the ratio $D/R = 7$ can be lowered to $D_{\text{dig}}/R_{\text{dig}} = 4$. From Tab. B-17.2 we obtain a valid cluster size of $N_{\text{cluster,dig}} = 7$ for a $D_{\text{dig}}/R_{\text{dig}} = 4.6$. This results in

   $$N_{\text{cell,dig}} = \frac{N_{\text{ch,dig}}}{N_{\text{cluster,dig}}} = \frac{125}{7} = 17.9 \tag{17.5}$$

   channels per cell. By using the figure on slide 18, a maximum blocking probability of 0.03 and $N_{\text{cell,dig}} = 17$ channels per cell, a cell capacity of approximately $C_{\text{cell,dig}} = 13$ Erlang is obtained. Then, since the cell size is the same, the network capacity is

   $$C_{\text{net,dig}} = \frac{C_{\text{cell,dig}}}{A_{\text{cell}}} = \frac{13}{12.6} = 1.03 \text{ Erlang/km}^2. \tag{17.6}$$

(c) By reducing the transmit power, the cell radius can be reduced to $R_{\text{new}} = 1$ km. Since the ratio $D_{\text{dig}}/R_{\text{dig}} = 4$ must be preserved, the cluster size will be the same. The number of channels is also the same, which means that the cell capacity is still $C_{\text{cell,dig}} = 13$. The cell area, however, will decrease to

$$A_{\text{cell,new}} = \pi R_{\text{new}}^2 = \pi \text{ km}^2. \tag{17.7}$$

Thus, the new network capacity is increased to

$$C_{\text{net}} = \frac{C_{\text{cell,dig}}}{A_{\text{cell,new}}} = \frac{13}{\pi} = 4.1 \text{ Erlang/km}^2. \tag{17.8}$$

Since it takes

$$\frac{A_{\text{cell}}}{A_{\text{cell,new}}} = \frac{R^2}{R_{\text{new}}^2} = 4 \tag{17.9}$$

new smaller cells to cover the same area as one old cell, 4 times as many base stations are required to obtain the same coverage.

2. Erlang B – the most commonly used traffic model. Erlang B is used to work out how many lines are required if the traffic figure during the busiest hour is known. This model assumes that all blocked calls are cleared immediately, and the probability of a blocked call is

$$P_{\text{block}} = \frac{T_{\text{tr}}^{N_C}}{N_C! \sum_{k=0}^{N_C} \frac{T_{\text{tr}}^k}{k!}} \tag{17.10}$$

With one operator the offered traffic is $T_{\text{tr}} = 12$ hence

$$0.05 \leq \frac{12^{N_C}}{N_C! \sum_{k=0}^{N_C} \frac{12^k}{k!}} \tag{17.11}$$

Hence, for $N_C = 17$ the blocking probability is 1.3%. With three operators, each operator needs 8 channels for $T_{\text{tr}} = 4$ to get a blocking probability of 3 %. A total of 24 channels is needed.

3. Erlang C – this model assumes that all blocked calls are queued in the system until they can be handled. Call centers can use this calculation to determine how many call agents to staff, based on the number of calls per hour, the average duration of class and the amount of time calls are left in the queue.

(a) Channels needed

$$0.05 \geq \frac{T_{\text{tr}}^{N_C}}{T_{\text{tr}}^{N_C} + N_C! \left(1 - \frac{T_{\text{tr}}}{N_C}\right) \sum_{k=0}^{N_C - 1} \frac{T_{\text{tr}}^k}{k!}} \tag{17.12}$$

Hence, for $N_C = 19$ the blocking probability is 4.4%. With three operators, each operator needs 9 channels for $T_{\text{tr}} = 4$ to get a blocking probability of 2.4%. A total of 27 channels is needed. Erlang C systems require more resources than Erlang B.

(b) What is the average waiting time if the average call duration is 5 min?

$$t_{\text{wait}} = P_{\text{wait}} \frac{T_{\text{call}}}{N_C - T_{\text{tr}}} \tag{17.13}$$

$$0.0238 \frac{5}{9 - 4} \tag{17.14}$$

$$0.0435 \frac{5}{19 - 12} \tag{17.15}$$

For one operator the waiting time is 0.031 minutes and for three it is 0.024 minutes.

4. TDMA requires a temporal guard interval.

(a) Hence a MS communicating with the BS could be 3000 m away and with the other very close to the BS. The propagation delay is

$$\frac{3000}{3 \cdot 10^8} = 10\mu\text{s} \tag{17.16}$$

The "echo" of the channel is 10 μs, hence the total guard time (propagation delay + excess delay) should be more than 20 μs. A TDMA slot in GSM is 577 μs which includes a guard time that is ≈ 30 μs.

(b) With timing advance, the transmitter knows the propagation delay and the guard time could be reduced.

5. For the downlink we have the approximation

$$\left(\frac{C}{I}\right) > \frac{1}{6}\left(\frac{R}{D-R}\right)^{-\eta}. \tag{17.17}$$

We make here the approximation that the distance from all BSs to the MS at the cell boundary is equal, namely $D-R$. This is a pessimistic approximation, as at least some BSs have a larger distance. The approximation holds the better the larger the reuse distance is.

For the uplink case, since all transmitter powers are assumed to be the same, $C \propto P_{\text{TX}} d_0^{-\eta}$ and $I \propto \sum_{i=1}^{6} P_{\text{TX}} d_i^{-\eta}$, where d_0 is the distance between MS-0 and BS-0 and d_i is the distance between MS-i and BS-0. The worst-case scenario is when MS-0 is on the boundary of its cell, i.e., $d_0 = R$, and the co-channel mobiles MS-i, $i = 1, 2, .., 6$, are located on the boundary of their cells, respectively, in the direction of BS-0, i.e., $d_i = D - R$, $i = 1, 2, .., 6$. Hence (since $\eta > 1$),

$$\left(\frac{C}{I}\right) = \frac{P_{\text{TX}} d_0^{-\eta}}{\sum_{i=1}^{6} P_{\text{TX}} d_i^{-\eta}} > \frac{P_{\text{TX}} R^{-\eta}}{6 P_{\text{TX}} (D-R)^{-\eta}} = \frac{1}{6}\left(\frac{R}{D-R}\right)^{-\eta}. \tag{17.18}$$

Consequently, the upper bound above also holds for the uplink case.

6. The received power of the user of interest, S, and received power from the interfering user, I, is equally strong at the receiver. The (signal-to-interference ratio) SIR is then

$$\gamma_{\text{SIR}} = \frac{S}{I} \tag{17.19}$$

The signal to noise ration (SNR) is 10 dB (= 10 in linear scale) and defined as

$$\gamma_{\text{SNR}} = \frac{S}{N} = 10 \tag{17.20}$$

The overlap, α, allowed to keep the signal-to-noise and interference ratio (SNIR) at (7 in dB is equal to 5 in linear scale)

$$\gamma_{\text{SNIR}} = \frac{S}{N+I} = \frac{S}{\frac{S}{\gamma_{\text{SNR}}} + \alpha \cdot \frac{S}{\alpha_{\text{SG}}}} = \gamma_{\text{SNIR}} \tag{17.21}$$

$$a = \left(\frac{1}{\gamma_{\text{SNIR}}} - \frac{1}{\gamma_{\text{SNR}}}\right)\alpha_{\text{SG}} = 1 \tag{17.22}$$

where α is the maximum overlap (normalized collision time) to fulfill the SNIR requirements. Hence, a full overlap of one packet is admissible.

The throughout without lost packets is $\lambda_p T_p$, where λ_p is the average transmission rate in packets per second. The effective throughput is the percentage of time during which the channel is used in a meaningful way, i.e., that packets are offered, and transmitted successfully. The probability of zeros or one collision is

$$p(0, T_p) + p(1, T_p) = e^{-\lambda_p T_p} + \lambda_p T_p e^{-\lambda_p T_p} \tag{17.23}$$

The effective throughput is then

$$\lambda_p T_p \left(e^{-\lambda_p T_p} + \lambda_p T_p e^{-\lambda_p T_p}\right) \tag{17.24}$$

The maximum of $\lambda_p T_p$ is found (derivative and set to zero) to be $\lambda_p T_p = \frac{1}{2} + \frac{1}{2}\sqrt{5} = 1.618$, thus the maximum effective throughput is 0.81. Remember that in the case when no interference is tolerated, the effective throughput is

$$\frac{1}{e} = 0.38 \tag{17.25}$$

which is less and follows intuition.

Chapter 18

Spread spectrum systems

1. For the following simulations, a generator for PN sequences is required. We use the following MATLAB program

```
function y = PN(G, Ain, N);
%
% This function generates the Pseudo Noise sequnece of length (N)
% according to Generation Polynomial and input state.

% Inputs:  G - Generation Polynom
% Ain - Initial state of SR
% N - The length of required PN sequence

% Outputs:  y - The resulting PN sequence

L = length(G);
A = Ain; % initiate the state of the SR

y = zeros(N, 1);
for i=1:N
 y(i)=A(L);
 SR_in=mod(sum(G.*A),2);
 A=[SR_in,A(1:L-1)];

end
```

Here a long sequence with an 8-state shift register is used and two users use different shifted sub-sequences. We next show the results for the received signals and the MATLAB programs used to obtain them.

1.
```
% --Chap.  18, Prob 1 abc----
clear all;

s1=[1,-1,1,1];
s2=[-1,1,-1,1];
```

```
%h1=1; % qestion (a)
%h2=1;

%h1=[1, 0.5, 0.1]; % qestion (b)
%h2=h1;

h1=[1, 0.5, 0.1]; % qestion (c)
h2=[1, 0, 0.5];

%----------------PN Seq.  Generation-----------------------------
%here a long sequence with L=8 state SR is used and two users use
%different shifted sequence with length N

N=128; % length of PN Seq.

G=[0,1,0,1,0,1,1,1]; % Ploynomial
A_ini=[0,1,0,0,0,0,1,1]; %initial state

C=PN(G, A_ini, 255);
C=2*C-1; % Antipodal Chips
c1=C(1:N)';
c2=C(4:N+3)';

%---Spreading------------------------
t1=[s1(1)*c1,s1(2)*c1,s1(3)*c1,s1(4)*c1];
t2=[s2(1)*c2,s2(2)*c2,s2(3)*c2,s2(4)*c2];

%---channel--------------------------
r1=conv(t1,h1);
r2=conv(t2,h2);
r=r1+r2; % assume the signals of two MS are synchronized (e.g.  by GPS)

%---Despreading & (hard)Detection--------------------
%Assume the receiver already made chip and symbol synchronizations for both users
d1(1)=sum(r(1:N)*c1');
d1(2)=sum(r(N+1:2*N)*c1');
d1(3)=sum(r(2*N+1:3*N)*c1');
d1(4)=sum(r(3*N+1:4*N)*c1');

d2(1)=sum(r(1:N)*c2');
d2(2)=sum(r(N+1:2*N)*c2');
d2(3)=sum(r(2*N+1:3*N)*c2');
```

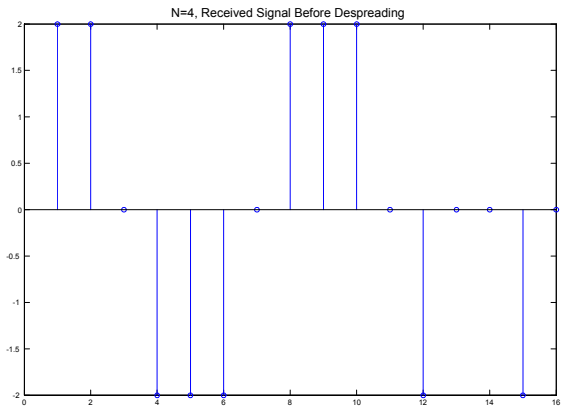

Figure 18.1: Received signal before despreading, $N = 4$, for Exercise 18.1

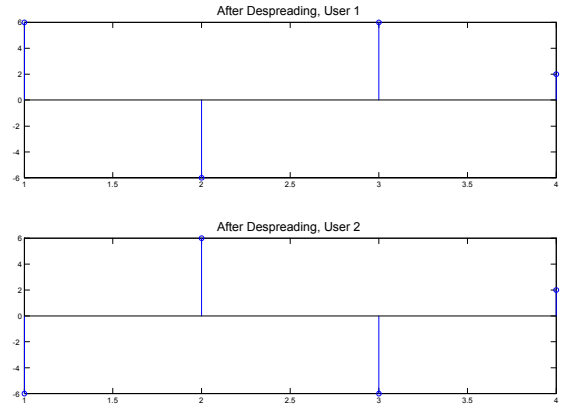

Figure 18.2: Received signal after despreading, $N = 4$, for Exercise 18.1

```
d2(4)=sum(r(3*N+1:4*N)*c2');

figure(1)
stem(r);
title('N=128, Received Signal Before Despreading')

figure(2)
subplot(2,1,1);
stem(d1);
title('After Despreading, User 1')
subplot(2,1,2);
stem(d2);
title('After Despreading, User 2')
```

The signals before and after spreading can be found in Figs. 18.1 - 18.6.

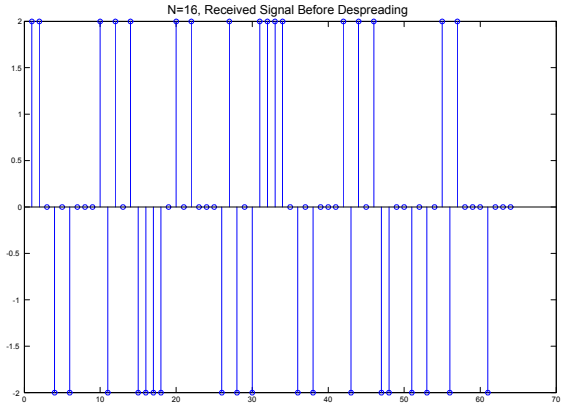

Figure 18.3: Received signal before despreading, $N = 16$, for Exercise 18.1

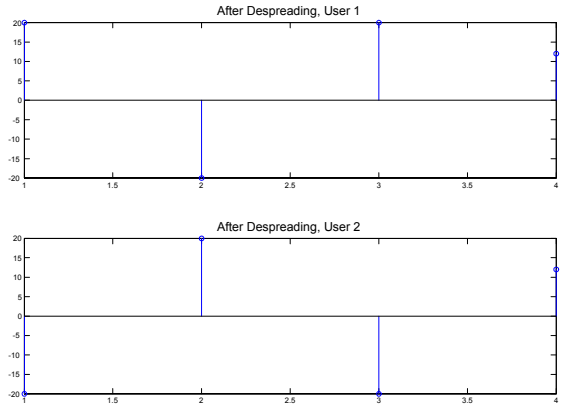

Figure 18.4: Received signal after despreading, $N = 16$, for Exercise 18.1

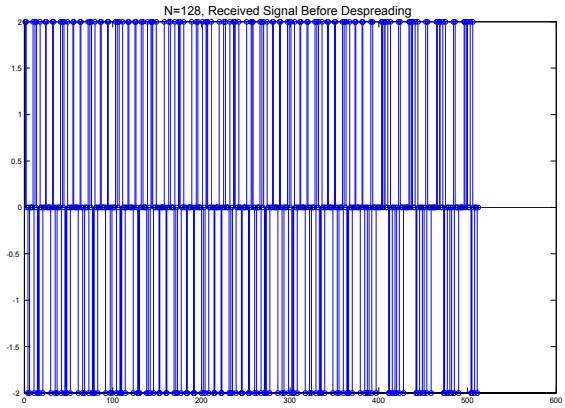

Figure 18.5: Received signal before despreading, $N = 128$, for Exercise 18.1

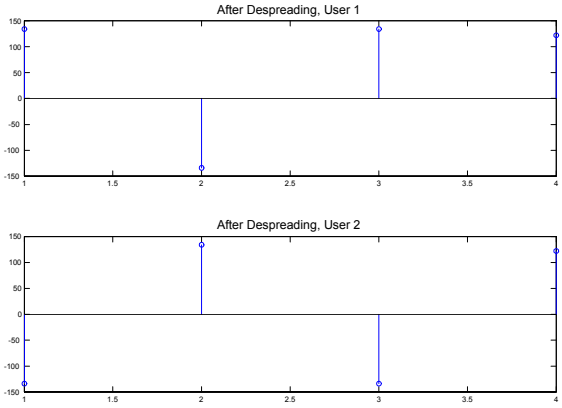

Figure 18.6: Received signal after despreading, $N = 128$, for Exercise 18.1

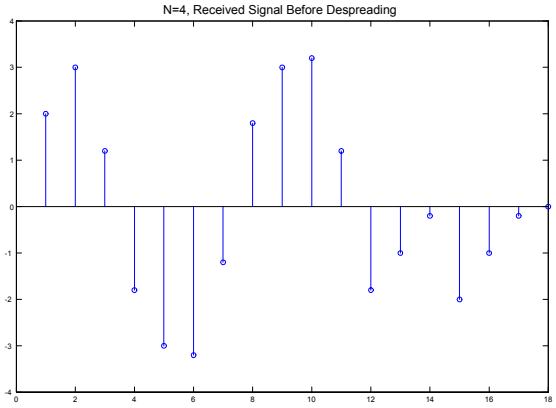

Figure 18.7: Received signal before despreading in delay-dispersive channel (identical for both signals); $N = 4$.

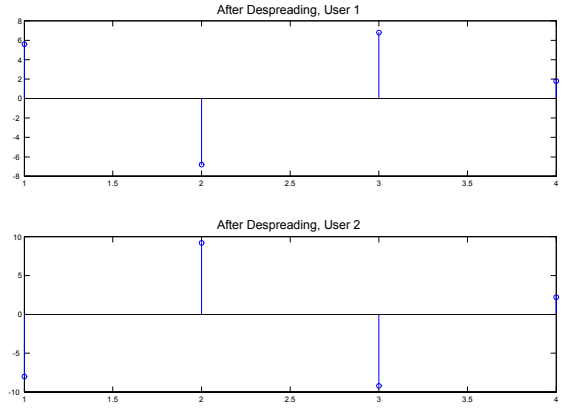

Figure 18.8: Received signal after despreading in delay-dispersive channel (identical for both signals); $N = 4$.

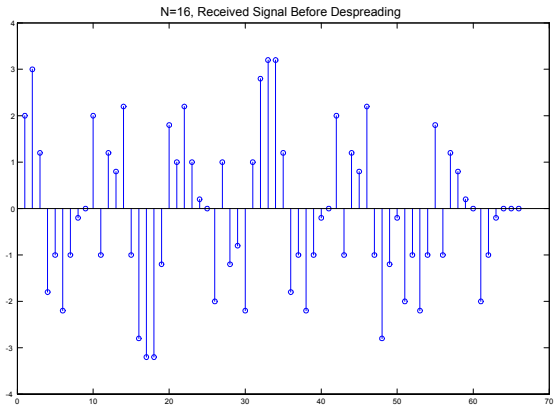

Figure 18.9: Received signal before despreading in delay-dispersive channel (identical for both signals); $N = 16$.

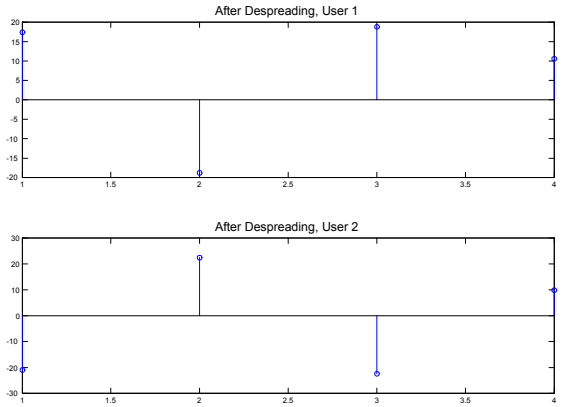

Figure 18.10: Received signal after despreading in delay-dispersive channel (identical for both signals); $N = 16$.

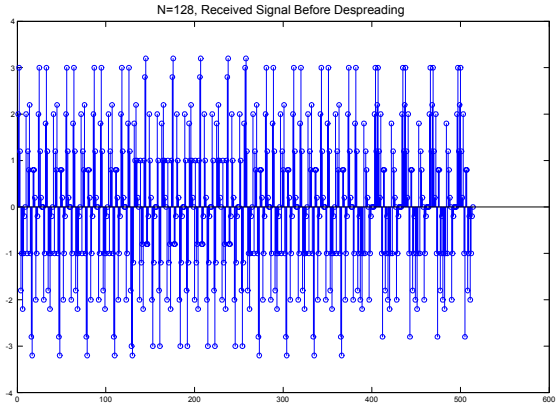

Figure 18.11: Received signal before despreading in delay-dispersive channel (identical for both signals); $N = 128$.

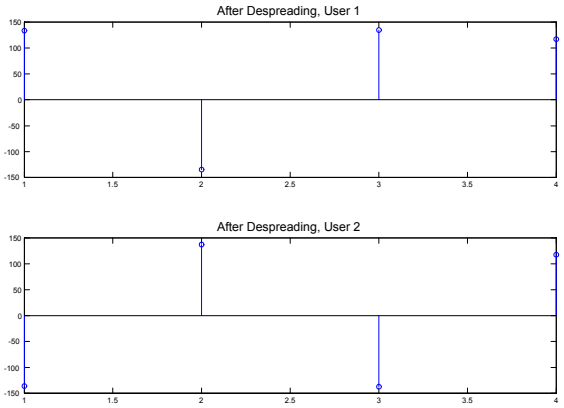

Figure 18.12: Received signal after despreading in delay-dispersive channel (identical for both signals); $N = 128$.

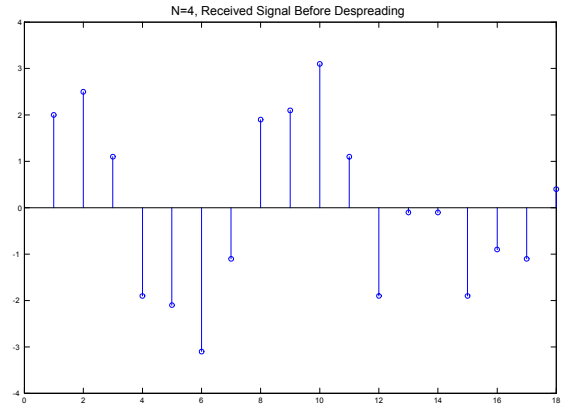

Figure 18.13: Received signal before despreading in delay-dispersive channel (different for the two signals); $N = 4$.

b. The results for a delay-dispersive channel (acting on both signals) are found in Figs. 18.7 - 18.12.

c. The results for delay-dispersive channels that are different for the two users can be found in Fig. 18.13-18.18.

d.
```
%----------------Hadamard Seq.  Generation-----------------------------
N=4; % length


H=hadamard(N);
c1=H(1,:);
c2=H(2,:);
```

From the figures we see that multipath channels will bring in inter-symbol interference (ISI) so SIR is reduced, if no RAKE receiver is used. For a longer spreading sequence, this effect is smaller. Hadamard sequences have better cross-correlation properties, therefore is less vulnerable to ISI, which can be seen from (d).

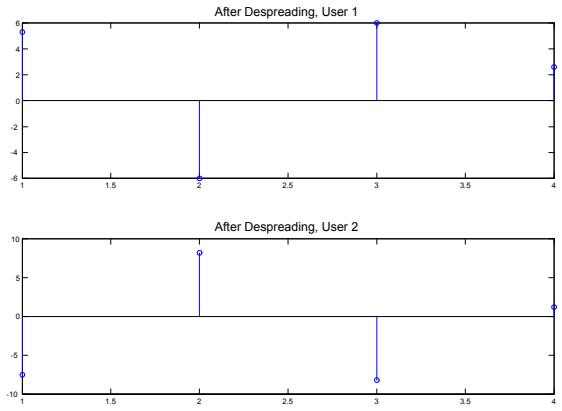

Figure 18.14: Received signal after despreading in delay-dispersive channel (different for the two signals); $N = 4$.

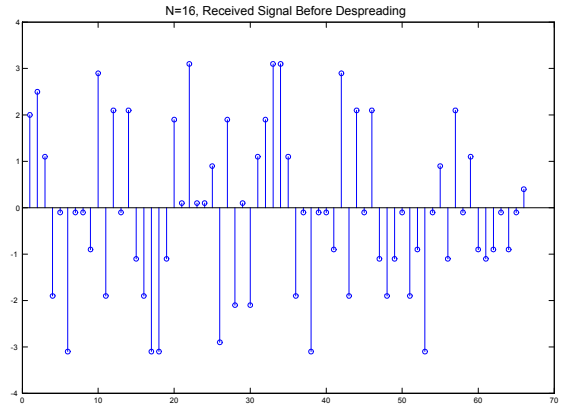

Figure 18.15: Received signal before despreading in delay-dispersive channel (different for the two signals); $N = 16$.

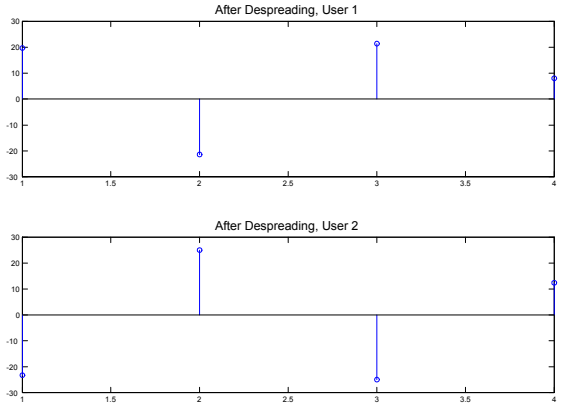

Figure 18.16: Received signal after despreading in delay-dispersive channel (different for the two signals); $N = 16$.

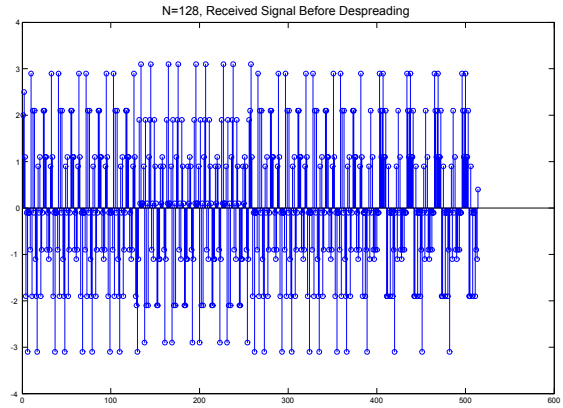

Figure 18.17: Received signal before despreading in delay-dispersive channel (different for the two signals); $N = 128$.

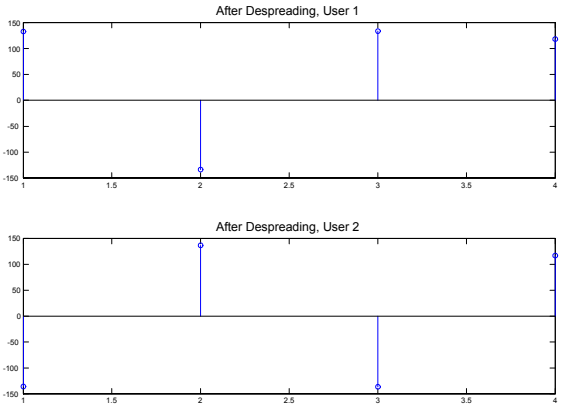

Figure 18.18: Received signal after despreading in delay-dispersive channel (different for the two signals); $N = 128$.

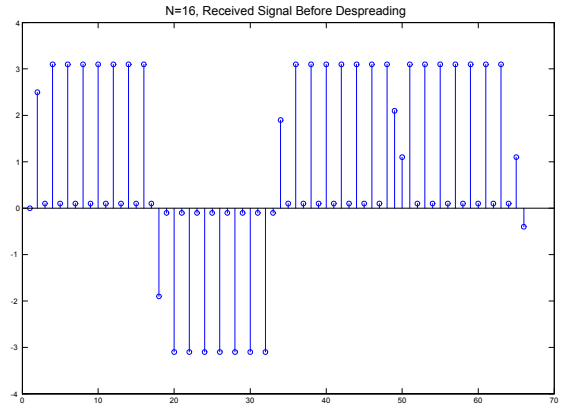

Figure 18.19: Received signal before despreading with Hadamard spreading.

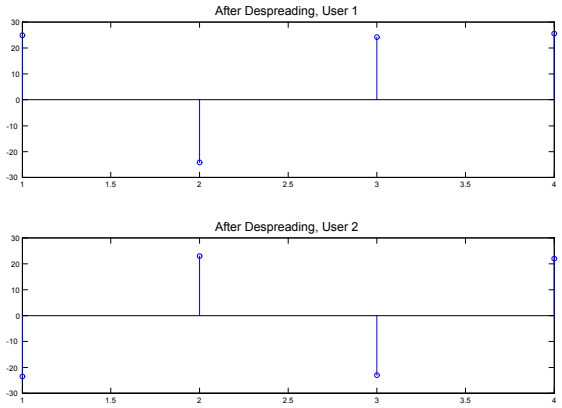

Figure 18.20: Received signal after despreading with Hadamard spreading.

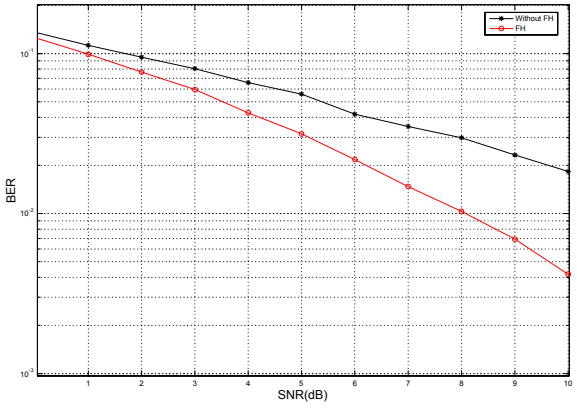

Figure 18.21: BER as a function of SNR with and without frequency hopping for Hamming encoding.

2. An exhaustive computer search shows that no such sequences exist. If no time shifts are applied, the following sequences have zero or one collision:

$$\begin{aligned} &1342, 1423, 2143, 2314, 2341, 2413, 2431, \\ &3124, 3142, 3241, 3412, 3421, 4123, 4132, \\ &4213, 4312, 4321 \end{aligned} \tag{18.1}$$

   However, when examining these, we see that all have the integers i and $\text{mod}(i+1, 4)$ following each other. For this interpretation, we have to actually consider periodically extended sequences, so that the first number "follows" the fourth one.

3. We assume a block fading channel model, i.e., the channel is constant over a block of L symbol intervals, which taking another independent value for the next block.

   When $L = 1$, FH assumes no advantage, because the temporally interleaved bits (by channel coding) also experience independent fading channels. When $L > 1$, FH achieves frequency diversity gain. In the simulation, we assume $L = 7$. The results are shown in Fig. 18.21.

   (a)
```
% --Chap.  18, Prob 3----
clear all;
```

```
N=100000; %transmit N symbols at each SNR
BF_length=7; %assuming block fading with correlation time of 7 symbols

for i=1:16
 i
 snr(i)=i-1; % SNR in dB

 % --Coding and BPSK Modulation, assuming N0=1 for AWGN----
 A=sqrt(2*(10^(snr(i)/10)));
 din=randint(1,N); %Source, original signal x
 x=encode(din,7,4); %encoding

 L=length(x);
 s=(x*2-1)*A;
 s=s';

 nr = wgn(1,L,0);
 ni = wgn(1,L,0);
 n=complex(nr,ni);

 %--Rayleigh Fading Channel for 7 carriers---
 h=(randn(7,L/BF_length)+j*randn(7,L/BF_length))/sqrt(2);



 %---received signals and coherent detection-----------
 for l=1:L
 BF_index=fix((l-1)/BF_length)+1;

 y1 = s(l)*h(1,BF_index) + n(l);
 r1(l)=conj(h(1,BF_index))*y1; % without FH
 y2 = s(l)*h(mod(l,7)+1,BF_index) + n(l);
 r2(l)=conj(h(mod(l,7)+1,BF_index))*y2; % FH
 end

 %--demod & decoding---
 c1=(r1>0);c2=(r2>0);
 dout1=decode(real(c1),7,4);
 dout2=decode(real(c2),7,4);

 num_err1=xor(din',dout1);
 num_err2=xor(din',dout2);
 BER1(i)=sum(num_err1)/N;
 BER2(i)=sum(num_err2)/N;
end

semilogy(snr,BER1, 'k-*',snr,BER2, 'r-o');
xlabel('SNR(dB)');
```

```
ylabel('BER');
legend('Without FH','FH');
grid;
```

4. For a slowly varying channel, i.e., $h(t,\tau)$ varying slowly over the time period on the order of a symbol duration, $R_{\rm h}(t_1-\alpha_1,t_2-\alpha_2;\tau_1,\tau_2)$ does not change appreciably over the two-dimensional region $(\alpha_1,\alpha_2)\in[0,T_{\rm s}]\times[0,T_{\rm s}]$, and it can be approximated by

$$R_{\rm h}(t_1-\alpha_1,t_2-\alpha_2;\tau_1,\tau_2)\approx R_{\rm h}(t_1-\frac{T_{\rm s}}{2},t_2-\frac{T_{\rm s}}{2};\tau_1,\tau_2)\,. \tag{18.2}$$

In this case, the output correlation becomes

$$\begin{aligned}R_{\rm yy}(t_1,t_2)=\int_{-\infty}^{+\infty}\int_{-\infty}^{+\infty}\quad & R_{\rm h}(t_1-\frac{T_{\rm s}}{2},t_2-\frac{T_{\rm s}}{2};\tau_1,\tau_2)\\ & R_{\rm s}^*(t_1-T_{\rm s}-\tau_1)R_{\rm s}(t_2-T_{\rm s}-\tau_2)\,d\tau_1 d\tau_2\ ,\end{aligned} \tag{18.3}$$

where

$$R_{\rm s}(t-T_{\rm s}-\tau)\triangleq\int_0^{+\infty}s(t-\alpha-\tau)f_{\rm M}(\alpha)\,d\alpha\,. \tag{18.4}$$

For an uncorrelated scattering (US) channel, defined as one with channel values at different path delays being uncorrelated,

$$R_{\rm h}(t_1,t_2;\tau_1,\tau_2)=R_{\rm h}(t_1,t_2;\tau_1)\delta(\tau_2-\tau_1)\,. \tag{18.5}$$

Therefore, the correlation function of the MFEP output for a slowly varying US channel becomes

$$\begin{aligned}R_{\rm y}(t_1,t_2)=\int_{-\infty}^{+\infty}\quad & R_{\rm h}(t_1-\frac{T_{\rm s}}{2},t_2-\frac{T_{\rm s}}{2};\tau)\\ & R_{\rm s}^*(t_1-T_{\rm s}-\tau)R_{\rm s}(t_2-T_{\rm s}-\tau)\,d\tau\,.\end{aligned} \tag{18.6}$$

For WSS channels, the correlation function depends on t_1 and t_2 only through the difference t_2-t_1, i.e.,

$$R_{\rm h}(t_1,t_2;\tau_1,\tau_2)=R_{\rm h}(t_2-t_1;\tau_1,\tau_2)\,. \tag{18.7}$$

With (18.7), the correlation function of the MFEP output for a slowly varying WSSUS channel becomes

$$\begin{aligned}R_{\rm y}(t_1,t_2)=\int_{-\infty}^{+\infty}\quad & R_{\rm h}(t_2-t_1;\tau)\\ & R_{\rm s}^*(t_1-T_{\rm s}-\tau)R_{\rm s}(t_2-T_{\rm s}-\tau)\,d\tau\,.\end{aligned} \tag{18.8}$$

In SS parlance, $R_{\rm s}(\tau)$ is the periodic time autocorrelation function of the baseband spread signature sequence. For a reasonable sequence design, $R_{\rm s}(\tau)$ possesses small side lobes and a narrow peak over the interval $|\tau|<1/W$, where W denotes the spreading BW. For DS-CDMA systems using pseudorandom sequences and rectangular chip pulse shape, the function $R_{\rm s}(\tau)$ can be written as

$$R_{\rm s}(\tau)=\begin{cases}E_{\rm S}\left[1-\frac{|\tau|}{T_{\rm c}}(1+\frac{1}{N})\right], & |\tau|<T_{\rm c}\\ -\frac{E_{\rm S}}{N}, & T_{\rm c}\le|\tau|\le NT_{\rm c}\,,\end{cases} \tag{18.9}$$

where $E_{\rm S}$ is the peak value of the autocorrelation function, $N=T_{\rm s}/T_{\rm c}$ is known as the processing gain, and $T_{\rm c}$ is the chip duration . The spreading BW W is roughly equal to the chip rate $R_{\rm c}$ which is defined by $R_{\rm c}=1/T_{\rm c}$. The sidelobes of $R_{\rm s}(\tau)$ relative to the peak value are $-1/N$. For DS-CDMA systems with large processing gain, $-1/N$ is small and, from a practical viewpoint, (18.9) can be approximated by

$$R_{\rm s}(\tau)=\begin{cases}E_{\rm S}\left[1-\frac{|\tau|}{T_{\rm c}}\right], & |\tau|<T_{\rm c}\\ 0, & T_{\rm c}\le|\tau|\le NT_{\rm c}\,.\end{cases} \tag{18.10}$$

This implies that

$$R_{\rm s}{}^*(t_1-T_{\rm s}-\tau)R_{\rm s}(t_2-T_{\rm s}-\tau)\approx 0\,,\qquad |t_2-t_1|\ge\frac{2}{W}\,. \tag{18.11}$$

Together with the slowly varying channel assumption, this gives

$$\begin{aligned} R_{\mathrm{h}}(t_2 - t_1; \tau) &\approx R_{\mathrm{h}}(0; \tau) \qquad |t_2 - t_1| < \frac{2}{W} \\ &\triangleq (0; \tau)\,. \end{aligned} \tag{18.12}$$

The function $(0;\tau)$ is known as the power delay profile or multipath intensity profile. By use of (18.12), the correlation function of the MFEP output for a slowly varying WSSUS channel reduces to

$$R_{\mathrm{y}}(t_1, t_2) = \int_{-\infty}^{+\infty} P_{\mathrm{h}}(0, \tau_1) \underbrace{R_{\mathrm{s}}{}^*(t_1 - T_{\mathrm{s}} - \tau) R_{\mathrm{s}}(t_2 - T_{\mathrm{s}} - \tau)}_{= 0 \;\forall \quad |t_2 - t_1| \geq \frac{2}{W}} d\tau\,. \tag{18.13}$$

The noise correlation function can be derived in a similar fashion as

$$\begin{aligned} R_{\mathrm{n}}(t_1, t_2) &= \int_0^{+\infty} \int_0^{+\infty} \mathbb{E}\left\{n^*(t_1 - \alpha_1) n(t_2 - \alpha_2)\right\} f_{\mathrm{M}}^*(\alpha_1) f_{\mathrm{M}}(\alpha_2)\, d\alpha_1 d\alpha_2 \\ &= 2N_0 \widetilde{R}_{\mathrm{s}}(t_2 - t_1)\,. \end{aligned} \tag{18.14}$$

5. (a) The diversity order of a Nakagami-fading channel is equal to the m-factor. With maximum-ratio combining, the diversity orders of the different branches add up. Therefore, the total diversity order is 8.

   (b) As we have seen in Chapter 13, the average BER for maximum-ratio combining is given as

$$\overline{SER} = \int_{\theta_1}^{\theta_2} d\theta\; f_1(\theta) \prod_{i=1}^{N_{\mathrm{r}}} M_\gamma\left(-f_2(\theta)\right) \tag{18.15}$$

   We have furthermore seen in Chapter 12 that the moment-generating function of Nakagami fading is

$$M_\gamma(s) = \left(1 - \frac{s\overline{\gamma}}{m}\right)^{-m}. \tag{18.16}$$

   Thus, the BER for BPSK is given as

$$\frac{1}{\pi} \int_0^{\pi/2} \left(1 + \frac{\overline{\gamma}_1}{m_1 \sin^2(\theta)}\right)^{-m_1} \left(1 + \frac{\overline{\gamma}_2}{m_2 \sin^2(\theta)}\right)^{-m_2} \left(1 + \frac{\overline{\gamma}_3}{m_3 \sin^2(\theta)}\right)^{-m3} d\theta \tag{18.17}$$

   (c) The resulting BER vs. SNR curve is plotted in Fig. 18.22.

6. Since the MS operates in a rich multipath environment, the available frequency diversity allows the Rake receiver to eliminate the small-scale fading. consequently, the pdf of the received power is determined by the shadow fading only. Since the MS is in soft handover, it has links to two BSs, whose shadow fading is independent. The Rake receiver at the MS is capable of adding up the contributions from the two MSs (note that for the uplink, typically the base station controller would only select the stronger of the two available components). Therefore, we need to find the probability that the sum of two independent, lognormally distributed variables falls below a certain threshold value.

   It is well known that the sum of two lognormally distributed variables can be approximated as another lognormally distributed variable. Matching the first and second moment of the approximation and of the sum of the two constituent random variables is the well-known Fenton-Wilkinson method.

$$E\{\exp(Z)\} = E\{\exp(Y1) + \exp(Y2)\} \tag{18.18}$$

$$E\{\exp(2Z)\} = E\{[\exp(Y1) + \exp(Y2)]^2\} \tag{18.19}$$

   Then

$$\exp\left[\mu_Z + \frac{1}{2}\sigma_Z^2\right] = 2\exp\left[\mu_Y + \frac{1}{2}\sigma_Y^2\right] = u_1 \tag{18.20}$$

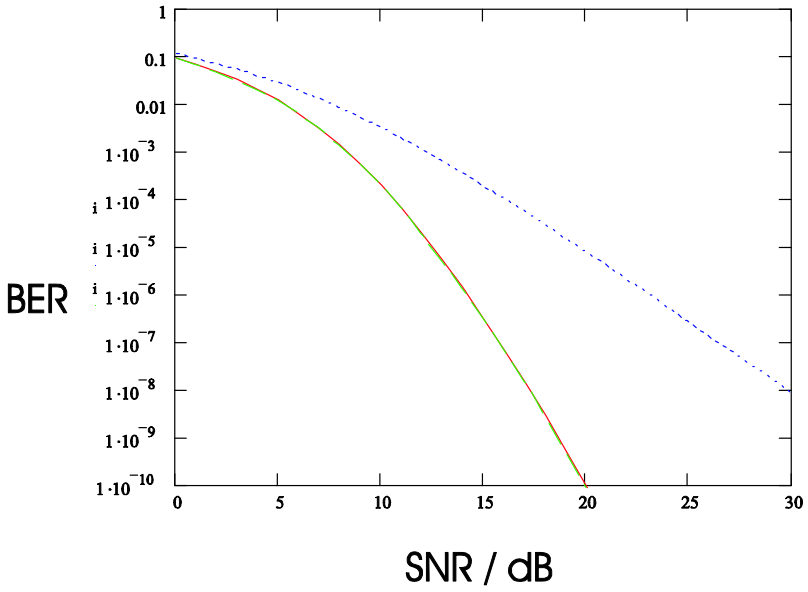

Figure 18.22: BER vs. SNR for a three-finger Rake in Nakagami fading and Rayleigh fading (Example 18.5.c).

$$\exp\left[2\mu_Z + 2\sigma_Z^2\right] = 2\exp\left[2\mu_Y + 2\sigma_Y^2\right] - 2\exp\left[2\mu_Y + \sigma_Y^2\right] = u_2 \tag{18.21}$$

from which we can solve for μ_Z and σ_Z.

This results in a lognormally distributed variable with a mean of 12 dB and a σ of 4 dB. Thus, the outage probability is the probability that a Gaussian variable has a value that is 2 standard deviations below its mean, which is 2.3%.

7. Assume the position of BS1 is $(0, 0)$, and that of BS2 is $(1000, 0)$. For the ease of simulations, we assume the cells have circular shapes. One MS is randomly located in Cell 1, and the average received interference power at BS2 is calculated by simulation. The transmit power of the MS is calculated based on the power control criteria (-90 dBm) and the path loss: $P_t = -90$ dBm $+ PL_1$, therefore the received interference power at BS2 is $P_{r2} = P_t - PL_2$.

   The simulation is performed using the following MATLAB program:

```
% --Chap.  18, Prob 7----
clear all;


fc=1800e6; %Carrier Freq.
lamda=3e8/fc; % wavelength
R=1000; %Cell size
pos_BS1=[0,0]; pos_BS2=[1000,0]; % BS locations
d0=100; %Distance threshold
Gain0=10*2*log10(lamda/(4*pi*d0)); % power gain at d0 in dB


N=100000; % number of samples


Pr=-90; %received pwr at associated BS (dBm)
```

```
for i=1:N
 r=rand(1,1)*R/2; theta=rand(1,1)*2*pi;
 pos=[r*cos(theta),r*sin(theta)]; %user position at cell 1
 d_BS1=sqrt(pos(1)^2+pos(2)^2); % distance to BS1
 d_BS2=sqrt((pos(1)-pos_BS2(1))^2+(pos(2)-pos_BS2(2))^2); % distance to BS2

 %--Power gain to BS1---
 if (d_BS1<=d0)
 Gain1=10*2*log10(lamda/(4*pi*d_BS1));
 else
 Gain1=Gain0+10*4*log10(d0/d_BS1);
 end

 %--Power gain to BS2---
 Gain2=Gain0+10*4*log10(d0/d_BS2);

 %--Rayleigh Fading-----
 h1=(randn+j*randn)/sqrt(2); % Channel to BS1
 h2=(randn+j*randn)/sqrt(2); % Channel to BS2
 Gain1=Gain1+10*log10(abs(h1)^2);
 Gain2=Gain2+10*log10(abs(h2)^2);

 %--TX Power per Pwr Control in Cell 1----
 Pt=Pr-Gain1;

 %--Received Pwer at BS2------
 Pr2(i)=Pt+Gain2;
end

mean(Pr2)
```

The simulation shows an average interference power from this handset to the neighboring BS is -117.7650 dBm.

8. The provided channel gains without power control represent a scenario with serious near-far effect, so the detections of users 1 and 2 are incorrect, because of the strong interference from user 3. With power control (the received signal of all the three users are the same and equal to the smallest one), the performance can be greatly enhanced and the data of all the users can be correctly detected. The results are plotted in Figs. 18.23 - 18.25.

```
% --Chap.  18, Prob 8----
clear all;

s1=[1,-1,1,1];
s2=[-1,-1,-1,1];
s3=[-1,1,-1,1];
```

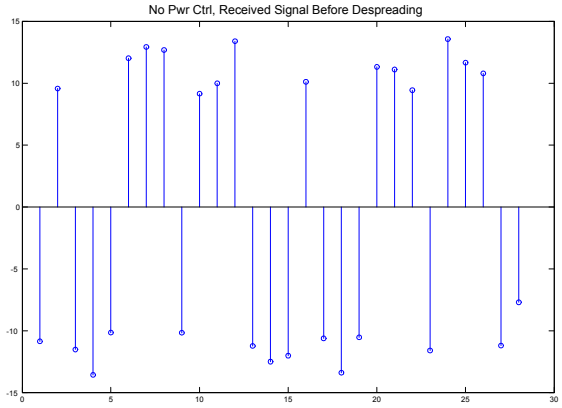

Figure 18.23: Received signal before despreading - no power control. Setup for Problem 18.8.

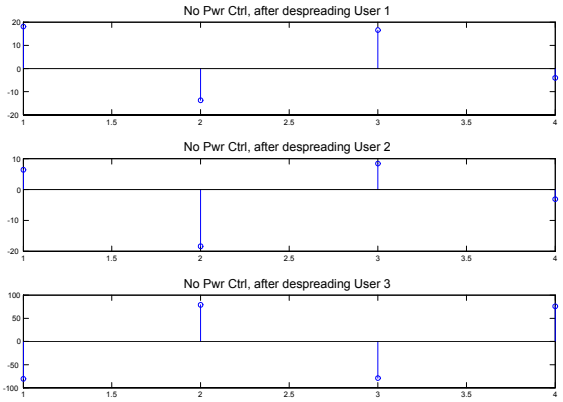

Figure 18.24: Received signal after despreading - no power control. Setup for Problem 18.8.

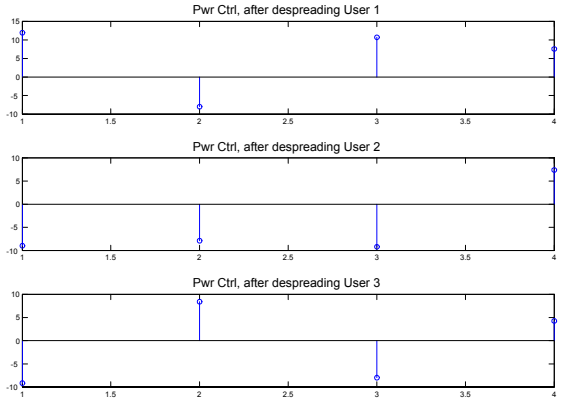

Figure 18.25: Received signal after despreading - with power control. Setup for Problem 18.8.

```
pwr_ctrl=1;

if (pwr_ctrl==0)
 h1=1; h2=0.6; h3=11.3;
else
 h1=1; h2=1; h3=1;
end

%--PN Seq.  Generation---
N=7; % length of PN Seq.
G=[0,1,1]; % Ploynomial
A1_ini=[1,0,0]; %initial state
A2_ini=[1,1,0]; %initial state
A3_ini=[1,0,1]; %initial state

C=PN(G, A1_ini, 7);
c1=(2*C-1)'; % Antipodal Chips
C=PN(G, A2_ini, 7);
c2=(2*C-1)'; % Antipodal Chips
C=PN(G, A3_ini, 7);
c3=(2*C-1)'; % Antipodal Chips


%---Spreading------------------------
t1=[s1(1)*c1,s1(2)*c1,s1(3)*c1,s1(4)*c1];
t2=[s2(1)*c2,s2(2)*c2,s2(3)*c2,s2(4)*c2];
t3=[s3(1)*c3,s3(2)*c3,s3(3)*c3,s3(4)*c3];

%---AWGN-----------------------------
n=randn(3,length(t1))*sqrt(0.3);
%---channel--------------------------
r1=conv(t1,h1)+n(1,:);
r2=conv(t2,h2)+n(2,:);
r3=conv(t3,h3)+n(3,:);

r=r1+r2+r3; % assume the signals of MS's are synchronized (e.g.  by GPS)

%---Despreading & (hard)Detection--------------------
%Assume the receiver already made chip and symbol synchronizations
d1(1)=r(1:N)*c1';
d1(2)=r(N+1:2*N)*c1';
d1(3)=r(2*N+1:3*N)*c1';
```

```
d1(4)=r(3*N+1:4*N)*c1';

d2(1)=r(1:N)*c2';
d2(2)=r(N+1:2*N)*c2';
d2(3)=r(2*N+1:3*N)*c2';
d2(4)=r(3*N+1:4*N)*c2';

d3(1)=r(1:N)*c3';
d3(2)=r(N+1:2*N)*c3';
d3(3)=r(2*N+1:3*N)*c3';
d3(4)=r(3*N+1:4*N)*c3';

figure(1)
stem(r);
title('Pwr Ctrl, Received Signal Before Despreading')

figure(2)
subplot(3,1,1);
stem(d1);
title('Pwr Ctrl, after despreading User 1')
subplot(3,1,2);
stem(d2);
title('Pwr Ctrl, after despreading User 2')
subplot(3,1,3);
stem(d3);
title('Pwr Ctrl, after despreading User 3')
```

9. The results with multiuser detection can be obtained using the following MATLAB program.

```
%---MUD--------------------
%Assume the receiver already made chip and symbol synchronizations
%------ZF-----------------------
C=[conv(c1,h1),
 conv(c2,h2),
 conv(c3,h3)];
R=C*C';
T=inv(R); %inverse of R

%--MF and ZF MUD---
d1=r(1:N)*C'*T;
d2=r(N+1:2*N)*C'*T;
d3=r(2*N+1:3*N)*C'*T;
d4=r(3*N+1:4*N)*C'*T;
```

```
dzf1=[d1(1),d2(1),d3(1),d4(1)];
dzf2=[d1(2),d2(2),d3(2),d4(2)];
dzf3=[d1(3),d2(3),d3(3),d4(3)];

%------Serial intf.  cancellation------------------
%---Symbol interval 1----------------------------
dsic3(1)=r(1:N)*c3'; %detect User 3 at first
rtp=r(1:N)-conv(sign(dsic3(1))*c3,h3); % cancel out User3's contribution
dsic1(1)=rtp*c1'; %detect User 1
rtp=rtp-conv(sign(dsic1(1))*c1,h1); % cancel out User1's contribution
dsic2(1)=rtp*c2'; %detect user 2

%---Symbol interval 2----------------------------
dsic3(2)=r(N+1:2*N)*c3'; %detect User 3 at first
rtp=r(N+1:2*N)-conv(sign(dsic3(2))*c3,h3); % cancel out User3's contribution
dsic1(2)=rtp*c1'; %detect User 1
rtp=rtp-conv(sign(dsic1(2))*c1,h1); % cancel out User1's contribution
dsic2(2)=rtp*c2'; %detect user 2

%---Symbol interval 3----------------------------
dsic3(3)=r(2*N+1:3*N)*c3'; %detect User 3 at first
rtp=r(2*N+1:3*N)-conv(sign(dsic3(3))*c3,h3); % cancel out User3's contribution
dsic1(3)=rtp*c1'; %detect User 1
rtp=rtp-conv(sign(dsic1(3))*c1,h1); % cancel out User1's contribution
dsic2(3)=rtp*c2'; %detect user 2

%---Symbol interval 4----------------------------
dsic3(4)=r(3*N+1:4*N)*c3'; %detect User 3 at first
rtp=r(2*N+1:3*N)-conv(sign(dsic3(4))*c3,h3); % cancel out User3's contribution
dsic1(4)=rtp*c1'; %detect User 1
rtp=rtp-conv(sign(dsic1(4))*c1,h1); % cancel out User1's contribution
dsic2(4)=rtp*c2'; %detect user 2


figure(1)
subplot(3,1,1);
stem(dzf1);
title('ZF Receiver, User 1')
subplot(3,1,2);
stem(dzf2);
title('ZF Receiver, User 2')
subplot(3,1,3);
```

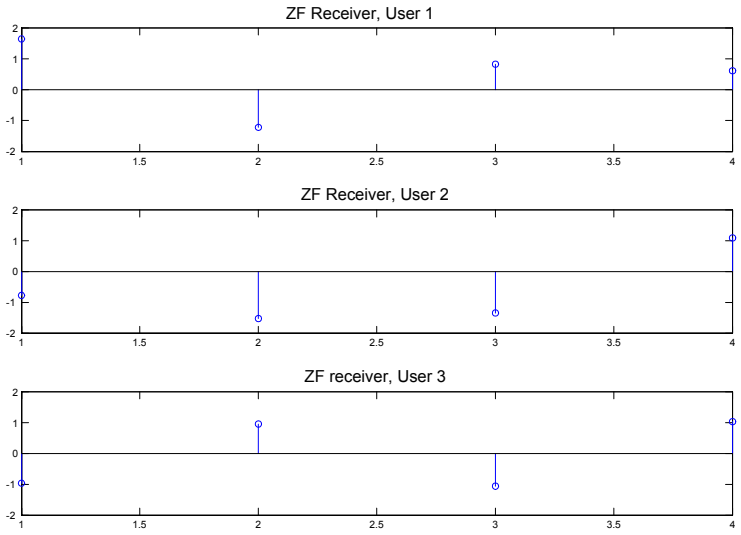

Figure 18.26: Signal received with zero-forcing multiuser detector, Exercise 18.9.

```
stem(dzf3);
title('ZF receiver, User 3')

figure(2)
subplot(3,1,1);
stem(dsic1);
title('SIC Receiver, User 1')
subplot(3,1,2);
stem(dsic2);
title('SIC Receiver, User 2')
subplot(3,1,3);
stem(dsic3);
title('SIC receiver, User 3')
```

The results obtained with that program are plotted in Figs.18.26-18.27.

10. For any modulation signal with independent input sequences, the power spectral density can be written generally as

$$G_s(f) = \frac{1}{T_s^2}.\sum_{n=-\infty}^{+\infty}\left(\left|\sum_{i=0}^{M-1}P_i.S_i\left(\frac{n}{T_s}\right)\right|^2\delta\left(f-\frac{n}{T_s}\right)\right) + \frac{1}{T_s}\left(\sum_{i=0}^{M-1}P_i.\left|S_i\left(f\right)\right|^2-\left|\sum_{i=0}^{M-1}P_i.S_i\left(f\right)\right|^2\right) \tag{18.22}$$

where M denotes the number of symbols, T_s the symbol period, $S_i(f)$ the Fourier transform of the i^{th} symbol of the constellation, and P_i the marginal probability of the i^{th} symbol. The spectrum of a

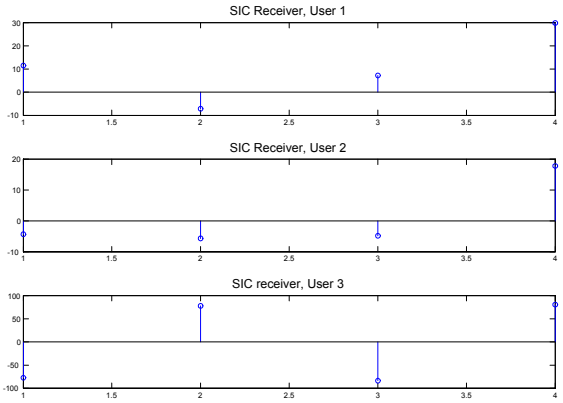

Figure 18.27: Signal received with serial interference cancellation multiuser detector, Exercise 18.9.

signal with a 2-PPM usually contains spectral lines spaced by the PRF. Rewriting Eq. (18.22) as the sum of a discrete and a continuous part with equiprobable input sequence, it becomes:

$$\begin{aligned} G_s(f) &= \frac{1}{M^2T_s^2}.\sum_{n=-\infty}^{+\infty}\left(\left|\sum_{i=0}^{M-1}S_i\left(\frac{n}{T_s}\right)\right|^2\delta\left(f-\frac{n}{T_s}\right)\right)+\frac{1}{M.T_s}.\left(\sum_{i=0}^{M-1}\left|S_i\left(f\right)\right|^2-\frac{1}{M}.\left|\sum_{i=0}^{M-1}S_i\left(f\right)\right|^2\right) \quad (18.23)\\ &= \frac{1}{2^2T_s^2}.\sum_{n=-\infty}^{+\infty}\left(\left|S_0\left(\frac{n}{T_s}\right)+S_1\left(\frac{n}{T_s}\right)\right|^2\delta\left(f-\frac{n}{T_s}\right)\right) \quad (18.24)\\ &\quad +\frac{1}{2.T_s}.\left(\left|S_0\left(f\right)\right|^2+\left|S_1\left(f\right)\right|^2-\frac{1}{2}.\left|S_0\left(f\right)+S_1\left(f\right)\right|^2\right) \end{aligned}$$

With

$$\begin{aligned} S_0(f) &= S(f).e^{-j0} = S(f)\\ S_1(f) &= S(f).e^{-j2\pi xT_sf} \end{aligned} \quad (18.25)$$

where x represents the time shift of the pulse expressed in % of T_s to code a '1', $S(f)$ is the Fourier transform of the basic pulse waveform and $S_0(f)$ and $S_1(f)$ are the Fourier transforms of the symbols 0 and 1. We find after some calculations

$$G_s(f)=\frac{1}{2T_s^2}\sum_{n=-\infty}^{+\infty}\left|S\left(\frac{n}{T_s}\right)\right|^2\left(1+\cos\left(2\pi nx\right)\right).\delta\left(f-\frac{n}{T_s}\right)+\frac{1}{2T_s}\left|S\left(f\right)\right|^2\left(1-\cos\left(2\pi fxT_s\right)\right) \quad (18.26)$$

For a short TH sequence, , the spectrum of the transmit signal (without modulation) can be written as

$$FT\{TH(t)\}=S(f).\sum_{k=0}^{N_s-1}e^{j2\pi(T_f.k+c_kT_c).f} \quad (18.27)$$

Replacing $S(f)$ in Eq. (18.23) by the Fourier transform of this TH code, the PSD of the signal is then:

$$\begin{aligned} G_s(f) &= \frac{1}{2T_s^2}\sum_{n=-\infty}^{+\infty}\left|S\left(\frac{n}{T_s}\right)\right|^2\left|\sum_{k=0}^{N_s-1}e^{j2\pi(T_f.k+c_kT_c).\frac{n}{T_s}}\right|^2.\left(1+\cos\left(2\pi n\frac{T_\mathrm{d}}{T_s}\right)\right).\delta\left(f-\frac{n}{T_s}\right) \quad (18.28)\\ &\quad +\frac{1}{2T_s}\left|S\left(f\right)\right|^2.\left|\sum_{k=0}^{N_s-1}e^{j2\pi(T_f.k+c_kT_c).f}\right|^2.\left(1-\cos\left(2\pi fT_\mathrm{d}\right)\right) \end{aligned}$$

with T_d the delay due to Pulse Position Modulation.

Chapter 19

Orthogonal Frequency Division Multiplexing (OFDM)

1. In order to generate the signal plots, we use the following MATLAB program

```
%---Chap.  19 Prob 1-----------------
s=[1 4 3 2 1 3 1 2]
h=[2 0 2 -1];
N=length(s); %# of OFDM tones
L=length(h)-1; % length of CP
sc=[s(N-L+1:N),s]; % adding CP
yc=conv(sc,h); % channel
y=yc(L+1:L+N); % CP deletion
Y=fft(y);
%---Get H(k)'s-----------
H=zeros(1,8);
for k=1:N
H(k)=0;
for i=1:length(h)
H(k)=H(k)+h(i)*exp(-j*2*pi*(i-1)*(k-1)/N);
end
end
S_hat=Y./H;
s_hat=real(ifft(S_hat));
figure(1)
subplot(2,2,1);stem(s);ylabel('s[n]');
subplot(2,2,2);stem(sc);ylabel('sc[n]');
subplot(2,2,3);stem(yc);ylabel('yc[n]');
subplot(2,2,4);stem(y);ylabel('y[n]');
figure(2)
subplot(2,2,1);stem(abs(Y));ylabel('Y[k]');
subplot(2,2,2);stem(abs(S_hat));ylabel('S-hat[k]');
subplot(2,2,3);stem(s_hat);ylabel('s-hat[n]');
```

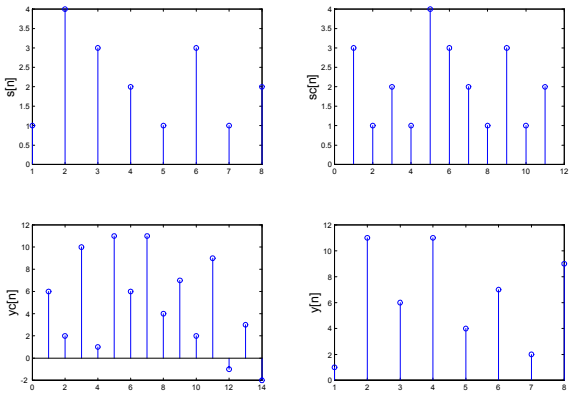

Figure 19.1: Signal vectors for OFDM system from Exercise 19.1: original signal; transmit signal with cyclic prefix, received signal; received signal after stripping off cyclic prefix.

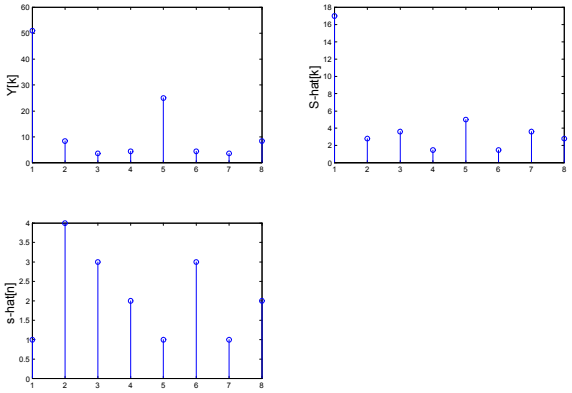

Figure 19.2: Signals for OFDM system from Exercise 19.1: received signal in frequency domain; signal in frequency domain after equalization; final signal in time domain.

(a) The block diagram of a baseband OFDM system can be found in Fig. B-19.4.

(b) The minimum CP length should be $4 - 1 = 3$. Observing that $\hat{s}[n] = s[n]$, the transmitted data can be fully recovered, because of the implementation of cyclic prefix. In another word, there is no intercarrier interference due to frequency selectivity. At the baseband, the receiver discards the first 3 received samples.

(c) The signal vectors are plotted in Figs. 19.1-19.2.

2. We need to find the backoff level that limits the probability of exceeding the desired amplitude level to $x\%$. As mentioned in Sec. 19.6, the distribution of in-phase and quadrature-phase amplitudes are Gaussian. The distribution of the total amplitude is thus Rayleigh

$$pdf(r) = \frac{r}{\sigma^2} \cdot \exp\left[-\frac{r^2}{2\sigma^2}\right] \qquad 0 \le r < \infty \tag{19.1}$$

Since the average mean power is unity, the σ in each of the branches must be $\sigma = 1/\sqrt{2}$, and the cdf can be written as

$$cdf(r) = 1 - \exp\left(-\frac{r^2}{1}\right) \tag{19.2}$$

Since we require that the amplitude does not exceed a level A_0, we find that

$$cdf(A_0) = 1 - \exp\left(-A_0^2\right) = 1 - x \tag{19.3}$$

Thus, the level A_0 must be

$$A_0 = \sqrt{\ln(1/x)} \tag{19.4}$$

which is 1.517, 2.146, 2.628, respectively.

3. Let the block $X_k^{(i)}$ be the i-th block of the transmission, with k indexing the N complex modulation symbols. The transmit signal in the time domain $x^{(i)}[n]$ can then be written as

$$x^{(i)}[n] = \frac{1}{N}\sum_{k=0}^{N-1} X_k^{(i)} e^{j\frac{2\pi}{N}nk} \quad , \quad -G \le n < N \tag{19.5}$$

where G is the length of the CP; if the CP is absent, we simply set $G = 0$. The channel performs the convolution with the impulse response of the channel $h[n,l]$, which consists of L multipath components, $0 \le l < L$, and is time-variant, as reflected by the double indexing. The received signal $y^{(i)}[n]$ (without noise added by the channel) is then

$$y^{(i)}[n] = (h * x^{(i)})[n] \ , \tag{19.6}$$

As the CP is discarded by the receiver, we henceforth consider only $0 \le n < N$. The first $L - G - 1$ samples of $y^{(i)}[n]$ are distorted by ISI from the previous symbol $x^{(i-1)}$, thus $y^{(i)}$ consists of two parts,

$$\begin{aligned} y^{(i)}[n] &= \sum_{l=0}^{L-1} h[n,l]x^{(i)}[n-l]\sigma[n-l+G] + \\ &\quad + \sum_{l=G+1}^{L-1} h[n,l]x^{(i-1)}[n-l+G+N](1-\sigma[n-l+G]) \\ &= y^{(i;i)}[n] + y^{(i;i-1)}[n] \ , \end{aligned} \tag{19.7}$$

where σ is the Heaviside function, and $y^{(i,i)}[n]$ and $y_i^{(i,i-1)}[n]$ are the contributions to $y^{(i)}[n]$ stemming from the $i-$th and $i-1$-th block, respectively. To reconstruct the sent symbols, the receiver performs a DFT on $y^{(i)}[n]$, $Y_k^{(i)} = \mathcal{DFT}\{y^{(i)}[n]\}[k]$ where again k is the subcarrier index. Throughout the paper we assume perfect synchronization of carriers and blocks, and further, if not otherwise stated, absence of noise.

We now write the Discrete Fourier Transform of Eq. (19.7) in the receiver as

$$\begin{aligned} Y_k^{(i)} &= \sum_{n=0}^{N-1}\left(y^{(i,i)}[n] + y_i^{(i,i-1)}[n]\right)e^{-j\frac{2\pi}{N}nk} = \\ &= \underbrace{\sum_{n=0}^{N-1}\sum_{l=0}^{L-1} h[n+iN,l]x^{(i)}[n-l]\sigma[n-l+G]e^{-j\frac{2\pi}{N}nk}}_{Y_{i,k}^{(i)}} + \\ &+ \sum_{n=0}^{N-1}\sum_{l=G+1}^{L-1} h[n+iN,l]x^{(i-1)}[n-l+G+N]\cdot \\ &\underbrace{\cdot(1-\sigma[n-l+G])\,e^{-j\frac{2\pi}{N}nk}}_{Y_{i,k}^{(i-1)}} . \end{aligned} \tag{19.8}$$

$Y_k^{(i,i)}$ and $Y_{i,k}^{(i,i-1)}$ are again the parts of $Y_k^{(i)}$ that originate from the own symbol i and the previous symbol $i-1$, respectively. If we use (19.5), these parts can then be written as

$$Y_k^{(i,i)} = \sum_{m=0}^{N-1} X_m^{(i)} H_{k,m}^{(i,i)} \ , \tag{19.9}$$

$$Y_k^{(i,i-1)} = \sum_{m=0}^{N-1} X_m^{(i-1)} H_{k,m}^{(i,i-1)} \tag{19.10}$$

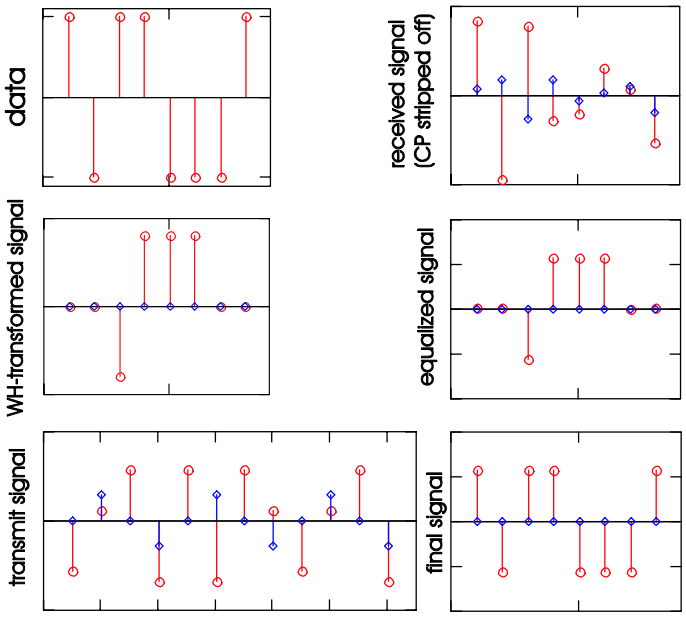

Figure 19.3: Signal waveforms for an 8-point MC-CDMA system (Exercise 19.4).

where

$$H_{k,m}^{(i,i)} = \frac{1}{N} \sum_{n=0}^{N} \sum_{l=0}^{L-1} h[n+iN, l] e^{j\frac{2\pi}{N}(nm-lm-nk)} \sigma[n-l+G] \tag{19.11}$$

and

$$H_{k,m}^{(i,i-1)} = \frac{1}{N} \sum_{n=0}^{N} \sum_{l=G+1}^{L-1} h[n+(i-1)N, l] e^{j\frac{2\pi}{N}(nm-lm-nk)} \tag{19.12}$$

This can be written in a compact form as a vector-matrix-product $\mathbf{Y}^{(i)} = \mathbf{Y}^{(i,i)} + \mathbf{Y}^{(i,i-1)} = \mathbf{H}^{(i,i)} \cdot \mathbf{X}^{(i)} + \mathbf{H}^{(i,i-1)} \cdot \mathbf{X}^{(i-1)}$ .where $\mathbf{Y}^{(i,i-1)}$ is the ISI term and $\mathbf{Y}^{(i,i)}$ contains the desired data disturbed by ICI. Note that if $\mathbf{X}^{(i-1)}$ was detected successfully (and the channel is completely known, as we always assume), $\mathbf{Y}^{(i,i-1)}$ can be computed and subtracted from $\mathbf{Y}^{(i)}$.

4. (a) The plots of the various signal components can be seen in Fig. 19.3.

   (b) The average noise enhancement with a zero-forcing receiver can be computed as

$$\left(\frac{1}{8}\sum \frac{1}{|H_i|^2}\right)\left(\frac{1}{8}\sum |H_i|^2\right) = 11.27 = 10.5 \text{ dB} \tag{19.13}$$

   (c) Simulation of the system with zero-forcing equalization is straightforward, though care must be taken about the correct normalizations in the spreading and despreading operation. A simulation plot is shown in Fig.

5. For the evaluation of this problem, we apply Eq. (19.14)

$$SINR = \frac{\frac{E_S}{N_0} P_{\text{sig}} \frac{N}{N_{\text{cp}}+N}}{\frac{E_S}{N_0} P_{\text{sig}} \frac{N}{N_{\text{cp}}+N} \frac{P_{\text{ISI}}+P_{\text{ICI}}}{P_{\text{sig}}} + 1} \ . \tag{19.14}$$

where P_{sig}, P_{ICI}, and P_{ISI} are given by Eqs. (B-19.21) - (B-19.23). Since the Doppler effect is negligible, the function $R(k,l)$ becomes the power delay profile, sampled at the OFDM sampling instants $k \cdot 1\mu s$

$$R(k,l) = \exp(-k/16) \tag{19.15}$$

Inserting this, and Eq. (B-19.20) into Eqs. (B-19.21) - (B-19.23), we obtain the values for P_{sig}, P_{ICI}, and P_{ISI}. The result is shown in Fig. 19.5.

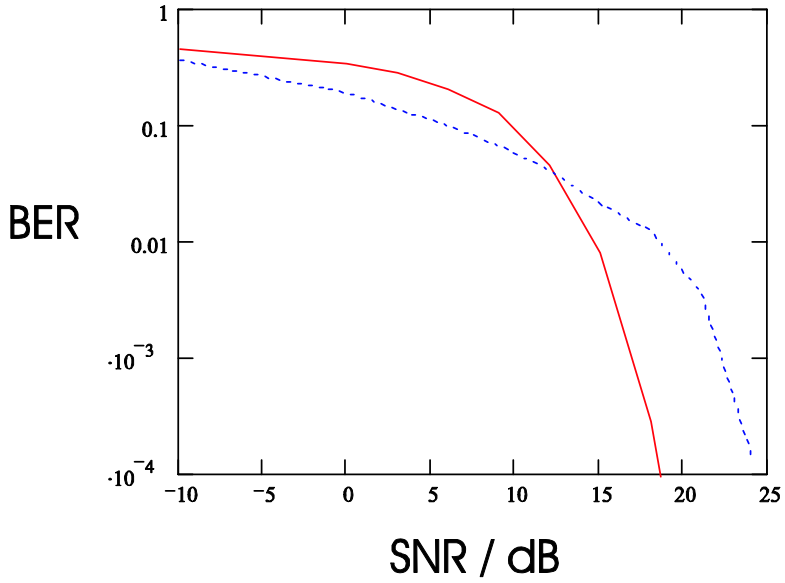

Figure 19.4: BER of the OFDM system with (solid) and without (dotted) WH transformation. See Exercise 19.4.

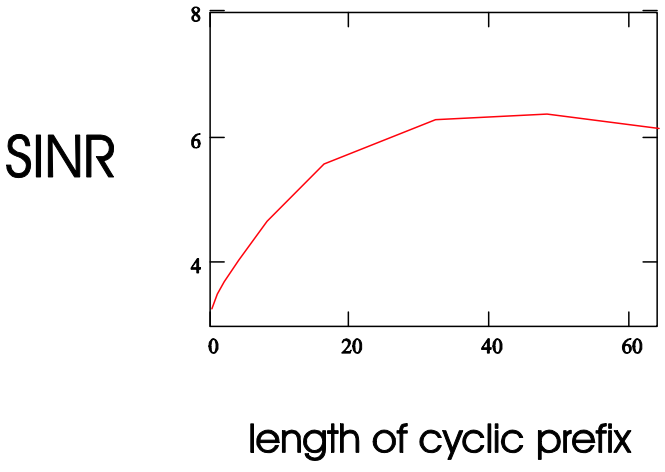

Figure 19.5: SINR as a function of the duration of the cyclic prefix for $SNR = 8$ dB (Exercise 19.5).

6. The capacity for waterfilling is given by Eq. (B-19.31), with the power constraint Eq. (B-19.32). We find by inspection that with $\alpha_n^2 = 1, 0.1, 0.01$, then $\varepsilon = 55.5$, so that $P_1 = 54.5$, $P_2 = 45.5$, and $P_3 = 0$. Thus, the third channel is not selected by the system. The SNRs in the two used channels are then 54.5 and 45.5. From this, we find that that the capacity in the first channel is

$$\log_2(1 + 54.5) = 5.79 \text{ bit/s/Hz} \tag{19.16}$$

while for the second channel it is

$$\log_2(1 + 54.5) = 5.54 \text{ bit/s/Hz} \tag{19.17}$$

and the total capacity is 11.33 bit/s/Hz.

When using BPSK, each of the channels can achieve at most 1 bit/s/Hz. Thus, the total capacity is limited to 2 bit/s/Hz if waterfilling is used. When equal power allocation is used, 3 bit/s/Hz can be used.

7. The key to this exercise is to recognize that the different carriers are fading independently, and thus the behavior of the coded system is the same as a properly interleaved block-coded single-carrier system in a flat-fading channel. Thus, Eq. (B-14.52) and the subsequent discussion applies without modifications. A diversity order of 4 can be achieved, so that the BER is proportional to $1/\gamma^4$.

8. The spectral efficiency of BPSK with rasied-cosine spectrum follows from Eq. (B-11.5). We find that the spectrum occupies a band of width

$$\Delta B = (1 + \alpha)/T_{\mathrm{B}} \tag{19.18}$$

where α is the rolloff factor; no energy exists outside that band (of course, that is an idealization; in practical circumstances, the rolloff is never perfect). Spacing the carriers at ΔB then ensures complete orthogonality. For OFDM, the spacing between the carriers is $1/T_{\mathrm{B}}$, which also guarantees perfect orthogonality, even though the bands on the different carriers do overlap. It thus seems that OFDM shows the better spectral efficiency. For this comparison, we disregard the possible introduction of a cyclic prefix: measures fighting delay dispersion have to be implemented in any system.

Chapter 20

Multiantenna systems

1. The advantages of using a smart antenna system include

   - Increase of coverage area
   - Increase of user capacity
   - Improvement of link quality
   - Decrease of delay dispersion
   - Improvement of user localization

2. For single antenna,

$$N = \frac{SF}{SIR_{\text{threshold}}} = \frac{128}{10^{0.6}} \approx 32 \tag{20.1}$$

   For $N = 4$ antennas,

$$N = \frac{SF \cdot N}{SIR_{\text{threshold}}} = \frac{128 \times 4}{10^{0.6}} \approx 128 \tag{20.2}$$

   Consider now the reduction of the received desired signal power due to angular spreading. The array factor is given as

$$|M_k(\phi)| = \left| \frac{\sin\left[\frac{N_\text{r}}{2}\left(\pi\cos\phi - \frac{k}{N_\text{r}}\right)\right]}{\sin\left[\frac{1}{2}\left(\pi\cos\phi - \frac{k}{N_\text{r}}\right)\right]} \right| \tag{20.3}$$

   The power reduction of the desired signal can thus be computed as

$$\frac{P}{P_{\text{unspread}}} = \frac{1}{N_\text{r}^2} \int \frac{6}{\pi} \exp\left(-\frac{|\phi - \pi/2|}{(\pi/12)}\right) \left| \frac{\sin\left[\frac{N_\text{r}}{2}\left(\pi\cos\phi\right)\right]}{\sin\left[\frac{1}{2}\left(\pi\cos\phi\right)\right]} \right|^2 d\phi \quad . \tag{20.4}$$

   which can be evaluated numerically as 0.805, 0.563, 0.348 for $N_\text{r} = 2, 4, 8$, respectively.

3. The three different purposes are:

   - beamforming
   - diversity
   - spatial multiplexing

   Spatial multiplexing has attracted by far the most attention since it enables the transmission of multiple data streams in parallel, which increases the channel capacity linearly with the number of data streams. The underlying mechanism is: spatially separated antennas are able to exploit independent fading across the antennas in a rich multipath environment to support independent single channels (or communication modes) via proper signal processing. More explicitly, the MIMO channel matrix $\mathbf{H}$ contains more of one significant singular values, each of which corresponds to the complex gain of the new single channels.

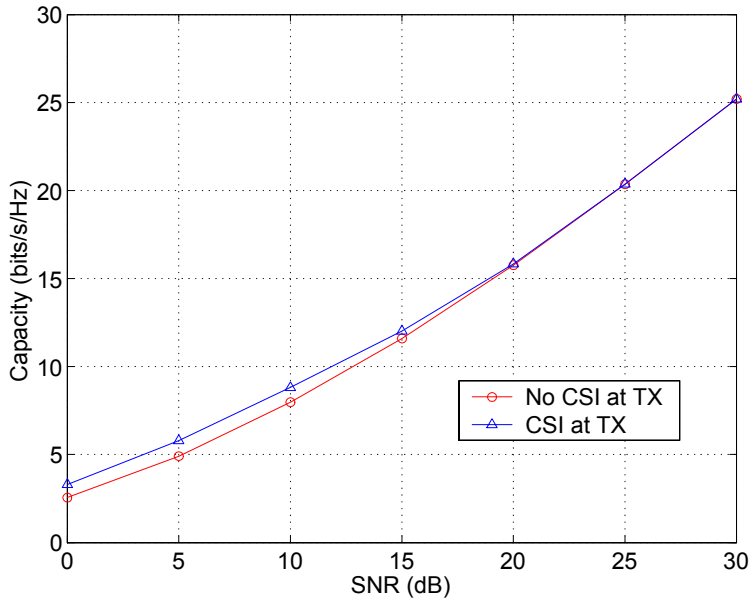

Figure 20.1: Capacity of 3×3 MIMO system with and without CSI at TX.

4. For the case of no channel information at the TX, equal transmit power is assigned to all the TX antennas,

$$C = \log_2 \det \left(\mathbf{I}_{N_r} + \frac{\bar{\Gamma}}{N_t} \mathbf{H}\mathbf{H}^\dagger \right) \tag{20.5}$$

For the case with channel information at the TX, waterfilling may be used to maximize the capacity. To perform waterfilling, let the eigenvalues of the matrix $\mathbf{H}\mathbf{H}^\dagger$ be $\lambda_1, \lambda_2, \lambda_3$. The waterfilling solution is then given by

$$C = \sum_{i=1}^{3} \log_2 \left(\mu \lambda_i \right)^+ \tag{20.6}$$

where μ must satisfy $\bar{\Gamma} = \sum_{i=1}^{3} \left(\mu - \lambda_i^{-1} \right)^+$. Using MATLAB to implement the above calculations for $\bar{\Gamma} = 0 : 5 : 30$ dB, the following Fig. 20.1 can be plotted. The MATLAB scripts used to plot the equal power and waterfilling capacities in bits/s/Hz for the given range of SNR (and the given $\mathbf{H}$ matrix) is as follows:

```
% main MATLAB script
snr=0:5:30;

for i=1:length(snr)
[Ceq(i),Cwf(i)]=calc_capacity(snr(i));
end

figure(1)
H=axes('FontSize',16)
plot(snr,Ceq,'r-o',snr,Cwf,'b-^')
legend('No CSI at TX','CSI at TX',0)
ylabel('Capacity (bits/s/Hz)')
xlabel('SNR (dB)')
```

```
grid on

figure(2)
H=axes('FontSize',16)
plot(snr,Cwf./Ceq,'b-^')
ylabel('Relative Capacity Gain with CSI at TX')
xlabel('SNR (dB)')
grid on

% function to generate capacities for a given SNR
function [Ceq,Cwf]=calc_capacity(snr)
Pt=10^(snr/10);
H=[-0.0688-1.1472*j -0.9618-0.2878*j -0.4980+0.5124*j
   -0.5991-1.0372*j  0.5142+0.4967*j  0.6176+0.9287*j
    0.2119+0.4111*j  1.1687+0.5871*j  0.9027+0.4813*j];

Ceq=real(log2(det(eye(3)+Pt/3*H*H'))); % capacity for equal power case

% capacity for waterfilling case
MINIMUM = [];
value=0;
stepsize = 0.01;
W=H*H';
[V2,S2]=eig(W);
S2=diag(S2);
start = real(min(1./S2))/stepsize;
for xvar=start:100000
 rho=0;
 if (xvar*stepsize-1/S2(1)) >= 0
 rho = (xvar*stepsize-1/S2(1));
 end
 if (xvar*stepsize-1/S2(2)) >= 0
 rho= rho + (xvar*stepsize-1/S2(2));
 end
 if (xvar*stepsize-1/S2(3)) >= 0
 rho= rho + (xvar*stepsize-1/S2(3));
 end
 if rho-Pt > 0
 value=xvar*stepsize;
 break
 end
end
```

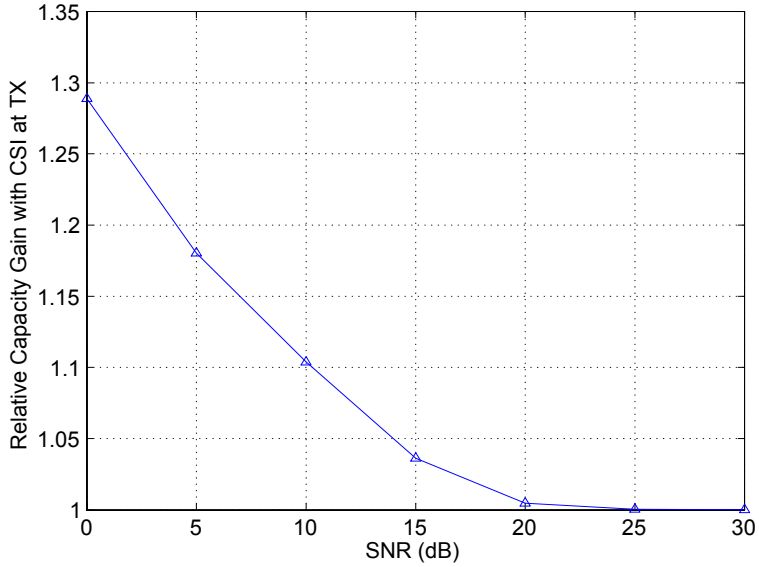

Figure 20.2: Relative capacity gain for different SNRs.

```
sum1=0;
for p=1:length(S2)
 term=log2(value*(S2(p)));
 if term>0
 sum1=sum1+term;
 end
end
Cwf=real(sum1);
return;
```

It appears in Fig. 20.1 that the improvement due to waterfilling suffers from diminishing return with increasing SNR. Figure 20.2 highlights this feature further with a plot of capacity gain due to waterfilling, relative to the equal power case.

The fact that feedback gain reduces at higher SNR levels can be intuitively explained by the following fact. Knowledge of the transmit channel mainly provides transmit array gain. In contrast, gains such as diversity gain and multiplexing gain do not require this knowledge as these gains can be captured by "blind" transmit schemes such as STCs and V-BLAST. Since the relative importance of transmit array gain in boosting average SNR decreases in the high SNR region, the benefit of channel state information at the transmitter is also reduced.

5 A single bounce channel model as described in the following may be used for this investigation: Each transmission traces a path from a TX antenna to one scatterer, and then to the RX antenna. The scatterer positions are placed according to random realizations of DoD and DoA of signal paths, denoted by θ_{t} and θ_{r}, respectively. θ_{t} and θ_{r} are random variables, uniformly distributed over the intervals $(-90°, 90°)$. Each signal path has a complex gain drawn from a Rayleigh distribution. Based on the above model, we obtain the capacity distribution for a 4×4 MIMO system for $N_{\mathrm{S}} = 1, 2, 4, 10, 50, 100$ (see Figure 20.3). The ideal Rayleigh case is also included for comparison. The impact of having fewer scatterers than N_{t} or N_{r} on the capacity distribution is obvious. It is also noted that the capacity gain

from having additional scatterers while the number of scatterers N_S are less than N_t or N_r is much more significant than when they are exceeded. In fact, a saturation point is eventually obtained when N_S is increased further. For example, there is practically no difference between the cases of $N_S = 50$ and $N_S = 100$. Also note that in this case, the capacity distribution tends towards the Rayleigh case for a large N_S. The MATLAB script used to generate the plot is given below.

(a)
```
M=4; % Number of TX antennas
N=4; % Number of RX antennas
d=2; % Spacing between antennas (in unit of wavelength)

NM=min(N,M);
Ntest=2000;  % Number of realizations to run

for Ns=[1 2 4 10 50 100 200]

for it=1:Ntest

% Distribution of angles and departure and arrival
theT=(rand(1,Ns)-0.5)*180;
theR=(rand(1,Ns)-0.5)*180;

a=(randn(1,Ns)+j*randn(1,Ns))/sqrt(2);

H=zeros(M,N);
tn=1:N;
tm=1:M;

for n=1:N
for m=1:M
   H(n,m)=sum(a.*exp(-j*2*pi*d*n*sin(pi/180*theR)).*exp(-j*2*pi*d*m*sin(pi/180*theT)));
end
end

if Ns==200
H=(randn(N,M)+j*randn(N,M))/sqrt(2); % ideal Rayleigh case
end

Ht(it,:,:)=H(:,:);
end

P=mean(abs(Ht(:,1,1).^2));

for it=1:Ntest
H(:,:)=Ht(it,:,:);

% Normalize H with respect to its (1,1) element over all realizations
H=H/sqrt(P);

C(it)=log2(det(eye(M)+100/M*H*H')); % Set SNR=20 dB
```

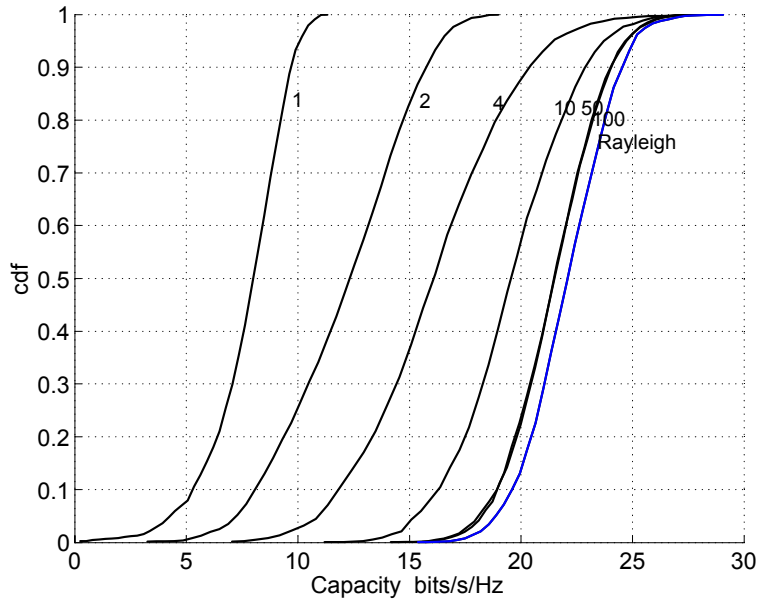

Figure 20.3: Capacity distribution for different number of scatterers.

```
end

C=real(C); % Getting rid of numerical errors in MATLAB resulting in non-zero imaginary
part

[n2,x2]=hist(C,40);
n2m=n2/Ntest;
a2=cumsum(n2m);
b2=a2;
plot(x2,b2,'k','LineWidth',1); hold on

if Ns==200 % Rayleigh case
plot(x2,b2,'b','LineWidth',1);
end

xlabel('Capacity, b/s/Hz','FontSize',16)
ylabel('CDF','FontSize',16)
grid on

end % end of loop for different number of scatterers
```

6 For the Kronecker model, we require the correlation matrices of the TX and the RX, denoted by $\mathbf{R}_{\mathrm{TX}}$ and $\mathbf{R}_{\mathrm{RX}}$, respectively. These are obtained from the structure of the TX and RX arrays and the DoD and DoA angular spectra $f(\theta)$.

$$[\mathbf{R}_{\mathrm{TX}}]_{n,m} = \frac{\int_0^{2\pi} a_n(\theta)\, a_m^*(\theta)\, f(\theta)\, d\theta}{\sqrt{\int_0^{2\pi} a_n(\theta)\, a_n^*(\theta)\, f(\theta)\, d\theta \int_0^{2\pi} a_m(\theta)\, a_m^*(\theta)\, f(\theta)\, d\theta}},$$

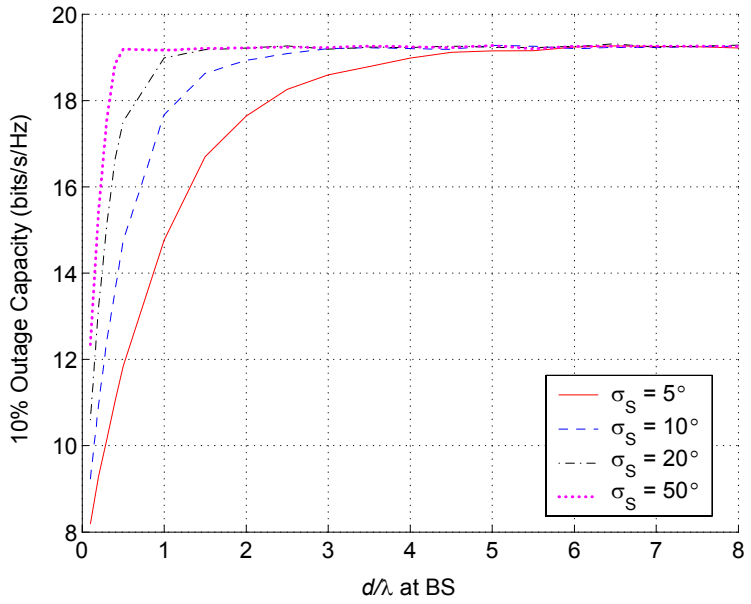

Figure 20.4: 10% outage capacity for Laplacian distribution at the BS and uniform distribution at the MS.

where $a_n(\theta)$ is the nth element of the steering vector of the uniform linear array $\mathbf{a}(\theta)$ at the TX. $\mathbf{R}_{\mathrm{RX}}$ is similarly defined.

10,000 realizations of the channel are obtained for each array spacing at the BS over the range $d \in [0.1\lambda, 8\lambda]$. Figure 20.4 shows the 10% outage capacity. From the figure, it is clear that the outage capacity suffers at lower array spacing, and particularly for lower angular spread. This is because when antennas are brought closer together, there is less fading diversity available for the received signals. Note, however, that here the effect of mutual coupling is neglected. In reality, mutual coupling can significantly affect the capacity performance at smaller array spacings.

The MATLAB script to generate the plot is as follows:

```
angspr=[5 10 20 50];% Put the range of desired angular spread
d=[0.1:0.1:0.4 0.5:0.5:10]; % Spacing between antenna elements (in wavelength)
C_1=zeros(size(d)); % Initialize 10% outage capacity vector
CC=zeros(length(d),length(angspr));

for ii=1:length(angspr)
for k=1:length(d)

Nt=4; % Number of ULA elements at TX
Nr=4; % Number of ULA elements at RX

MC=1e4; % Number of trials to obtain capacity distribution
snr=20; % in dB
snr=10^(snr/10); % SNR at the receiver
Np=1e4; % Number of paths

% Spatial correlation at the TX
```

```
st=2*pi*rand(1,Np); % Assume uniform distribution at TX
At=exp(j*(0:(Nt-1))'*sin(st)*2*pi*0.5)/sqrt(Np);
Rt=At*At';

% Assume Laplacian distribution at RX
AS=angspr(ii)/180*pi;
b=1/sqrt(2);
sr=rand(1,Np);
sr(find(sr<=0.5))=AS*b*log(2*sr(find(sr<=0.5)));
sr(find(sr>0.5))=-AS*b*log(2*(1-sr(find(sr>0.5))));
Ar=exp(j*(-(Nr-1)/2:(Nr-1)/2)'*sin(sr)*2*pi*d(k))/sqrt(Np); % broadside
%ULA, middle of array as reference, seems to be same as element 1 as reference
Rr=Ar*Ar'; % correlation matrix at RX

% Use Kronecker model to generate channel matrix H and calculate capacity C
Q=snr*eye(Nt); % Signal covariance matrix
C=zeros(1,MC); % initialize capacity vector
sqrt_tr_Rt=sqrt(trace(Rt));
sqrt_Rt=Rt^0.5;
sqrt_Rr=Rr^0.5;

for i=1:MC
 G=1/sqrt(2)*(randn(Nr,Nt)+j*randn(Nr,Nt));
 H=1/sqrt_tr_Rt*sqrt_Rr*G*(sqrt_Rt).';
 C(i)=log2(det(eye(Nr)+H*Q*H'));
end

C=real(C); % Getting rid of numerical errors in MATLAB resulting
%in non-zero imaginary part
C=sort(C);
C_1(k)=C(MC*0.1);% Capacity at 10% level
end

CC(:,ii)=C_1.';
end

% plotting results
H=axes('FontSize',16);
hold on
plot(d,CC(:,1),'r',d,CC(:,2),'b--',d,CC(:,3),'k-.')
plot(d,CC(:,4),'m:','LineWidth',2)
legend('\sigma_S = 5{\circ}','\sigma_S = 10{\circ}','\sigma_S = 20{\circ}','\sigma_S =
50{\circ}',0)
```

```
xlabel('{\itd/{\lambda}} at BS')
ylabel('10% Outage Capacity (bits/s/Hz)')
grid on
```

7 The channel matrix for the system consists of LOS and non-LOS components.

$$\mathbf{H} = \sqrt{\frac{\bar{\Gamma}_{\mathrm{LOS}}}{N_{\mathrm{t}}}}\mathbf{H}_{\mathrm{LOS}} + \sqrt{\frac{\bar{\Gamma}_{\mathrm{NLOS}}}{N_{\mathrm{t}}}}\mathbf{H}_{\mathrm{NLOS}} \tag{20.7}$$

The LOS component is given by

$$\mathbf{H}_{\mathrm{LOS}} = \mathbf{a}_{\mathrm{r}}\left(\theta_{\mathrm{r}}\right)\mathbf{a}_{\mathrm{t}}^{T}\left(\theta_{\mathrm{t}}\right) \tag{20.8}$$

where $\mathbf{a}_{\mathrm{t}}^{T}\left(\theta_{\mathrm{t}}\right)$and $\mathbf{a}_{\mathrm{r}}^{T}\left(\theta_{\mathrm{r}}\right)$ are the steering vectors of the arrays at the transmitter and receiver, respectively, and the LOS SNR $\bar{\Gamma}_{\mathrm{LOS}} = 6/1 = 7.78$ dB.

The non-LOS component is given by

$$\mathbf{H}_{\mathrm{NLOS}} = \begin{bmatrix} h_{11} & h_{12} & h_{13} \\ h_{21} & h_{22} & h_{23} \\ h_{31} & h_{32} & h_{33} \end{bmatrix} \tag{20.9}$$

where h_{nm} are channel coefficients from the $n-$th transmitter to the $m-$th receiver, normalized such that

$$\sum_{n=1}^{3}\sum_{m=1}^{3}\left|h_{nm}\right|^{2} = N_{\mathrm{r}}N_{\mathrm{t}} = 9. \tag{20.10}$$

By definition, h_{nm} is a circularly symmetric complex Gaussian random variable with i.i.d. zero mean and unit variance.

Using MATLAB, the capacity distribution of LOS and NLOS cases can be computed for a large number of realizations of the channel. The channel capacity for each channel realization is given by

$$C = \log_2 \det\left(\mathbf{I}_{N_r} + \mathbf{H}\mathbf{H}^{\dagger}\right) \tag{20.11}$$

In Figure 20.5, the cdf for the LOS case is given as the solid line. The cdf for the NLOS case is given as the dotted line. The increase of transmit power (by trial and error) brings the expected capacity back to that of the LOS case is shown as the dot-dashed line. And finally the increase of transmit power to bring the 5% outage capacity back to that of the LOS case is given as the dashed line.

Case	Channel Capacity	Add. RX power	required power increase
Equal expected capacity (TX power 1)	7 bits/s/Hz	3.8 mW	+127%
Equal 5% outage capacity (TX power 2)	5.6 bits/s/Hz	5.2 mW	+173%

Table 20.2. Change in TX power for NLOS case to match LOS capacity.

It is clear from this exercise that the LOS component is very important to MIMO capacity. A loss of LOS path can cause a large drop in capacity, which can only be compensated for by a large increase in TX power.

We also observe that the slope of the NLOS cases with increased TX power is smaller than the LOS case, since the LOS case is less susceptible to fading (no fading in the LOS component!). As a direct consequence, much greater power (additional 173 %, or 273 % relative to original) is needed in the 5 % outage case in order to restore the LOS capacity.

```
MC=5e4; % Number of realizations
d=0.5; % Antenna separation distance (in wavelength)
Nr=3; % Number of RX
Nt=3; % Number of TX
theta_r=0; % Angle of arrival of LOS component at RX
```

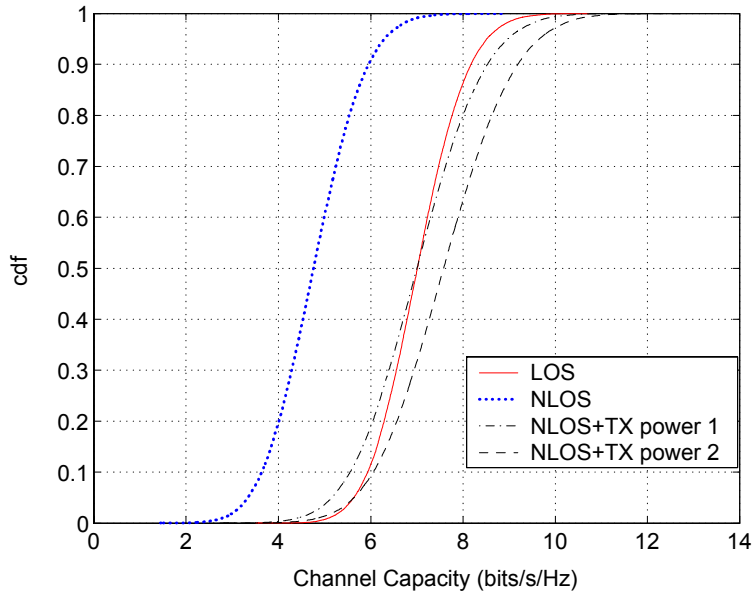

Figure 20.5: Cdfs of indoor LOS and NLOS cases.

```
theta_t=0; % Angle of departure of LOS component at TX
snrLOS=6/1;

ar=exp(j*2*pi*d*sin(theta_r)*(0:(Nr-1)));
at=exp(j*2*pi*d*sin(theta_t)*(0:(Nt-1)));

HLOS=sqrt(snrLOS/Nt*eye(Nr))*ar.'*at;

C1=zeros(1,MC);
C2=C1;
C3=C1;

for i=1:MC
    H=1/sqrt(2)*(randn(Nr,Nt)+j*randn(Nr,Nt));

    H1=sqrt(eye(Nr)*3/(1*Nr))*H+HLOS;
    C1(i)=log2(det(eye(Nr)+H1*H1')); % LOS+NLOS capacity
    H3=sqrt(eye(Nr)*3/(1*Nr))*H;
    C3(i)=log2(det(eye(Nrx)+H3*H3')); % Pure NLOS capacity

% Pure NLOS capacity + additional Tx Power for expected
    % channel capacity to be equal to mixed LOS+NLOS case
    H2=sqrt(eye(Nr)*6.8/(1*Nr))*H;
    C2(i)=log2(det(eye(Nr)+H2*H2'));
```

```
% Pure NLOS capacity + additional Tx Power for 5% outage
    % channel capacity to be equal to mixed LOS+NLOS case
    H4=sqrt(eye(Nr)*8.22/(1*Nr))*H;
    C4(i)=log2(det(eye(Nr)+H4*H4'));
end

% plotting cdfs of the different cases
cdf(real(C1),'r');
cdf(real(C3),'b:');
cdf(real(C2),'k-.');
cdf(real(C4),'k--');

xlabel('Channel Capacity (bits/s/Hz)','Fontsize',16)
ylabel('cdf','Fontsize',16)
legend('LOS','NLOS','NLOS+TX power 1','NLOS+TX power 2')
grid on


function y1=cdf(x,color) % function to plot cdf curves
[nx,cx]=hist(x,1000);

for i=1:1000
 y(i)=sum(nx(1:i));
end

y=y/length(x);
plot(cx,(y),color); hold on
return;
```

8 (a) The 10 %, 50 % and 90 % outage capacities for the different numbers of TX antennas relative to the capacity in the SISO case are given in Fig. 20.6. Here we assume equal power at the TX antennas, i.e., no CSI available at the TX. The MATLAB script used to generate the plot is given below

```
C_1=zeros(1,8); % Initialize 10% outage capacity vector
C_5=zeros(1,8); % Initialize 50% outage capacity vector
C_9=zeros(1,8); % Initialize 90% outage capacity vector

Nt=1:8; % Number of ULA elements at TX
Nr=4; % Number of ULA elements at RX
MC=1e4; % Number of trials to obtain capacity distribution
snr=20; % Assume 20dB SNR
snr=10^(snr/10); % SNR at the receiver

for k=1:length(Nt)
```

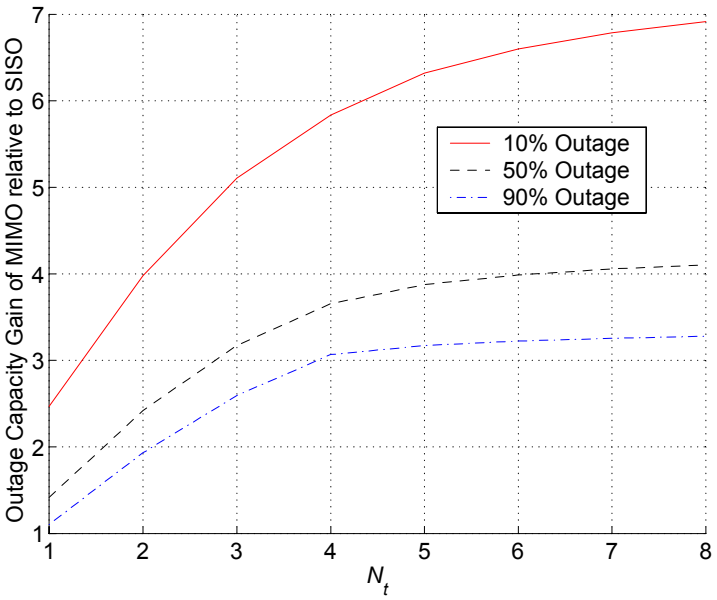

Figure 20.6: 10%, 50%, and 90% outage capacities.

```
Q=snr/Nt(k)*eye(Nt(k)); % Signal covariance matrix
C=zeros(1,MC); % initialize capacity vector

for i=1:MC
 H=1/sqrt(2)*(randn(Nr,Nt(k))+j*randn(Nr,Nt(k)));
H=H/norm(H,'fro')*sqrt(Nr*Nt(k));
 C(i)=log2(det(eye(Nr)+H*Q*H'));
end

C=real(C); % Getting rid of numerical errors in MATLAB resulting in non-zero imaginary
part
C=sort(C);
C_1(k)=C(MC*0.1); % Capacity at 10% level
C_5(k)=C(MC*0.5); % Capacity at 50% level
C_9(k)=C(MC*0.9); % Capacity at 90% level
end

% SISO case
 h=1/sqrt(2)*(randn(1,MC)+j*randn(1,MC));
 C_S=real(log2(1+snr*abs(h).^2));
 C_S=sort(C_S);
C_S1=C_S(MC*0.1); % Capacity at 10% level
C_S5=C_S(MC*0.5); % Capacity at 50% level
C_S9=C_S(MC*0.9); % Capacity at 90% level

C_1=C_1/C_S1; % Capacity at 10% level
C_5=C_5/C_S5; % Capacity at 50% level
C_9=C_9/C_S9; % Capacity at 90% level
```

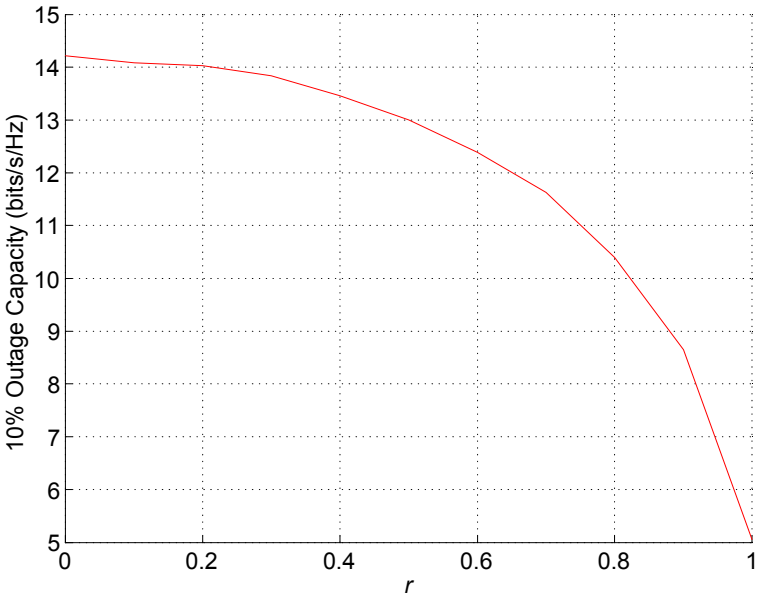

Figure 20.7: 10% outage capacity for different r values.

```
% plotting results
H=axes('FontSize',16);
hold on
plot(Nt,C_1,'r',Nt,C_5,'k--',Nt,C_9,'b-.')
legend('10% Outage','50% Outage','90% Outage',0)
xlabel('{\itN_t}')
ylabel('Outage Capacity Gain of 3x3 MIMO relative to SISO case')
grid on
```

As mentioned in the text, when the TX has no channel knowledge, then there is little point in having more transmit than receive antennas: the number of data streams is limited by the number of receive antennas. Of course, we can transmit the same data stream from multiple transmit antennas, but that does not increase the SNR for that stream at the receiver (without channel knowledge at the TX, the streams add up incoherently at the receiver).

9 The 10 % outage capacity plot for the different values of r are given in Fig. 20.7.

The following MATLAB script may be used to generate the required plot.

```
r=[0:0.1:1];
C_1=zeros(size(r)); % Initialize 10% outage capacity vector
 for k=1:length(r)
Nt=3; % Number of ULA elements at TX
Nr=3; % Number of ULA elements at RX
MC=1e4; % Number of trials to obtain capacity distribution
snr=20; % Assume 20dB SNR
snr=10^(snr/10); % SNR at the receiver
 Rt=[1 r(k) r(k)^2;r(k) 1 r(k);r(k)^2 r(k) 1];
```

```
Rr=Rt;
 % Use Kronecker model to generate channel matrix H and calculate capacity C
Q=snr*eye(Nt); % Signal covariance matrix
C=zeros(1,MC); % initialize capacity vector
sqrt_tr_Rt=sqrt(trace(Rt));
sqrt_Rt=Rt^0.5;
sqrt_Rr=Rr^0.5;
 for i=1:MC
 G=1/sqrt(2)*(randn(Nr,Nt)+j*randn(Nr,Nt));
 H=1/sqrt_tr_Rt*sqrt_Rr*G*(sqrt_Rt).';
 C(i)=log2(det(eye(Nr)+H*Q*H'));
end
C=real(C); % Getting rid of numerical errors in MATLAB resulting in non-zero imaginary
part
C=sort(C);
C_1(k)=C(MC*0.1);% Capacity at 10% level
end
 % plotting results
H=axes('FontSize',16);
hold on
plot(r,C_1,'r')
xlabel('{\itr}')
ylabel('10% Outage Capacity (bits/s/Hz)')
grid on
```

10 For the RHS (right-hand side), we know from the text that the singular value decomposition of $\mathbf{H}$ is given by $\mathbf{H} = \mathbf{U}\mathbf{\Sigma}\mathbf{W}^\dagger$, where $\mathbf{U}$ and $\mathbf{W}$ are unitary matrices, and $\mathbf{\Sigma}$ the eigenvalue of $\mathbf{H}$.

$$\begin{aligned}
\log\det\left(\mathbf{I}_{N_\mathrm{R}} + \frac{\overline{\gamma}}{N_\mathrm{T}}\mathbf{H}\mathbf{H}^\dagger\right) &= \log\det\left(\mathbf{I}_{N_\mathrm{R}} + \frac{\overline{\gamma}}{N_\mathrm{T}}\mathbf{U}\mathbf{\Sigma}^2\mathbf{U}^\dagger\right) \\
&= \log\det\left[\mathbf{U}\left(\mathbf{I}_{N_\mathrm{R}} + \frac{\overline{\gamma}}{N_\mathrm{T}}\mathbf{\Sigma}^2\right)\mathbf{U}^\dagger\right] \\
&= \log\det\left(\mathbf{I}_{N_\mathrm{R}} + \frac{\overline{\gamma}}{N_\mathrm{T}}\mathbf{\Sigma}^2\right) \text{(by property of determinant and unitary matrix)} \\
&= \log\left[\prod_{k=1}^{M}\left(1 + \frac{\overline{\gamma}}{N_\mathrm{T}}\sigma_k^2\right)\right] \\
&= \sum_{k=1}^{M}\log\left(1 + \frac{\overline{\gamma}}{N_\mathrm{T}}\sigma_k^2\right) \quad .
\end{aligned} \tag{20.12}$$

Chapter 21

GSM - Global System for Mobile communications

1. As we have seen in Part II, the pathloss is significantly lower at lower frequencies; this is partly related to the lower free-space pathloss, and also to the diffraction around obstacles. More quantitative results about the frequency dependence can be found from the Okumura-Hata models described in Chapter 7. Finally, the maximum allowed transmit power is usually higher for GSM-900 than for GSM-1800. For all these reasons, the carrier frequencies around 900 MHz are mostly suitable for covering larger areas. On the other hand, the lower propagation loss implies that the interference to neighboring cells can be higher, so that the reuse distance might have to be increased (compared to GSM-1800). Furthermore, the available absolute bandwidth is three times larger at 1800 MHz, so that it is typically cheaper to buy spectrum in this frequency range. Thus, the 1800 MHz cells are better suited for high-capacity areas. Summarizing, it is preferable to use GSM-1800 in urban areas where a high capacity is desired, while GSM-900 should be applied in rural areas where a large coverage area can be achieved.

   In many cases, an operator can only buy a *nationwide* spectral license. In that case, GSM 900 can be gainfully used in urban areas to establish "umbrella cells". Such cells have a larger coverage area, and can accomodate users that move fast without having an excessive numbers of handovers. Alternatively, GSM 900 can also be established to provide better indoor coverage. In either case, the GSM 900 and GSM 1800 networks have to be planned jointly.

2. BTS and BSC must be from the same vendor, as the Abis interface is not completely specified.

3. Since the DOAs are uniformly distributed, the Doppler spectrum has a Jakes shape. From Eq. (B-5.47), it then follows that the envelope autocorrelation function is

$$J_0^2(2\pi\nu_{\max}\Delta t) \tag{21.1}$$

   The Δt between the beginning of a burst and its end is after 148 bit durations. Thus, the time between the training sequence and the end of the burst is about $74 \cdot 3.7\ \mu s = 274\ \mu s$. In order to obtain $\nu_{\max}$, we first convert the speed to units of m/s, namely $250/3.6 = 70$ m/s. The the maximum Doppler frequency is

$$\nu_{\max} = \mathrm{v}\frac{f_\mathrm{c}}{c_0} = 70\frac{1.8 \cdot 10^9}{3 \cdot 10^8} = 420 \text{ Hz} \tag{21.2}$$

   The correlation coefficient is thus

$$J_0^2(2\pi \cdot 420 \cdot 274 \cdot 10^{-6}) = J_0^2(0.724) = 0.76 \tag{21.3}$$

   Between the beginning and the end of the burst, the argument of the Bessel function is doubled, so that the correlation coefficient becomes

$$J_0^2(2 \cdot 0.724) = 0.29\ . \tag{21.4}$$

4. The power delay profile for the TU-GSM model can be well approximated as a single-exponential profile (compare App. 7C)

$$P_h(\tau) = \exp(-\frac{\tau}{\mu s}) \tag{21.5}$$

From that, the envelope correlation coefficient can be computed as (see Eq. (B-13.4))

$$\rho_{xy} = \frac{1}{1 + (2\pi)^2 S_\tau^2 \left(f_2 - f_1\right)^2} \tag{21.6}$$

The frequency differences $f_2 - f_1$ that we consider are (i) 200 kHz, (ii) 5 MHz, and (iii) 80 MHz. Note that the latter value is specific to the DCS 1900 system in the US; the values are different for GSM 900 and GSM 1800. Inserting those values into the above equation, we get (i) 0.39, (ii) 10^{-3}, and (iii) $4 \cdot 10^{-6}$. We thus see that for cases (ii) and (iii), there is complete decorrelation.

5. The slow associated control channels SACCH carry the information about the properties of a specific TCH or a SDCCH. The MS informs the BS about the strength and quality of the signal received from the serving, as well as from the neighboring, BSs. The BS sends data about the power control and runtime of the signal from the MS to the BS. This information need not be transmitted very often, and therefore the channel is called *slow*; however, the information needs to be transmitted continuously. The SACCH is sent in the 13−th frame of a multiframe.

   The fast associated control channel FACCH carries the information that is required for a handover. This information has to be transmitted fast, but only rarely. Thus, the FACCH is transmitted using bits that would normally be used to carry payload data. The signalling bits just before and after the midamble in a burst signify whether the contained information is payload data or FACCH data.

6. The block FEC of the voice data is only an error-detecting code, to determine whether the class 1a voice bits were received correctly (after convolutional decoding). For this reason, it only contains 3 parity check bits for the 50 class 1a data bits. None of the other voice data are encoded with a block encoder.

   The signalling bits, on the other hand, are encoded with a $(224, 184)$ Fire code. Fire codes are block codes which are capable of correcting burst errors. The stronger protection is used because transmission errors in the control data can have catastrophic results for a link.

7. All midambles have an autocorrelation function that has a peak of amplitude 26 (for delay 0), and value 0 for at least 4 sample values to the left and right of this peak. Several sequences of length 26 fulfill this requirement. Different BSs use the different midambles. The reason is that this allows the MSs to distinguish signals from different BSs, and thus to better track the received power from those BSs. This provides important information for the handover procedure.

8. Yes, by entering the *Personal Unblocking Key* (PUK).

9. Subscriber A pays for international call charges (Denmark to Finland), as well as for roaming charges (being outside the coverage area of the home network), and possibly a fee for "conference call". Subscriber C pays for a call (forwarding) from France to England. Subscribers B and D do not pay any fees.

10. As a first step, we analyze the worst-case phase deviation of GMSK. We know that for regular MSK, the phase deviation in each bit is 0.5π. For GMSK, we insert Eq. (B-11.17) into Eq. (B-11.12) to obtain the modulation phase of a GMSK signal. By plotting this phase for a bit sequence of alternating $+1/-1$, we find that the phase deviation between a positive and negative bit can be as low as 0.15π. Applying a phase-derotation of $\pi/2$, we find that the distance between two points in the signal constellation diagram has decreased from $d_{ik} = 2$ to

$$\begin{aligned} d_{ik} &= \sqrt{(1 - \cos(0.65\pi))^2 + \sin^2(0.65\pi)} && (21.7) \\ &= 1.7 && (21.8) \end{aligned}$$

so that the effective SNR is decreased by 1.4 dB. We furthermore observe that 4.3 dB results in a BER of 0.01 for pure MSK; as a consequence, the required SNR would be 5.7 dB for GMSK.

The symbol error probability for 8-PSK can be computed from Eq. (B-12.66). With an SNR of 12 dB, the SER becomes 0.03. Assuming that each symbol error leads to one bit error, this results in a BER of 0.01.

Chapter 22

IS-95 and CDMA 2000

1. The spreading factors are independent of the rate set; it is the code rate that is different. For the downlink, the data rate (after encoding) is 19.2 kbit/s, so that the spreading factor is 64. For the uplink, the data rate is 28.8 kbit/s, so that the spreading factor becomes 42.7.

2. IS-95 can adjust the power by 1 dB in each 1.25 ms interval. In the following, we derive a simplified estimate. We find that the envelope correlation between two signals with 1 dB difference is 0.9. This is achieved (for a Jakes spectrum) when

$$2\pi\nu_{\max}\Delta t = 0.45 \tag{22.1}$$

since $J_0^2(0.45) = 0.9$. Inserting the equation for the maximum Doppler frequency, we obtain

$$2\pi\frac{\mathrm{v}}{c_0}f_c\Delta t = 0.45 \tag{22.2}$$

so that the maximum Doppler frequency is 21.5 m/s at 800 MHz and 9 m/s at 1.9 GHz.

3. Typically, 20% of the total transmit power is used for the transmission of the pilot. Reducing that percentage to 10% implies that each user could increase the power assigned to it by about 12%. As the capacity is limited by interference, the capacity per cell is not affected by this increase (assuming that the pilot does not act as a significant interferer, which can be achieved, e.g., by interference cancelation). On the other hand, the increase of the power allows an increase of the cell radius, by a factor $1.12^{1/4}$, assuming that the decay exponent is $n = 4$. This implies an increase in cell size by 6%. Note that an increase in the cell size leads to a corresponding decrease in the area spectral efficiency.

   From this we can conclude that a significant decrease in pilot power is not beneficial for capacity, and also does not lead to a significant increase in range. On the other hand, weak reception of the pilot tone leads to a host of other problems. It is thus sensible to keep the pilot tones at the mentioned 20 % of the considered power.

4. In IS-95, three different code rates are used: 1/3, 1/2, and 3/4. The rate 1/3 is used for rateset 1 in the uplink. The rate 1/2 is used for rateset 1 in the downlink, and rateset 2 in the uplink. The rate 3/4 is used for rateset 2 in the downlink.

5. In IS-95, different channels are assigned different channelization codes (either Walsh codes or spreading codes, for downlink or uplink). The receiver can separate the channels by correlating with the different channelization codes. In GSM, different channels are assigned different timeslots and frequencies, where bits can also have different meanings depending on their position within a superframe.

6. In the uplink, transmission always occurs at full power. If the data rate is lower than the maximum considered for a rateset, then bits are repeated. A gating algorithm described in Sec. 22.5 determines how the repeated bits are "punctured" (selectively not transmitted) depending on a randomization algorithm. In the downlink, the channels with a lower data rate are transmitted with lower power.

7. In the uplink, the 3x mode uses a higher chip rate. Thus, each symbol is inherently spread over the whole transmission bandwidth, and (assuming that a Rake receiver is used), the frequency diversity

can always be obtained to its full extent. For the downlink, the information is first encoded, and then multiplexed onto the three used carriers. The drawback of this method is that for a low coding rate, the distribution onto the carriers may not be as effective for obtaining diversity as spreading by using shorter chip durations.

Chapter 23

WCDMA/UMTS

1. The service classes in UMTS are: (i) conversational: this class is mainly intended for speech services, similar to GSM. The delays for this type of service should be on the order of 100 ms or less; larger values are experienced as unpleasant interruptions by users. BERs should be on the order of 10^{-4} or less; (ii) streaming: audio and video streaming are viewed as one important application of WCDMA. Larger delays (in excess of 100 ms) can be tolerated, as the receiver typically buffers several seconds of streaming material. The BERs are typically smaller, as noise in the audio (music) signal is often considered to be more irksome than in a voice (telephone) conversation; (iii) interactive: this category encompasses applications where the user requests data from a remote appliance. The most important category is web-browsing, but database retrievals and interactive computer games also fall into this category. Also for this category, there are upper limits to the tolerable delay - the time between choosing a certain website and its actual appearance on the screen should not exceed a few seconds. BERs have to be lower; typically 10^{-6} or less; (iv) background class: this category encompasses services where transmission delays are not critical. These services encompass email, Short Message Service (SMS), etc.

2. We assume that the sensitivity level of the MS is -117 dBm; since our considered MS is operating at 3 dB above sensitivity, the received power is -114 dBm. The receiver is still functional if the interfering power is equal to the noise power, assumed to be -124 dBm. We furthermore see from Fig. B-23.4 that the admissible out-of-band emission is -6 dBm (integrated over the whole 5 MHz band). Thus, we require a pathloss of more than 118 dB. At a carrier frequency of 1800 MHz, this means that the attenuation from 1 m to the desired distance is 80 dB.

   Also note that the interfering signal is not necessarily suppressed: two users on adjacent frequencies can use the same codes. For this reason, some coordination between operators is desirable.

3. In IS-95, the pilot is transmitted on a separate channel, i.e., with a separate spreading code. A considerable amount of the energy transmitted by a BS (about 20 %) is used for the transmission of the pilot. Furthermore, it is noteworthy that the transmission of the pilot channel is independent of the channels.

   In UMTS, there is a common pilot channel that is transmitted with a specific spreading code, and thus bears resemblance to the pilot channel in IS-95. However, in addition, there is also a pilot transmitted as part of each dedicated channel. The pilot is part of the dedicated control channel that is mapped onto the quadrature-phase component of the transmit signal. Within that control channel, the position of the symbols within each frame determines whether the bits carry pilot information or other types of control information.

4. The maximum data rate is 2 Mbit/s. That rate is achieved the following way: six data channels are transmitted: three on the I-branch, and three on the Q-branch. Each of those three codes has a spreading factor of 4. Thus, the datarate for each of the channels is 3.88/4 Mbit/s $\approx$ 1 Mbit/s. Thus, the total aggregate datarate is 6 Mbit/s. Considering that coding at these high data rates is done with a rate 1/3 encoder, the throughput as seen by the user is $6/3 = 2$ Mbit/s.

   Note, however, that this is the maximum possible throughput. It assumes that the desired user can take up most of the capacity in the cell, does not suffer from significant interference, and is close enough

so that repetitions of data blocks (as requested, e.g., by a higher-layer protocol) are not required. Also note that inefficiencies of higher layers are not considered for this number.

5. Feedback information is transmitted once in every timslot, which has a duration of 0.67 ms. A transceiver can now determine the channel state from the pilot tones during one timeslot, and transmit it in the subsequent timeslot. The other station can make use of that information in yet another timeslot. Thus, the time between the observation of the CSI and its use is two timeslots, 1.33 ms.

   Since the azimuthal power spectrum is uniform, the autocorrelation is $J_0^2(2\pi\nu_{\max}\Delta t) = 0.9$, so that

$$2\pi\nu_{\max}\Delta t = 0.45 \tag{23.1}$$

   from which we obtain

$$2\pi\frac{\mathrm{v}}{c_0}f_\mathrm{c}\Delta t = 0.45 \tag{23.2}$$

   and

$$\mathrm{v} = \frac{0.45c_0}{2\pi f_\mathrm{c}\Delta t} = 8.5 \text{ m/s}. \tag{23.3}$$

   If the angular power spectrum is isotropic (and similarly the antenna pattern), then the Doppler spectrum is uniformly distributed between $-\nu_{\max}$ and $\nu_{\max}$. The temporal autocorrelation function is the Fourier transform of the Doppler spectrum, i.e., a $sin(x)/x$ function. The requirement for the velocity in that case is

$$\mathrm{v} = \frac{0.55c_0}{2\pi f_\mathrm{c}\Delta t} = 10.4 \text{ m/s}. \tag{23.4}$$

   Note that there is an interesting contrast to the maximum velocity that is often mentioned in the literature. It is stated there that since feedback occurs in every slot 0.67 ms), a Doppler frequency of 1500 Hz can be compensated, at least for power control purposes. However, this neglects the effects of the delay between measurement and useage of the information, and also assumes that full information can be transmitted by the feedback bits in one slot.

Chapter 24

Wireless Local Area Networks

1. (a) While 802.11a uses a 64-point FFT, only 52 tones carry any information, and 4 of that are pilot tones (i.e., do not carry payload). Thus, the loss of spectral efficiency is

$$\frac{64-(52-4)}{64} = 25\% \tag{24.1}$$

   (b) The cyclic prefix is 0.8 μs, while the total OFDM symbol is 4 μs. The loss in spectral efficiency is thus

$$\frac{0.8}{4} = 20\% \tag{24.2}$$

   (c) The total duration of the training field and signalling field is 20 μs = 5 OFDM symbol durations, as can be seen from Fig. B-24.6. Thus, the loss in spectral efficiency is

$$\frac{5}{16+5} = 23.8\% \tag{24.3}$$

   The total loss in spectral efficiency due to all of the above effects is

$$1-[(1-0.25)(1-0.2)(1-0.24)] = 54.4\% \tag{24.4}$$

2. 1 Mbit/s (802.11), 11 Mbit/s (802.11b), and 54 Mbit/s (802.11a).

3. The use of OFDM allows better use of the assigned spectral band, since OFDM can more easily achieve a sharp rolloff of the spectrum than can single-carrier modulation. Thus, the required guard bands are smaller. Furthermore, 802.11a allows the use of large symbol alphabets (up to 64 QAM), which have an inherently high spectral efficiency. Note, however, that such a high-order modulation format can only be employed for good SINR.

4. There is a number of N-bit long codewords, and - depending on the data symbol to be transmitted - one out of those possible code vectors is transmitted. Since the codewords can be complex, we have in principle 4^N codewords available. If actually all of those 4^N codewords are valid codewords, then the transmission scheme becomes just standard QPSK, using a 1:1 mapping between 16-bit groups of data symbols and the codewords. The point of CCK is to define a *subset* of codewords with "good" properties as valid codewords, while other codewords are not valid. In the 802.11b standard, the length of the codewords is $N = 8$, so that more than 65000 codewords are possible. Out of those, only 64 codewords are actually admissible ones, representing 6 bits. These 64 codewords are further DQPSK modulated, i.e., a phase rotation of 0, 90,180, or 270 degrees is applied, depending on the 2 additional bits. Thus, a total of 8 bits is transmitted in one codeword.

   CCK (or in general, M-ary Orthogonal Keying, MOK) has a strong similarity to non-systematic block codes. In either case, each symbol (combination of K input bits) is associated with a transmit symbol of length N. The association can be done via a lookup table (as in the case of MOK or block codes), or by some algebraic rules (the more common form for block codes).

5. PLCP header and preamble are *always* transmitted with 1 Mbit/s, and are $144 + 48 = 192$ bits long (see Fig. B-24.). Thus, the transmission lasts 192 μs. In order to achieve 80% spectral efficiency, the data transmission must be

$$\frac{0.8}{0.2} 192\ \mu\text{s} = 768\ \mu\text{s} \tag{24.5}$$

long. With a 1 Mbit/s data rate, this implies a transmission of 768 bits. With 11 Mbit/s, more than 8 kbit need to be transmitted.